BUREAU OF MINERAL RESOURCES GEOLOGY AND GEOPHYSICS

REPORT 243

BMR MICROFORM MF197

CAINOZOIC VOLCANISM OF THE TABAR, LIHIR, TANGA, AND FENI ISLANDS, PAPUA NEW GUINEA: GEOLOGY WHOLE-ROCK ANALYSES, AND ROCK-FORMING MINERAL COMPOSITIONS

by

D.A. Wallace[1], R.W. Johnson, B.W. Chappell[2], R.J. Arculus[3,4]
M.R. Perfit[3,5] and I.H. Crick[1]
Appendices by D.J. Belford and H.R. Lord

---

1. Formerly Geological Survey of Papua New Guinea.
2. Department of Geology, Australian National University, P.O. Box 4, Canberra, A.C.T. 2600
3. Research School of Earth Sciences, Australian National University, P.O. Box 4, Canberra, A.C.T. 2600
4. Present address: Department of Geological Sciences, University of Michigan, Ann Arbor, Michigan 48109, U.S.A.
5. Present address: Department of Geology, University of Florida, 1112 General Purpose Building A, Gainesville, Florida 32611, U.S.A.

DEPARTMENT OF RESOURCES & ENERGY

Minister: Senator the Hon. Peter Walsh

Secretary: A.J. Woods

BUREAU OF MINERAL RESOURCES, GEOLOGY AND GEOPHYSICS

Director: R.W.R. Rutland

Published for the Bureau of Mineral Resources, Geology and Geophysics
by the Australian Government Publishing Service

ISSN 0084-7100

Abstract

Geological surveys have been made of the Tabar, Lihir, Tanga, and Feni island groups, which constitute a dominantly alkaline volcanic chain, roughly parallel to, and northeast of, the Tertiary island arc of New Ireland in northeastern Papua New Guinea. The islands consist mainly of Pliocene and Pleistocene lava flows and volcaniclastic deposits, but pre-Middle Miocene volcanic rocks are known in the Tabar Islands. Quartz trachytes (the only silica-oversaturated rocks of the chain) represent the youngest extrusive rocks in each island group. Raised Pleistocene coral reefs form fringing terraces on many of the islands, and Miocene reef limestone is preserved on Simberi Island in the Tabar Islands. Present-day thermal activity is found in each of the island groups, but is best developed on Lihir and Feni Islands, where the thermal areas mostly occupy the calderas of Quaternary volcanoes. Whole-rock chemical analyses have been compiled for 116 Tabar-to-Feni rocks (major and trace elements, and, for some rocks, rare-earth-element abundances and $^{87}Sr/^{86}Sr$ values). Rock-forming minerals in many rocks have also been analysed using the electron microprobe. The analysed alkaline rocks are mainly phonolitic tephrite and trachybasalt, but more mafic types are basanite, tephrite, alkali basalt, transitional basalt, and ankaramite. Clinopyroxene-rich cumulate inclusions are a common feature of some lava flows.

Contents

Tables

Tabar Islands:

Lihir Islands:

Tanga Islands:

Feni Islands:

INTRODUCTION

One of the most curious features of the Cainozoic geology of Papua New Guinea is the chain of dominantly alkaline volcanoes making up the Tabar, Lihir, Tanga, and Feni Islands off the northeastern coast of New Ireland (Fig. 1). Their alkaline character was first reported by Glaessner (1915), but the islands were neglected by petrologists and geologists for more than fifty years - until 1969, when the late G.A.M. Taylor undertook a geological investigation of them, and collected a suite of rock specimens for petrological study.

The alkaline compositions of most Tabar-to-Feni rocks are the main petrological feature of interest in this volcanic province, as they are in marked contrast to the dominantly silica-oversaturated character of rocks from other volcanic provinces in Papua New Guinea. However, another equally important aspect of Tabar-to-Feni volcanism is the tectonic setting of the islands. The analysed volcanic rocks are thought to have some chemical features in common with arc-trench-type rocks, but there is no consensus on the nature of the tectonic setting in which the magmas originated. All suggestions made in the literature to date are little more than speculation (see Johnson 1979 for a review).

Taylor's 1969 field study was the first of a series of geological investigations of the Tabar-to-Feni Islands by the Bureau of Mineral Resources (BMR) and Geological Survey of Papua New Guinea (GSPNG). Taylor returned to the islands in 1971, and collected more rock samples. Wallace and Crick then undertook surveys of the islands, in 1972 and 1973, as part of the routine geological mapping of Papua New Guinea at 1:250 000 scale. Wallace and Johnson visited the islands in 1974, specifically to collect additional rock samples, as most of Taylor's original specimens had by then been lost(though thin sections and rock powders of many of them survived).

Many of the rocks collected by Taylor and to a lesser extent, by Wallace and Crick were analysed routinely for major elements in the early 1970s, but in recent years the entire collection of existing material has been subjected to relatively intensive petrological and geochemical investigations - particularly trace-element and isotopic analysis of whole-rock samples and electron-microprobe determination of mineral compositions. Interpretation of these analytical results is still underway, and our aim in this report is mainly to present analytical data - together with geological descriptions of

the islands - as a basis for interpretative reports that are still in progress. Some initial interpretations are given in the Discussion section. Taylor did not write a report of his early work (he died in August 1972), but a preliminary (now outdated) account of the geology and petrology of the islands was given by Johnson, Wallace, & Ellis (1976; see also: Arculus, Johnson, & Perfit, 1978; Arculus, Johnson, & Chappell, 1978: Arculus & Johnson, 1981; Perfit, Johnson & Chappell, 1981). The results of an independent petrological study of Ambitle Island (one of the Feni Islands) were also presented by Heming (1979).

A breakdown of responsibilities for the authors of this Report is as follows:

Wallace - geological mapping, rock-sample collection, geological interpretations, sample-locality identifications (plotting on maps, and grid references):

Johnson - rock-sample collection, overall compilation and editing of report, tabulation of major-element and XRF trace-element analyses, rock nomenclature;

Chappell - X-ray fluorescence (XRF) analysis, computer data storage, tabulation programming;

Arculus - electron-microprobe analysis, tabulation of mineral compositions;

Perfit - spark-source mass spectrographic (SSMS) analysis of trace elements, mass spectrometric analysis of Sr-isotopes, and tabulation of results from both methods;

Crick - geological mapping, rock-sample collection, descriptions of thermal areas on Lihir and Feni Islands.

Rock-sample numbering system and locality identification

Major-element chemical analyses of 116 Tabar-to-Feni rocks are listed in ten Tables labelled TB1 to FN2. The coding of these Tables allows identification of each analysed sample. The island group of any one sample is identified by a two-letter abbreviation (TB, LH, TG, FN), followed by a number that corresponds to one of the individual islands listed in Table 1,

followed by a slash and the number of the rock analysis in the appropriate Table. Analyses in each Table are listed in order of decreasing MgO content, so, for example: TB2/12 refers to a sample from Tatau Island in the Tabar Islands (Table 1) that is twelfth in order of decreasing MgO content in Table TB2; FN1/2 is a sample from Ambitle Island that has the second highest MgO content of all the analysed rocks from this island listed in Table FN1.

Rock names are given in an index at the bottom of each Table page, and these are followed by an eight-digit BMR registered sample number. The particular survey during which the sample was collected may be identified by using the first two digits of the BMR sample number in conjunction with Table 1. Some samples from the Wallace-and-Crick surveys have two BMR registered numbers- one prefixed 74, the other by 73.

Grid references and locality descriptions for each sample follow the BMR registered sample number in Tables TB1 to FN2. The grid references refer to the following series of 1:100 000-scale topographic maps of the Tabar-to-Feni Islands published in 1975 by the Royal Australian Survey Corps (Series T601): Tabar Islands - Tatau 9292, Tabar, 9392; Lihir Group - Lihir, 9491; Tanga Islands - Tanga, 9591; Feni Islands - Feni, 9689. The topographic maps have also been used as bases for the geological maps given in Figures 4-6, 9, 12, and 15. A legend for the geological maps is given in Figure 2.

The 1975 maps became available after the geological surveys had been completed, so there were problems in accurately relocating sample sites - particularly those of rocks collected by Taylor. However, most other samples are probably reasonably well located to within 100m or so. We have also used the 1975 maps as our source for place names and spellings, even though these may not necessarily conform to local usage.

A palaeomagnetic survey of the Bismarck Archipelago, including the Tabar-to-Feni Islands, was undertaken in 1979 and 1980 by D.A. Falvey then of the Department of Geology and Geophysics, University of Sydney (now BMR). Sampling sites in the Tabar-to-Feni Islands are also plotted on the geological maps (Figs 4-6, 9,12,15), by courtesy of Dr Falvey (personal communication, 1982).

Rock nomenclature

The rock names used in Tables TB1 to FN2 derive from the CIPW-normative system of rock nomenclature adopted by Johnson & others (1976; see also Johnson, Mackenzie, & Smith, 1978). This system is based on a plot of Differentiation Index (Thornton & Tuttle, 1960) against normative nepheline or normative quartz plus the silica of normative hypersthene (Fig. 3), and the

fields are broken into arbitrarily defined areas which are assigned familiar rock names. Two kinds of prefixes are given to most of the rock names: (1) Q, hy, or ne, depending on whether the rock is quartz-, hypersthene-, or nepheline-normative, respectively; (2) potassic or sodic, depending on whether K_2O/Na_2O values are, respectively, greater or less than 0.5.

The system is dependent on the CIPW norm, which, in turn, is sensitive to the oxidation state of iron. Johnson & others (1976) recalculated all their analyses and standardised Fe_2O_3 values according to the method of Irvine & Baragar (1971). Here, however, we have reverted to use of the 'raw' major-element analyses, and have neither recalculated analyses volatile-free nor standardised the oxidation state, on the grounds that the relatively high Fe_2O_3/FeO values and high volatile contents of Tabar-to-Feni rocks may at least in part be intrinsic features of the magmas, and that transforming the data by the above criteria may be an overcompensation. The result of using raw analyses rather than transformed ones is that data points in Figure 3 correspond to slightly lower degrees of silica-undersaturation, and that two analysed rocks formerly called nephelinites (because they were leucite normative) are now classified as tephrites (albite normative); no analysed Tabar-to-Feni rocks are now termed nephelinites. The numbers of the different analysed rock types are listed in Table 2.

Analytical techniques

The samples collected between 1969 and 1974 were analysed for major elements by the Australian Mineral Development Laboratories (Amdel), Adelaide, between 1971 and 1978, on contract to BMR and GSPNG. Amdel analytical techniques are a combination of atomic-absorption spectroscopy and conventional gravimetric and colourimetric methods, and levels of precision for many elements were probably not the same throughout the entire seven-year period of analysis. This contrasts with the 1976-series rocks, which were all analysed during the same period in late 1977 mainly by X-ray fluorescence spectrometry. Consequently, the 1976-series values are probably the most reliable of all the major-element data. XRF analyses were done on rock-powder pellets, following the methods of Norrish & Chappell (1977) on the automated Philips PW1220 spectrometer at the Department of Geology, Australian National University (ANU). XRF techniques were also used for the determination of all trace-element values listed in Tables TB1 to FN2.

Abundances for 21 trace elements, including the rare-earth elements (REE), in 27 rocks have been determined. These were obtained by spark-source mass spectrography, using techniques described by Taylor & Gorton (1977), and (with one exception) using samples from the same powders used for the major-element and XRF analyses. Chondrite-normalised REE patterns for the 26 samples are shown for each island group in Figures 8, 11, 14, 17 and 18.

Strontium-isotope ratios (Table 3) were measured using the Nuclide Analysis Associates (NAA) machine (30.5 cm radius, 60° sector) at the Research School of Earth Sciences (ANU; see also Page & Johnson, 1974). Rhenium triple-filament sources were used, and the samples were loaded as chlorides with water. The NAA mass spectrometer uses 6 kV accelerating voltage, a Faraday cup collector, and a Cary electrometer (model 31), and is operated on-line by an HP-2116B computer, which also controls the magnetic-field peak switching. One or two sets of twelve $^{87}Sr/^{86}Sr$ values were measured between sets of $^{88}Sr/^{86}Sr$ measurements and normalised to a value of 8.3752 for $^{88}Sr/^{86}Sr$. ^{85}Rb was measured repeatedly to correct for ^{87}Rb in ^{87}Sr, but corrections were mostly negligible. No runs required tail corrections. The $^{87}Sr/^{86}Sr$ value measured by Page & Johnson (1974) for the Eimer and Amend standard was 0.70813 ± 0.00004, and the mean value for standard NBS 987 measured during the new runs was 0.71032 ± 0.00006.

About 2500 mineral analyses for analysed lava samples were carried out on the TPD electron microprobe at the Research School of Earth Sciences. Analytical procedures used were those of Reed & Ware (1973, 1975) and Ware (1981). Samples of cumulate rocks whose bulk-rock compositions were not determined have also been studied with the electron microprobe; a list of these additional samples is given in Table 4. The mineral analyses have been compiled in an unpublished data catalogue (Arculus, 1982) two copies of which have been made. One copy has been lodged in the BMR Library, and the other in the Library of the Research School of Earth Sciences.

Data presentation

The Sr-isotope data for Tabar-to-Feni samples are presented in Table 3, but all other analytical data are listed in groups of tables after the geological descriptions and illustrations for each island group. The first table in each group is from the TB1-to-FN2 series of tables, and is followed by tables of SSMS analyses and mineral compositions.

Table 1. Rock-sample codes and numbers of analysed samples on an island-by-island and survey-by-survey basis

Island groups and abbreviations	Individual islands and numbers	First two numbers of BMR registered sample no.*			Totals
		69, 71	74(73)	76	
Tabar Islands TB	1. Simberi	2	3	-	5
	2. Tatau	5	3	6	14
	3. Tabar	3	6	2	11
					Σ30
Lihir Group LH	1. Lihir	11	12	7	Σ30
Tanga Islands TG	1. Malendok	6	1	4	11
	2. Lif	3	1	1	5
	3. Tefa	3	-	1	4
	4. Bitiik & Bitbok	3	1	-	4
					Σ24
Feni Islands FN	1. Ambitle	7	11	10	28
	2. Babase	3	1	-	4
					Σ32
	Totals	46	39	31	116

*Collectors: 69, 71 - Taylor (1969 & 1971 surveys, respectively).
74(73) - Wallace & Crick (1972 and 1973 surveys).
76 - Wallace & Johnson (1974 survey).

Table 2. Numbers of different, chemically analysed rock types for each island group

	Tabar	Lihir	Tanga	Feni	Total
Ankaramite & cumulates	-	1	-	1	2
Transitional basalt	4	4	1	1	10
Alkali basalt	2	7	-	2	11
Tephrite	-	1	-	2	3
Basanite	1	1	-	1	3
Hy-trachybasalt	8	9	-	1	18
Ne-trachybasalt	7	5	6	4	22
Phonolitic tephrite	3	2	9	11	25
Hy-trachyandesite	2	-	-	1	3
Ne-trachyandesite	1	-	-	4	5
Tephritic phonolite	-	-	-	2	2
Q-trachyte	2	-	5	2	9
Ne-trachyte	-	-	3	-	3
(Phonolite)	-	-	-	-	-
Total	30	30	24	32	116

Table 3. $^{87}Sr/^{86}Sr$ values for 28 Tabar-to-Feni Rocks

New results[a]:	Rb/Sr	$^{87}Sr/^{86}Sr$	$\pm 2\sigma$
TB2/3	0.020	0.70400	3
TB2/9	0.029	0.70405	7
TB2/12	0.031	0.70436	3
TB2/14	0.039	0.70433	4
TB3/4	0.028	0.70365	5
TB3/10	0.075	0.70422	5
LH1/3	0.010	0.70452	4
LH1/9	0.039	0.70435	5
LH1/10	0.042	0.70398	5
LH1/22	0.052	0.70397	14
Lh1/23	0.036	0.70387	7
TG1/1	0.041	0.70392	7
TG1/2	0.056	0.70410	3
TG1/8	0.038	0.70438	6
FN1/9	0.037	0.70392	5
FN1/10	0.036	0.70402	5
FN1/13	0.043	0.70422	4
FN1/22	0.033	0.70403	5
FN1/27	0.028	0.70384	4
Page and Johnson (1974) results[b]:			
TB2/12	0.031	0.7044	
TB3/7	0.039	0.7041	
LH1/12	0.090	0.7042	
374	0.038	0.7040	
TG1/6	0.010	0.7041	
TG1/7	0.030	0.7042	
TG2/3	0.077	0.7040	
TG3/1	0.059	0.704	
FN1/19	0.030	0.7041	
FN1/23	0.028	0.7041	

a Measured values for NBS 987 = 0.71032; 0.71026; 0.71029. All values quoted to 2 standard errors of the mean ($\pm 2\sigma$).

b Rb/Sr values are new. Measured value for E and A $SrCO_3$ standard = 0.70813 $\pm$ .00004.
Sample 374 not analysed for major elements and hence not listed in Tables TB1 to FN2 (BMR registered number is 69400374)

Table 4. List of cumulate samples whose whole-rock chemical compositions have not been determined, but whose minerals have been analysed by the electron microprobe.

Sample No.	Grid reference and locality description
TB2/15	LB816935. In stranded boulder on cultivated alluvium at Kopo Plantation, western side of Tatau Island.
TB2/16	LB806982. In *in situ* lava flow in stream east of Tupinaminda Bay, Tatau Island.
TB2/17	LB863968. In loose boulder in stream southwest of Pekinberiu village, Tatau Island.
TB2/18	LB862967. In loose boulder in stream southwest of Pekinberiu village, Tatau Island. Same locality as TB2/7.
TB2/19	LB863968. In loose boulder in stream southwest of Pekinberiu village, Tatau Island. Same locality as TB2/17.
TB2/20	LB862899. In loose boulder on flank of ridge across bay west of Matua, Tatau Island.
LH1/31	MB584604. In *situ* highly porphyritic lava flow in stream on western part of Londolovit Plantation, Lihir Island. Same locality as LH1/1.
FN1/32	NA680480 (approximate). Loose block on surface of Q-trachyte dome, central Ambitle Island.
FN1/33	NA631469. In loose boulder on beach near Tabulam village, Ambitle Island.
FN1/34	NA655456. In *in situ* lava flow exposed in road cut on southern side of Nanum Bay, Ambitle Island.
FN1/35	NA656452. In *in situ* lava flow (analysed sample FN1/25) in roadcut on southern side of Nanum Bay, Ambitle Island.

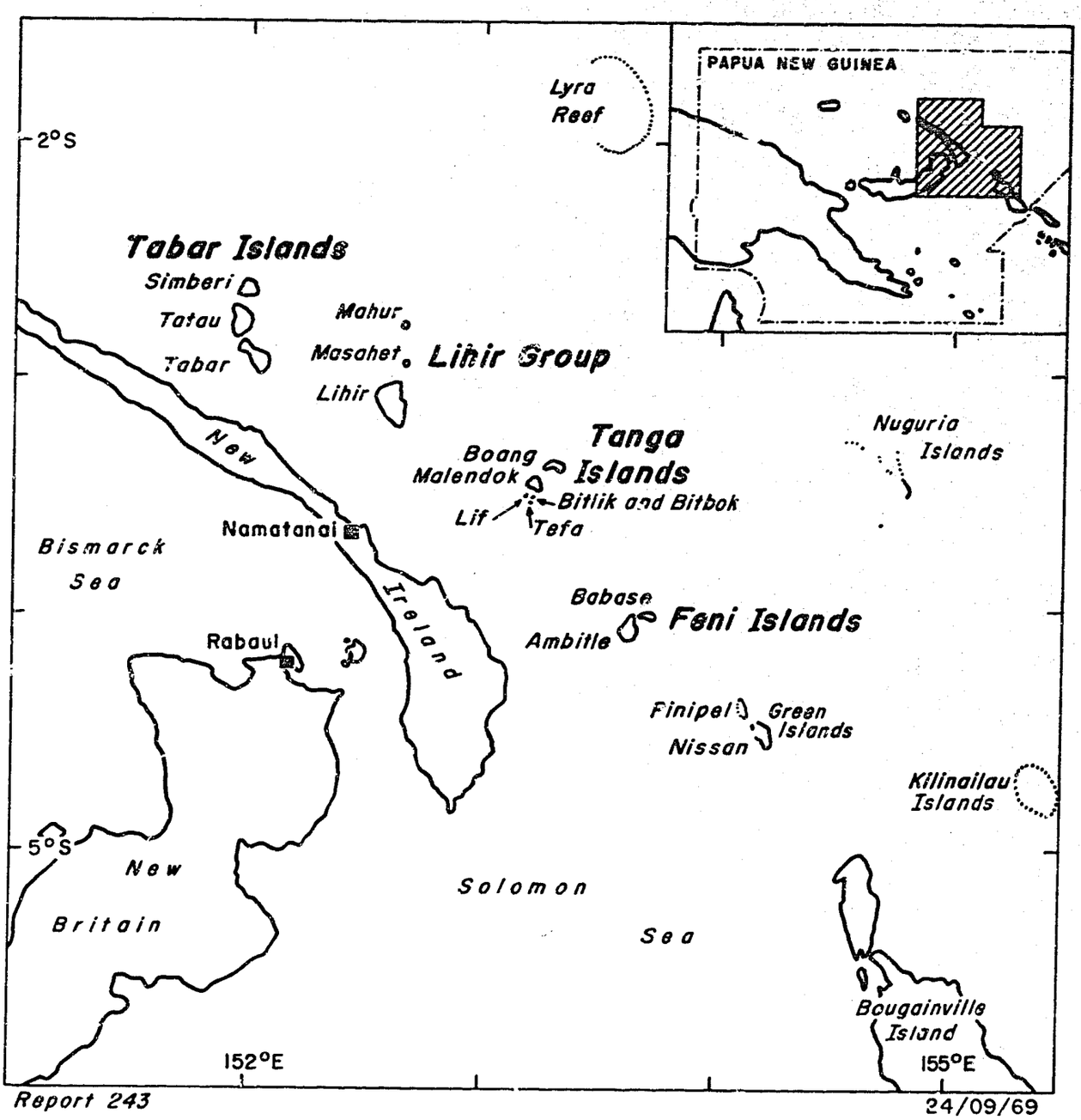

Figure 1. Locality maps.

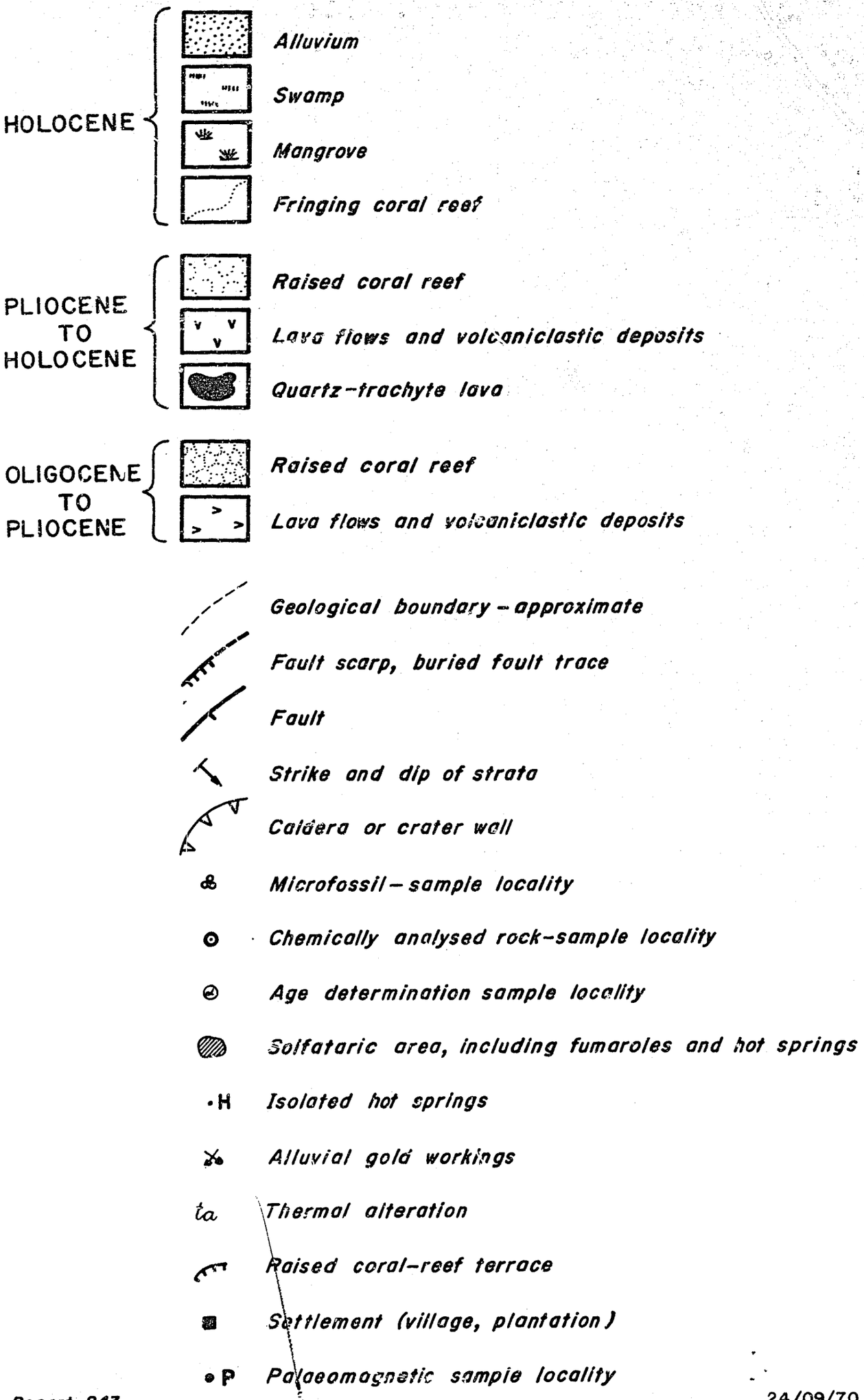

Figure 2. Legend to geological maps (Figs 4-6, 9, 12, 15).
For convenience this figure is repeated after each geological map.

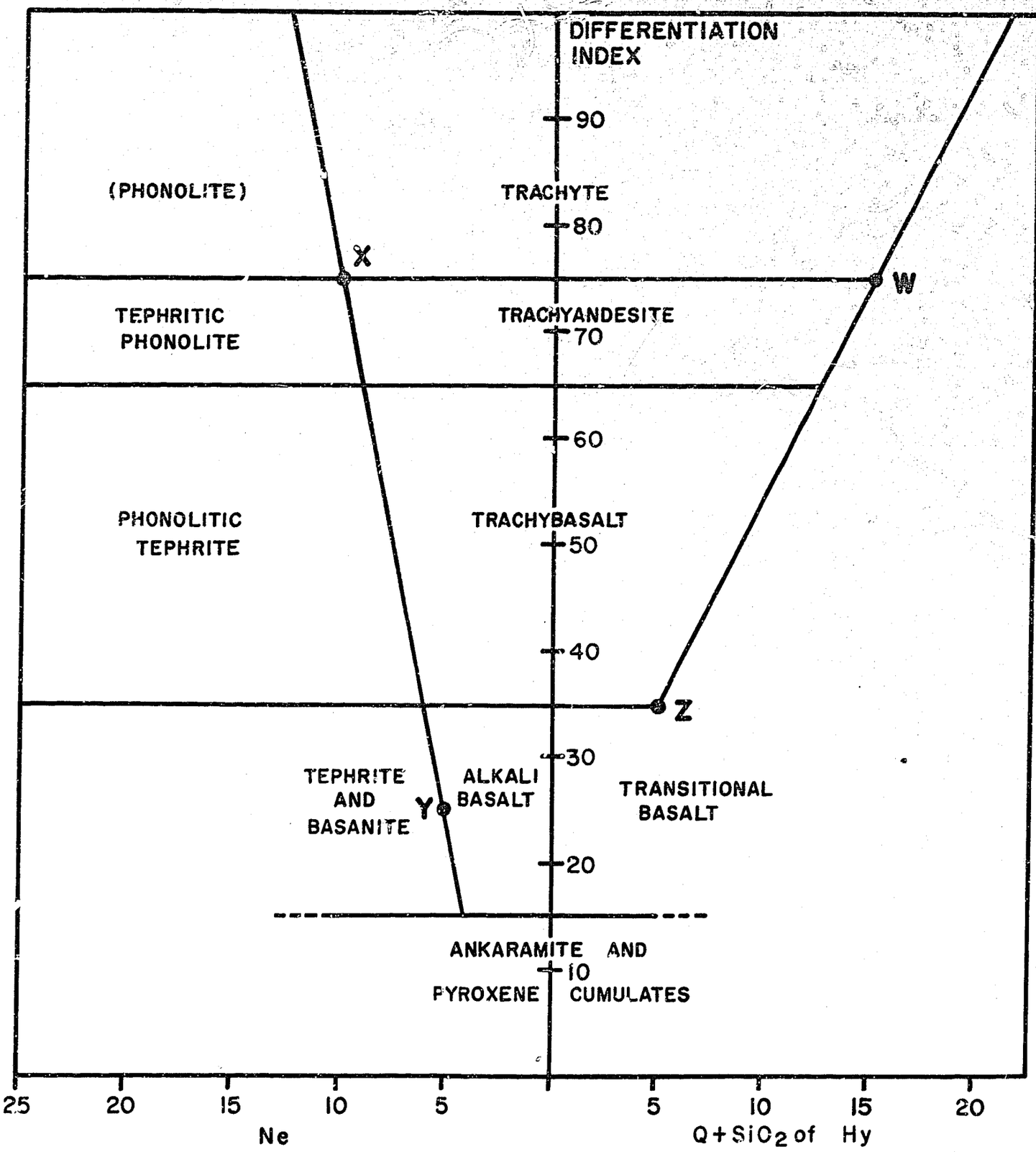

Figure 3. Rock-nomenclature grid. Ne, Q, and Hy are the CIPW normative components nepheline, quartz, and hypersthene, respectively. Differentiation Index is the summation of the CIPW normative components nepheline, quartz, orthoclase, albite, leucite, and kalsilite (Thornton & Tuttle, 1960). X-Y is the arbitrary line used by Coombs & Wilkinson (1969) to separate mildly undersaturated rocks from strongly undersaturated ones (X = /I75, Ne 10; Y = /I25, Ne 5). The line through W (DI = 75, Q + SiO_2 of Hy = 15) and Z (DI = 35, Q + SiO_2 of Hy = 5) is also an arbitrary boundary chosen specifically for rocks from Papua New Guinea (Johnson & others, 1978). Basanites contain significant amounts of modal olivine, whereas olivine is absent or rare (less than 1 percent by volume) in tephrites.

TABAR ISLANDS

Introduction

The Tabar Islands are the northernmost of the four island groups, and consist of three main islands (Fig. 1) - Simberi (Fig. 4), in the north, and the larger Tatau and Tabar Islands, which are separated by a narrow strait known as Saraware Passage (Figs. 5,6). The Tabar Islands consist of volcanic rocks of mid-Tertiary age - the oldest exposed in the Tabar-to-Feni chain - to Pleistocene, and Tatau Island is still thermally active, though not as strongly as Lihir and Ambitle Islands.

Simberi: topography and general geology

Simberi Island covers about 56 km^2, and is more-or-less circular - except in the south, where the coastline is straight for about 7 km (Fig. 4). Its maximum diameter is about 10 km from southwest to northeast. The highest point, Mount Manumbur, is northeast of the centre of the island, and is 292 m above sea-level. Simberi has four copra plantations, five missions, and several coastal villages. Except for the plantations, the island is thickly vegetated, and rock exposure is poor. Coral reef fringes the island for most of its perimeter, and swamp fills an embayment east of Simberi village (Fig. 4).

Simberi consists of a raised Quaternary coral-reef platform that surrounds a high, steep-sided, central plateau of volcanic rocks, which is partly capped and mantled by lower Miocene to Pliocene reef limestone (Fig. 4). The top of the central plateau is an area of moderate relief, mostly 120-290 m above sea-level; it is incised by radial valleys, and has a broad dome-like profile. The Tertiary limestone crops out mainly at the western and northern edges of the central plateau, and is exposed in many of the steep cliffs, up to 160 m high, that mark the contact of the Quaternary reef platform with the older rocks of the central plateau. The contact of the Tertiary limestone with the volcanic rocks is also marked by cliffs, a few tens of metres high, that face towards the centre of the island. The middle of the volcanic plateau is east of the centre of the island, and the widest part of the Quaternary reef platform is in the west. Faulting has affected parts of the central area of volcanic rocks; four faults shown in Figure 4 have a mainly northwesterly trend. Thermal alteration of country rock is associated with the faulting.

Simberi therefore appears to be an old volcano that has been inactive since the Miocene, and which, following submergence during the Miocene and Pliocene, has been raised and tilted.

Simberi: volcanic rocks

The volcanic rocks of Simberi Island can be divided into two broad units - a younger one, consisting predominantly of volcaniclastic deposits, and an older one that appears to be made up largely of mafic-to-intermediate lava flows. The apparent increase in the relative volume of fragmental rocks between the older and younger unit is probably an indication that, in its later stages, Simberi changed from a predominantly effusive to a more explosive type of volcanism.

The rocks of the older unit are exposed in the central part of Simberi, and its lava flows appear to dip away from the centre of the island. This and the dome-like profile of the dissected central plateau, are evidence that Simberi was originally a central-type volcano. Fragmental rocks are known to be associated with the lava flows, and Simberi could, therefore, be a stratovolcano, although more detailed fieldwork is required to confirm this.

A distinctive volcaniclastic rock type crops out in the lower reaches of a stream bed 2 km southeast of Napekur village. It consists of fine-grained, grey, angular to sub-angular clasts of basalt in a yellow-stained matrix, and forms a 1-m thick horizon that underlies southward-dipping volcanic rudites. The clasts are roughly equidimensional, mostly about 4 cm across, and their margins have been chilled against the matrix. Differential weathering has resulted in the clasts showing higher relief then then the matrix, giving a studded, or embossed, appearance on exposed surfaces, and the apparent fit of adjacent clasts with one another produces a 'jigsaw' effect. Hot lava may have come into contact with water, producing the rapid chilling and brecciation.

Thermal alteration of the rocks of the older unit to white, pyritised clay at least two localities, one of which coincides with a fault showing evidence of shearing. In addition, the condition of boulders in a stream west of Pigibut Plantation may be indicative of a third area of thermal alteration.

The younger unit of volcanic rocks consists of rudites made up of sub-angular to rounded clasts of dark lava, from a few centimetres up to 40 cm in diameter, in a weathered fine-grained matrix. The rudites are exposed along the southern edge of the central plateau and on the upper parts of high ridges in the south. They are crudely bedded, and dip at 30-40^{o} away from

the centre of the island, clearly overlying the older area of lava flows to the north. The long axes of large elongate clasts are roughly parallel to the direction of dip. Lava flows and beds of volcanic arenite and scoriae in some parts of the unit are intercalated with the rudites. Two dykes cut rudites in the southeast, one of which is intensely sheared. At the southwest edge of the central plateau, where the older unit crops out as a prominent tongue flanked by outcrops of the younger unit, horizons of volcanic arenite, dipping a few degrees to the northeast, are exposed in a stream section. These appear to be the youngest volcanic deposits on Simberi. Their age is uncertain, but they may be Miocene.

Five volcanic rocks from Simberi have been chemically analysed (Table TB1, Table 5, Figs 7, 8). They range from a quite mafic basanite, to alkali basalt and trachybasalt, to trachyandesite.

Simberi: raised-reef limestones

The older reef limestone on Simberi forms a semi-circular line of outcrop around the western, northern, and - to a lesser extent - eastern edges of the central plateau of volcanic rocks, only part of which is higher than the limestone cappings. The limestone has a maximum elevation of about 180 m above sea level in the north, and must have been raised by at least this amount to its present position. The limestone is not present at the southern edge of the central platform (Fig. 4). This may be due to a southward tilt of the reef, which, seen on the aerial photographs and in the field, dips beneath the Quaternary reef platform in the south. Other islands of the Tabar-Feni chain also have a similar southward tilt of a few degrees (see below).

The microfaunas of four limestone samples collected by G.A.M. Taylor in 1969 were identified by D.J. Belford, whose report is given in Appendix 1. The faunas of the three oldest samples, considered together, are consistent with an early to late Miocene age, and the fourth sample is Pliocene or younger. The limestone is, therefore, stratigraphically equivalent to other limestones that are widespread throughout the Bismarck Archipelago (for example, the Lelet Limestone of New Ireland - Hohnen, 1978; and the Yalam Limestone of New Britain - Davies, 1973) and which seem to mark a major cessation of volcanic activity throughout the region.

Samples of the limestone examined in the field are typically massive, containing limestone clasts and remains of corals, algae, and molluscs, most of which are fragmented. Some corals are seen in their

original growth positions, but much of the limestone appears to be detrital. Primary volcanic rocks do not seem to be present within the limestone, and no volcanism, therefore, appears to have taken place after the early Miocene. Rudimentary wave-cut notches in coral about 15 m above ground level east of Maragon village, on the west coast, may indicate that uplift continued up to the Holocene. The Miocene reef may, therefore, have been uplifted in stages, rather than in one period of rapid uplift.

The Quaternary coral platform surrounding the older rocks of Simberi represents a period of uplift that seems to have been distinct from that which raised the Miocene limestone. Because the platform is widest in the southwest (1.5 km) and narrowest in the northeast (less than 500 m), the tilting was probably to the northeast, but this was insufficient to drastically alter the older southward tilt of the Miocene reef.

Tatau: topography

Tatau is the central island of the Tabar group (Fig. 1). It is about 5 km south of Simberi Island and is separated from Tabar Island to the south by Sarawere Passage which, in parts, is only a few tens of metres wide. Tatau is shaped like an inverted comma, and covers about 120 km^2 (Fig. 5). Apart from low-lying coastal platforms in the north and east, the island is mountainous and has rugged relief; many parts of the island are more than 200 m above sea-level. The northeastern half of the island contains the two highest points, Mount Panalia (about 360 m above sea-level) and Mount Sokosung (320 m). The two highest points in the lower, southwestern part are Mount Letam (283 m), in the west, and Mount Tiro (about 280m), in the extreme south.

The drainage of Tatau is controlled by an axial watershed that follows a sinuous course northwards from Mount Tiro, west of the centre of the island, to a point northwest of Mount Panalia, where it swings abruptly northwestwards, passing through Mount Sokosung towards Cape Tiwi. A series of prominent, steep-sided spurs falls steeply westwards from the watershed to the coast between Maragat and Sambuari villages.

Apart from three coastal plantations and small cultivated village gardens, the island is densely covered by thick primary vegetation. A wide, almost unbroken, belt of mangrove swamps extends from Tupinaminda Bay on the northwest coast, around the south coast, to Mabua village in the east. Tatau

is surrounded almost entirely by fringing and offshore reef, which extends up to 2 km from the shore. Breaches in the reef allow access to many of the small bays and inlets around the island, which provide anchorages for small vessels.

Tatau: geology

Tatau Island is a volcanic complex that has been so extensively modified by erosion and tectonism that its original form has been largely destroyed. The age of the volcanism is also uncertain, although by comparison with the volcanic area of Simberi Island, much of the central area could be pre-Miocene (Fig. 5).

Lava flows and volcaniclastic rocks, together with a few dykes, form the bulk of the island. The watershed in the north lies close to a major boundary between two major rock units, which are broadly comparable with the two volcanic units identified on Simberi Island: (1) northward-dipping, volcaniclastic deposits, which crop out in the north (Fig. 5); (2) older flows and less common associated rocks, making up the centre of the island. Mount Tiro appears to be the remnant flank of a younger volcanic centre that has been modified by faulting.

The older effusive rocks are subaerial in origin, and range widely in grain-size. Some rocks have prominent phenocrysts of green pyroxene and crystals of plagioclase up to 3 mm long. Nodules of pyroxenite, up to 4 cm in diameter, are present as inclusions in many lava flows, particularly on the western side of the island, between Sambuari and Maragat villages. Spheroidal weathering is developed in jointed, fine-grained rocks that cover much of the central part of the island. An outcrop of tough, compacted, brecciated lava, similar to that described from Simberi Island, is found at 20 m above sea-level, 2 km north of Tugitug village.

The younger volcaniclastic succession in the northern part of the island is about 300 m thick, and consists of northward-dipping, interbedded volcanic rudites, arenites, and argillites. Good exposures are in the middle reaches of the stream draining into Tupinaminda Bay and cutting through the succession parallel to the strike. There, massive blocks up to 20 m across have been dislodged from a steep escarpment to the north, and are distributed chaotically in the stream bed. The clastic succession, which can be recognised as the northern part of a large composite volcano, is downfaulted

in the west along an arcuate fracture.

Most of the younger volcaniclastic succession is well consolidated, and consists of north-dipping, bedded, angular to sub-angular, mafic clasts, up to 50 cm across. These are subordinate to a matrix of unsorted ash and breccia, containing fragments of pumice, and pyroxenite nodules a few centimetres wide. The structure of the succession is generally chaotic, apart from some concentrations of rudaceous clasts that form discontinuous bands sub-parallel to the dip. The generally unsorted character in the upper 100 m is replaced by progressively thinner beds of lapilli tuffs, welded scoriae, and interlaminated ash beds a few centimetres thick. Soft, creamy-yellow, tuffaceous blocks are found in some streams. Dips of up to 70° can be seen in the western part of the succession, and they tend to decrease eastwards. These dips are higher than would be expected for the flanks of a stratovolcano (about 30-40°), and may be evidence that tilting has taken place towards the north and west, at least in the western downfaulted sector. Highly weathered and brecciated lava flows underlie the volcaniclastic succession.

Raised reef limestone is exposed on the northern and eastern sides of the island, reaching a maximum height of 20 m above sea-level along parts of the coast between Mabua and Pekinberiu villages, where it forms prominent headlands. Raised reef in the north forms a low-lying coastal platform that broadens westwards to widths of more than 2 km at Cape Tiwi. Palaeontological investigation of limestone samples yielded no conclusive ages. The general disposition of the raised reefs, and the presence of swampy ground around the west and south coasts, is indicative that Tatau Island may have been tilted a few degrees towards the southwest. Alternatively, the entire island may have been raised, except for the southern and western parts, which were downfaulted along a fault running west of the axial watershed (Fig. 5).

The island is strongly faulted. The two most prominent faults run north-south on either side of the watershed (Fig. 5). The western one curves northwestwards at its northern end, displaces the contact between the volcaniclastic unit and the lava flows, and is downthrown to the west. In general, other faults are less well defined, but on the aerial photographs most of them appear to have a northwesterly trend. A northwest-trending fault zone appears to mark the boundary between the higher northeastern part

of the island and the southwestern half. A northwest-trending fault cuts Mount Tiro.

The manager of Tomalabatt Plantation reported that in 1971 he felt a small earth tremor which lasted about two minutes and coincided with welling-up of water in Sarawere Passage. This may indicate that faulting is still taking place, possibly along a northeast-trending fault that may mark the line of the Passage.

Fifteen rock samples from Tatau Island have been chemically analysed (Table TB2, Table 5, Figs 7,8), and all but one - an alkali basalt - have relatively fractionated compositions - trachybasalt, phonolitic tephrite, and trachyandesite.

Tatau: thermal activity and alteration

Several areas of thermal alteration are present on the island. Each of these (marked 'ta' in Fig. 5) appears to be limited in area, but they are widespread throughout the island. Thermal alteration in the southeast of the island, within a lobe of volcanic rocks, appears to be associated with a series of northwest-trending faults (Fig. 5).

The most obvious effect of thermal alteration is the gradual change in colour from originally dark rock, to shades of grey and, finally, almost to white. In addition, the rocks become much more tough and compact, and develop a brittle fracture. Phenocrysts become less discernible and tend to merge with the darker groundmass minerals through recrystallisation and propylitisation. Pyritisation is a ubiquitous feature of the altered rocks. Good examples of these gradations in thermal alteration are seen 1.5 km up the stream flowing past Tugitug village and also near the headwaters of the stream to the southwest, where the alteration appears to have been related to the intrusion of a dyke. Veins of quartz are found throughout the faulted, lobe-shaped area north of Tomalabatt Plantation (Fig. 5). Minerals disseminated in cavities throughout the quartz have been identified by X-ray diffraction as hematite, goethite, and amorphous iron oxides ('limonite'). Local people reported that alluvial gold is found in streams draining this area, but no traces were revealed by panning during the field investigation of 1973.

Alluvial gold was mined on a small scale in the Tugitug stream before the Second World War, and several adits, up to 10 m deep, are scattered above the headwaters of the stream (Pearson, 1934). The bedrock

of the upper parts of the stream, from which the gold was presumably derived, is thermally altered mafic lava. Panning the stream sediment in 1973 yielded a few specks of gold in each pan, although it was found necessary to first remove the upper 50 cm of surface alluvium, which yielded no visible colour. Quartz crystals are disseminated throughout the stream sediment, but no quartz veins, or other bodies were observed in the country rocks.

According to the local people, present-day thermal activity on Tatau Island is limited to one small hot spring at the head of the bay southeast of Sambuari village. In 1973, this spring had a temperature of 36°C.

Grey, unconsolidated, alluvial mud is being deposited at the present by streams flowing through the swampy, low-lying area north of Tomalabatt Plantation, and resembles the mud currently being generated in hot bubbling pools on Lihir and Feni Islands (see below), and also in central New Britain (Wallace, 1976). Similar thermal phenomena may therefore have existed in the recent past near Tomalabatt, probably within the nearby, low-lying swampy terrain, which, however, is difficult to penetrate on foot.

Tabar: topography and general geology

Tabar Island is the southernmost of the Tabar group (Figs 1, 6). It covers about 110 km^2, and consists of two high areas connected by a low-lying isthmus, forming an elongate, club-shaped structure about 20 km long from northwest to southeast. The southern area is a steep-sided volcanic cone, modified by erosion, the highest parts of which are about 600 m above sea-level (Mounts Beirari, Wanwangar, Kambari). This cone is radially incised by steep-sided valleys. Its core is deeply dissected by two major river systems: a northwestern one (Buka River), which reaches the west coast north of Tumundar village; and a larger southeasterly one (Danolango River), which occupies the eroded remnant of an old breached crater, and which reaches the southeast coast at Banesa village. The northern part of Tabar covers less than half the area of the southern part. It is a relatively low-lying region of irregular topography, most of which is less than 200 m above sea level, but part of which, in the north, rises abruptly to a prominent peak called Mount Soraramba (526 m above sea level).

Tabar Island therefore seems to consist of two volcanic centres, about 12 km apart, which partly coalesced during their later stages of growth, forming a single unit. The composite structure was subsequently modified to

its present form by faulting, erosion, and explosive volcanism.

Tabar Island is thickly vegetated, except for four large plantations and limited cultivation around coastal villages. Mangrove swamps border the northern margin of the island - along Sarawere Passage, and between Kowamarara and Tumundar villages on the west coast. Raised fringing reef forms an almost unbroken belt around the coast, narrowing to less than 100 m along parts of the eastern and southern coastline (Fig. 6). The reef rarely extends more than 500 m inland, and reaches a maximum height of about 50 m between Matlik village and Banesa Bay. No palaeontological dates have been obtained, but the transgressive nature of the reef against the southern cone is consistent with a Quaternary age. The distribution of the reef is evidence that Tabar Island may have been tilted towards the southwest.

Tabar: geology of southern cone

The southern cone can be identified as a composite volcanic cone in the late 'planeze-stage' of dissection (terminology of Kear, 1957). Its central part has collapsed or has been destroyed by late-stage explosive activity and faulting, leaving a 3-5 km wide crater that is breached in the southeast. The northwestern flank of the cone is an exceptionally large planeze. Applying the scheme of Kear (1957), by which the age of a volcano can be determined empirically from its degree of dissection, and taking into account the more rapid rates of erosion in tropical regions (Blake & McDougall, 1973), a Pleistocene age can be assigned to the southern centre.

The rocks of the southern cone consist of roughly equal proportions of mafic lava flows and volcanic rudites. Dips are directed radially outwards from an area at the centre of the cone, and generally decrease from about 30° to zero with increasing distance from the centre of the cone. These observations are consistent with the southern cone being the remnant of a central-type stratovolcano. The lava flows also extend northwestwards onto the narrow central part of the island, where they are largely covered by reworked volcanic rudites.

Moderately well-consolidated rudaceous deposits mantle much of the middle and lower flanks or the southern cone. Rounded and sub-angular clasts, ranging from 2 cm to 1 m across, are embedded in a fine-grained matrix of the same composition. The rudites are reworked at the centre of the island, and are horizontal or have dips of only a few degrees. About 1 km up the Buka River, the rudites have an abrupt contact with a 6-m thick succession of finely bedded tephra. According to Dampier Mining (1974), these beds are as thin as 4 mm and graded from fine yellow clay to particles of grey-brown ash. The

beds are horizontal.

A northwesterly trending fault runs through the centre of the southern cone, from Banesa in the east to the west coast north of Tumundar. A branch of this fault extends northwards from a point about 2 km west of Banesa. Bedrock in the lower 2 kilometres of the Danolango River, adjacent to the fault zone, is strongly weathered and fractured, up to a point where the subsidiary fault swings northwards away from the valley. There, a small, porphyritic, and somewhat altered intrusion crops out in the river bed below a waterfall. For a further 2 km upstream from this point, the bedrock is thermally altered to bluish-grey or white, and is similar in appearance to the altered rocks seen on Tatau Island. Pyrite is found in thin veins and as crystals scattered throughout this zone of alteration ('ta' in Fig. 6). The central position of the thermally altered zone within the southern cone probably means it marks the position of a former vent.

Tabar: geology of northern cone

In contrast to the southern cone, the original form of the northern volcanic complex between Fotombar Point and Sarawere Passage has been largely obscured by faulting, and possibly also by explosive volcanism (Fig. 6). A major, north-south linear fault - here called the Tabar Fault - is colinear with the west coast of the island. In the north, it cuts diagonally across the island to the northern tip, and may continue (perhaps after an off-set in Sarawere Passage) as the eastern north-trending major fault on Tatau Island; it may even continue to Simberi Island (cf. Figs 4,5). Two other prominent faults intersect the Tabar Fault and appear to converge westwards to a point west of Tiripats village, isolating the triangular-shaped pinnacle of Mount Sororamba (Fig. 6). The most southerly of these faults also intersects a low-lying area to the south, which appears to have been downfaulted along an arcuate fracture, concave to the west, that may represent an old crater.

Mount Sororamba is a sequence of interbedded lava flows and volcanic rudites that dip steeply to the southeast. They contain rare cognate xenoliths consisting mainly of clinopyroxene. Mafic dykes intrude the sequence. The volcanic rocks are mainly lighter in colour than those from the southern cone, and they are generally less mafic (compare analyses in Table TB3). Four analysed samples from the southern area are mainly

transitional basalts, whereas most samples from the northern part of the island (except two quartz trachytes - see below) are trachybasalts (Table TB3, Table 5, Figs 7, 8).

The crater-like area bounded by the arcuate fault (Fig. 6) consists of thermally altered mafic rocks in which the original minerals have been replaced by epidote, sericite, and calcite. These rocks are typically pyritised, grey to white, and weathered to russet-brown. Jointing is well-developed. Mafic dykes intrude the altered rocks, and crop out along the coastal track as far as Fotombar Point. The dykes appear to be associated with small northwest-trending lineations which can be recognised on aerial photographs (Fig. 6).

The youngest feature of the thermally altered area is a Q-trachyte cumulodome, about 300 m across, that crops out in the centre of the crater-like area. The contact between the trachyte and the altered rocks can be seen near the headwaters of a small stream that starts on the northern flanks of the cumulodome and flows past the buildings of Tiripats Plantation. Sediments in this stream are distinctively cream-coloured. Chemical analyses of two Tabar trachyte samples are given in Table TB3, and a rare-earth-element pattern (Table 5) is given in Figure 18.

K-Ar radiometric dating of the trachyte gave a Pleistocene age of 0.986 $\pm$ 0.08 million years (Appendix 2). This is consistent with the empirically derived Pleistocene age for the southern centre. The trachyte is therefore thought to represent late stage volcanism in the north of the island that was synchronous with volcanic activity in the south. The younger age of the rocks of Tabar Island compared with the pre-middle-Miocene ages of rocks from Simberi and, possibly, Tatau Islands appears to indicate a southward migration of activity. The youthful appearance of the southern cone may represent a further shift of activity to the south during the middle or late Pleistocene.

No thermal activity has been observed, or reported, from Tabar Island. However, a 6-m thick deposit of soft blue clay overlying the altered rocks southeast of Tiripats Plantation (and overlying the trachyte cumulodome) resembles the thermally generated muds of Lihir and Feni Islands (see below), and may have been produced by a similar process.

Table TB1. Simberi Island

	1	2	3	4	5
SiO_2	46.6	45.0	48.7	48.2	56.2
TiO_2	0.75	1.07	0.87	0.81	0.51
Al_2O_3	12.9	15.1	16.8	17.1	19.5
Fe_2O_3	3.95	5.30	4.60	5.55	4.3
FeO	5.10	5.30	4.10	3.75	1.15
MnO	0.18	0.19	0.14	0.19	0.17
MgO	11.0	6.70	5.90	5.5	1.2
CaO	12.3	13.5	10.8	10.2	4.25
Na_2O	2.7	2.75	3.20	3.65	4.8
K_2O	1.6	0.65	1.62	2.0	4.4
P_2O_5	0.38	0.41	0.33	0.37	0.33
S	0.03	0.01	0.02	0.06	0.02
H_2O+	1.79	1.35	1.68	1.76	1.63
H_2O-	0.35	1.05	1.00	0.32	1.05
CO_2	0.25	1.35	0.20	0.05	<0.05
rest		0.34			
	99.88		99.96	99.51	99.51
O=S	0.01		0.01	0.03	0.01
Total	99.87	100.07	99.95	99.48	99.50

Trace elements	
Ba	145
Rb	10.0
Sr	1550
Zr	75
Nb	1.0
Y	16
La	18
Ce	45
Nd	24
Sc	37
V	318
Cr	132
Co	
Ni	31
Cu	101
Zn	81
Ga	17.5

1. Potassic basanite. 74400037 (also 73680045). LC879115. Boulder in stream southeast of Napekur village.
2. Sodic alkali basalt. 74400033 (also 73680041). LC909085. Lava at summit of small hill north of Pigibut Plantation.
3. Potassic ne-trachybasalt. 74400032 (also 73680038). LC842099. Lava flow in escarpment east of Maragan village.
4. Potassic ne-trachybasalt. 69400377. LC847098. Sample at southeastern boundary of Maragan Plantation.
5. Potassic hy-trachyandesite. 69400387. LC891085. Near head of Darum Creek west of Pigibut Plantation.

Table TB2. Tatau Island

	1	2	3	4	5	6	7	8
SiO_2	46.6	43.4	50.16	49.56	49.8	49.0	49.88	49.37
TiO_2	0.91	0.86	0.80	0.74	1.44	0.78	0.68	0.68
Al_2O_3	15.5	15.6	17.82	17.60	16.9	16.6	18.14	18.78
Fe_2O_3	6.7	7.45	5.81	4.99	5.90	5.15	5.40	4.83
FeO	3.95	3.75	2.65	3.35	3.20	3.30	3.32	3.26
MnO	0.19	0.19	0.15	0.16	0.21	0.17	0.19	0.19
MgO	6.75	5.95	5.13	4.95	4.50	4.30	4.21	3.72
CaO	11.6	10.8	10.31	10.52	10.3	9.50	9.75	10.04
Na_2O	2.6	1.90	3.19	3.55	3.50	3.65	3.07	4.35
K_2O	2.4	3.1	2.25	2.42	2.10	2.80	2.83	2.58
P_2O_5	0.49	0.42	0.27	0.36	0.56	0.39	0.39	0.42
S	0.03	0.06	0.02	0.07	0.02	0.13	0.02	0.08
H_2O+	1.22	2.15	0.80	0.81	0.78	1.02	1.21	1.03
H_2O-	0.54	1.6	0.68	0.45	0.86	0.54	0.70	0.21
CO_2	0.05	2.45	0.06	0.26	0.05	2.65	0.04	0.26
rest	0.35		0.30	0.33		0.43	0.41	0.33
	99.88	99.68	100.40	100.12	100.12	100.41	100.24	100.13
O=S	0.01	0.03	0.01	0.03	0.01	0.06	0.01	0.04
Total	99.87	99.65	100.39	100.09	100.11	100.35	100.23	100.09
Trace elements								
Ba	240		310	270		315	430	330
Rb	31.5		25.5	30.5		35.0	35.0	38.5
Sr	1580		1260	1580		2320	2067	1618
Zr	87		65	77		101	71	72
Nb	1.5		1.5	1.5		2.0	1.0	1.0
Y	18		18	17		15	19	18
La	16		14	15		16	17	15
Ce	38		29	36		39	36	38
Nd	22		16	19		20	20	21
Sc	31		29	25		26	18	17
V	319		276	267		259	269	253
Cr	66		56	38		51	9	16
Co			31	28			33	26
Ni	29		27	20		21	13	10
Cu	188		145	135		104	153	109
Zn	74		73	75		90	78	74
Ga	17.0		19.5	20.0		21.0	20.0	18.5

1. Potassic alkali basalt. 69400395. LB829952. Sample at summit of ridge east of Maragat Bay.
2. Potassic hy-trachybasalt. 69400412. LB872948. Sample in stream northwest of Tugitug village.
3. Potassic hy-trachybasalt. 76400008. LB811984. Clast in volcanic rudite east of Tupinaminda Bay.
4. Potassic ne-trachybasalt. 76400009. LB809982. Boulder in stream east of Tupinaminda Bay.
5. Potassic hy-trachybasalt. 74400029 (also 73680035). LB821933. Boulder in stream near eastern boundary of Kopo Plantation.
6. Potassic hy-trachybasalt. 74400027 (also 73680033). LB874945. Boulder in stream northwest of Tugitug village.
7. Potassic hy-trachybasalt. 76400016. LB862967. Boulder in stream southwest of Pekinberiu village.
8. Potassic phonolitic tephrite. 76400005. LB816934. Boulder in stream near Kopo Plantation.

continued on next frame

Table TB2 cont. Tatau Island

	9	10	11	12	13	14
SiO_2	48.59	50.9	51.3	50.3	58.0	55.02
TiO_2	0.65	0.57	0.61	0.52	0.59	0.35
Al_2O_3	18.59	18.8	18.3	19.3	17.6	19.89
Fe_2O_3	4.30	4.4	3.85	3.95	3.54	2.51
FeO	2.98	2.15	2.75	2.55	2.00	1.63
MnO	0.19	0.17	0.21	0.18	0.13	0.20
MgO	3.05	2.95	2.55	2.30	2.04	1.06
CaO	8.40	6.75	7.70	7.95	5.85	5.71
Na_2O	4.76	5.3	3.80	5.85	4.69	6.40
K_2O	3.45	3.25	3.55	4.05	2.82	4.06
P_2O_5	0.40	0.40	0.40	0.37	0.23	0.19
S	0.04	<0.01	0.03	0.27	0.06	0.40
H_2O+	3.73	3.1	1.43	1.79	0.92	1.84
H_2O-	0.61	0.42	1.21	0.24	0.13	0.25
CO_2	0.12	0.34	2.40	0.11	0.95	0.58
rest	0.34			0.37	0.26	0.34
	100.20		100.09	100.10	99.81	100.43
O=S	0.02		0.01	0.13	0.03	0.20
Total	100.18	99.50	100.08	99.97	99.78	100.23
Trace elements						
Ba	350			415	495	450
Rb	47.0			57	44.5	69
Sr	1624			1870	1050	1783
Zr	76			111	144	116
Nb	2.0			2	2.5	2.5
Y	18			19	28	22
La	19			25	16	27
Ce	42			59	32	55
Nd	22			26	16	24
Sc	12			6	14	3
V	252			195	151	119
Cr	4			10	6	1
Co	24					7
Ni	7			4	6	4
Cu	142			131	51	42
Zn	70			64	48	74
Ga	19.5			20.5	20.5	22.0

9. Potassic phonolitic tephrite. 76400023. LB869939. Boulder in stream west of Tugitug village.

10. Potassic ne-trachybasalt. 69400402. LB823941. Sample from ridge east of Kopo Plantation.

11. Potassic hy-trachybasalt. 74400026. LB806890. Lava flow near hot spring east of Sambuari Bay.

12. Potassic phonolitic tephrite. 69400404. LB823941. Sample from ridge east of Kopo Plantation.

13. Potassic hy-trachyandesite. 69400424. LB822874. Sample in stream north of Korumba village.

14. Potassic ne-trachyandesite. 76400002. LB818933. Boulder in stream east of Kopo Plantation.

Table TB3. Tabar Island

	1	2	3	4	5	6	7	8
SiO_2	48.4	47.1	49.0	49.0	50.1	50.0	46.4	51.20
TiO_2	0.73	0.80	1.18	1.50	1.00	0.93	0.73	0.87
Al_2O_3	11.8	12.3	13.8	14.2	16.1	16.8	19.5	16.84
Fe_2O_3	5.3	6.05	4.50	5.30	5.20	4.85	5.15	5.50
FeO	4.5	4.75	6.15	4.65	4.40	4.60	3.45	3.61
MnO	0.18	0.21	0.20	0.18	0.18	0.19	0.21	0.19
MgO	9.15	8.35	7.50	5.65	5.20	4.85	4.75	4.69
CaO	13.9	13.6	11.8	12.1	11.0	9.65	8.40	9.80
Na_2O	2.05	1.96	2.10	2.80	3.40	2.95	3.95	4.35
K_2O	0.72	0.87	1.70	1.38	1.94	2.90	3.00	2.21
P_2O_5	0.23	0.31	0.29	0.31	0.39	0.45	0.37	0.38
S	0.03	0.03	0.02	0.02	0.01	0.01	0.02	<0.02
H_2O+	1.58	1.88	1.08	0.68	0.27	0.83	1.38	0.23
H_2O-	1.16	1.38	0.80	1.50	0.31	0.69	0.49	0.14
CO_2	0.37	0.62	0.10	0.80	0.20	0.10	<0.02	0.06
rest	0.23	0.27		0.24		0.33	0.33	0.29
	100.33	100.48	100.22	100.31			100.13	
O=S	0.01	0.01	0.01	0.01			0.01	
Total	100.32	100.47	100.21	100.30	99.70	100.13	100.12	100.07
Trace elements								
Ba	220	370		175		500	330	325
Rb	18.5	77		23.0		36.5	60	37.0
Sr	595	795		835		1360	1560	1174
Zr	43	49		65		72	88	86
Nb	1.5	1.5		1		2	3	2.5
Y	14	13		28		18	17	19
La	6	8		12		13	18	12
Ce	14	20		28		31	37	29
Nd	9	12		16		15	19	16
Sc	38	33		30		15	19	25
V	254	270		261		239	230	249
Cr	287	200		125		62	72	44
Co								32
Ni	47	43		29		14	30	16
Cu	119	110		145		156	95	95
Zn	71	78		81		71	76	73
Ga	13.0	13.5		15.5		16.0	18.0	18.0

1. Sodic transitional basalt. 69400446. LB899710. Sample at shore of inlet at village on Dataru Plantation.
2. Sodic transitional basalt. 69400439. LB899710. Sample at shore of inlet at village on Dataru Plantation.
3. Potassic transitional basalt. 74400028 (also 73680034). LB903732. Lava flow south of Datava village.
4. Sodic transitional basalt. 74400030 (also 73680036). LB855792. Lava flow on track near Fotombar Point.
5. Potassic ne-trachybasalt. 74400034 (also 73680042). LB842840. Boulder in Cigaregare Plantation on northwestern flank of Mount Sororamba.
6. Potassic hy-trachybasalt. 74400036 (also 73680044). LB937733. Boulder near head of Danolango River.
7. Potassic ne-trachybasalt. 69400434. LB850810. Sample from southeastern base of crater wall southeast of Tiripats Plantation.
8. Potassic ne-trachybasalt. 76400029. LB839843. Boulder in Cigaregare Plantation on northwestern flank of Mount Sororamba.

continued on next frame

Table TB3 cont. Tabar Island

	9	10	11
SiO_2	50.4	67.95	68.5
TiO_2	0.95	0.23	0.30
Al_2O_3	16.0	17.20	16.3
Fe_2O_3	8.60	1.44	1.46
FeO	1.94	0.40	0.46
MnO	0.18	0.04	0.04
MgO	4.40	0.44	0.42
CaO	9.80	0.74	0.55
Na_2O	3.20	6.76	5.95
K_2O	2.20	4.18	4.85
P_2O_5	0.39	0.01	0.01
S	0.02	0.03	0.02
H_2O+	0.64	0.57	0.29
H_2O-	1.14	0.15	0.33
CO_2	0.05	0.01	0.10
rest	0.26	0.20	
	100.21	100.35	99.58
O=S	0.01	0.01	0.01
Total	100.20	100.34	99.57
Trace elements			
Ba	295	340	
Pb	37.5	68	
Sr	930	910	
Zr	79	164	
Nb	1.5	7.5	
Y	22	8	
La	13	7	
Ce	30	12	
Nd	18	9	
Sc	29	3	
V	262	70	
Cr	67	8	
Co		4	
Ni	22	5	
Cu	109	12	
Zn	75	20	
Ga	18.5	24.0	

9. Potassic hy-trachybasalt. 74400035 (also 73680043). LB880794. Lava flow in stream northeast of Fotombar Point.

10. Potassic Q-trachyte. 76400028. LB845815. Boulder from stream east of Tiripats Plantation.

11. Potassic Q-trachyte. 74400031 (also 73680037). LB845815. Lava from cumulodome east of Tiripats Plantation.

Table 5. Additional trace-element data for 8 rocks from Tabar Islands determined by spark-source mass spectrography

	TB1/1	011[a]	TB2/3	TB2/12	TB3/4	TB3/6	TB3/7	TB3/10
Cs	0.50	0.40	0.31	1.2	0.08	1.6	n.d.[b]	0.47
Pb	4.8	8.5	7.9	5.8	13	40	6.5	9.7
La	17.4	14.7	12.2	26.4	8.51	14.3	14.7	6.61
Ce	42.1	32.9	24.7	56.8	21.5	31.0	33.8	10.0
Pr	5.87	4.33	3.44	6.80	2.99	4.34	4.52	2.00
Nd	25.9	19.4	16.7	27.7	15.3	21.2	21.8	8.17
Sm	5.75	4.35	3.83	5.83	3.90	4.53	4.87	1.70
Eu	1.64	1.31	1.16	1.69	1.24	1.45	1.68	0.50
Gd	4.33	3.38	3.43	4.97	4.11	4.35	4.92	1.33
Tb	0.58	0.53	0.51	0.65	0.62	0.62	0.73	0.20
Dy	2.92	3.18	3.05	3.27	3.63	3.47	3.77	1.17
Ho	0.56	0.62	0.64	0.66	0.79	0.76	0.68	0.26
Er	1.34	1.67	1.68	1.80	2.24	1.96	1.70	0.82
Tm	0.16	0.23[c]	0.21	0.30[c]	0.30[c]	0.29[c]	0.28[c]	0.14
Yb	1.11	1.63	1.49	2.05	2.07	2.01	1.94	1.14
Lu[c]	0.17	0.25	0.23	0.32	0.32	0.31	0.30	0.18
Th	1.10	1.56	1.52	3.05	0.54	0.94	1.20	3.23
U	0.82	1.38	0.61	2.41	0.39	0.71	0.89	3.10
Hf	2.04	1.90	1.90	2.58	1.54	1.94	2.27	4.25
Sn	0.77	0.95	0.67	0.96	0.96	1.2	1.0	0.57
Mo	0.51	0.76	n.d.	1.5	0.52	1.5	0.65	n.d.

a. Sample 011 from Tatau Island not analysed for major elements by conventional methods, and hence not listed in Tables TB1 to FN2. Collected downstream from sample TB2/3. Grid reference: AB807982. BMR registered number: 76400011. Electron-microprobe analysis of fused sample gave following results: SiO_2 50.6%, TiO_2 0.72%, Al_2O_3 17.8%, FeOt 8.43%, MgO 5.50%, CaO 11.0%, Na_2O 3.35%, K_2O 2.34%, P_2O_5 0.20%. Sample is therefore slightly more mafic than TB2/3.

b. n.d.: not determined.

c. Interpolated value.

Table 6. Summary of mineral compositional data for the Tabar Islands.

Sample	Clinopyroxene	Amphibole	Olivine
Lavas:			
TB1/1	diopside/Al-salite/salite	magnesiohastingsite	Fo_{92-73}
TB2/3 host	salite/augite	magnesiohastingsite	
TB2/3 incl.	salite/augite	magnesiohastingsitic hornblende/edenitic hornblende	
TB2/9	Al-salite/salite	magnesiohastingsite	
TB3/3	salite/augite		Fo_{68}
TB3/10		magnesiohastingsite/actinolite/magnesioarfvedsonite	
TB3/11		actinolite/magnesioarfvedsonite/magnesioriebeckite	
Cumulates:			
TB2/15 host	salite	magnesiohastingsite	
incl.	salite	magnesiohastingsite	
TB2/16	Al-salite/salite	magnesiohastingsite	
TB2/17	salite	magnesiohastingsite	
TB2/18	Al-salite/salite	magnesiohastingsite	
TB2/19	diopside/salite	magnesiohastingsite	
TB2/20	Al-salite/salite	magnesiohastingsite	

	Biotite	Oxide	Feldspar	Feldspathoid	Other
Lavas:					
TB1/1		chromite/mt	$An_{75}-Or_{81}$		
TB2/3 host	Mg_{77-50}	mt	$An_{89}-Or_{53}$	haüyne	zeolite
TB2/3 incl.		chromian-mt/mt	$An_{25}-Or_{55}$		opx (Mg_{77-66}), zeolite
TB2/9	Mg_{74-64}	mt	$An_{82}-Or_{62}$		apatite, analcite, zeolite
TB3/3		mt	An_{91-45}, Or_{4-60}		zeolite
TB3/10	Mg_{60}	exsolved mt	$Ab_{95}-Or_{91}$		silica mineral
TB3/11	Mg_{58}	exsolved mt	$Ab_{87}-Or_{43}$		silica mineral
Cumulates:					
TB2/15 host	Mg_{80-77}	mt	$Ab_{60}-Or_{76}$		apatite
TB2/15 incl.	Mg_{80-77}	mt	$An_{55}-Or_{57}$		
TB2/16		mt	$An_{86}-Or_{55}$		
TB2/17		spinel/mt	An_{92-88}		apatite, sulphide (po)
TB2/18		mt	An_{92-88}		calcite, sulphide (po)
TB2/19	Mg_{77-75}	chromian-mt/mt			apatite, calcite, zeolite
TB2/20	Mg_{70-67}	mt	An_{86-56}		apatite, analcite, zeolite

Abbreviations. incl.: inclusion; Fo: forsterite; mt: magnetite; An: anorthite; Ab: albite; Or: orthoclase; opx: orthopyroxene; po: pyrrhotite.

Slash between two mineral names refers to compositional continuity (solid solution) between the minerals.

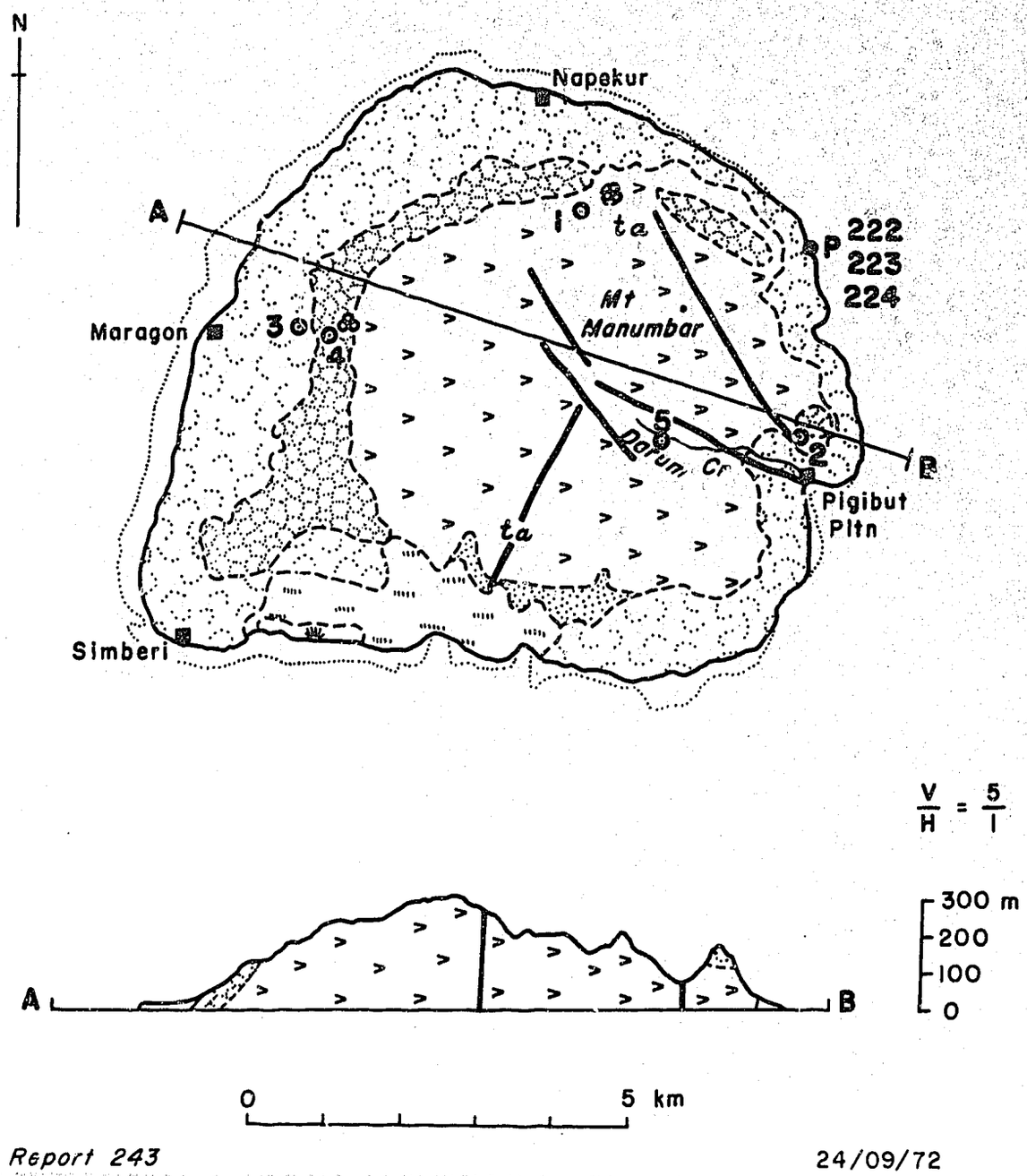

Figure 4a. Geology of Simberi Island, Tabar Islands (see legend in Fig. 2).

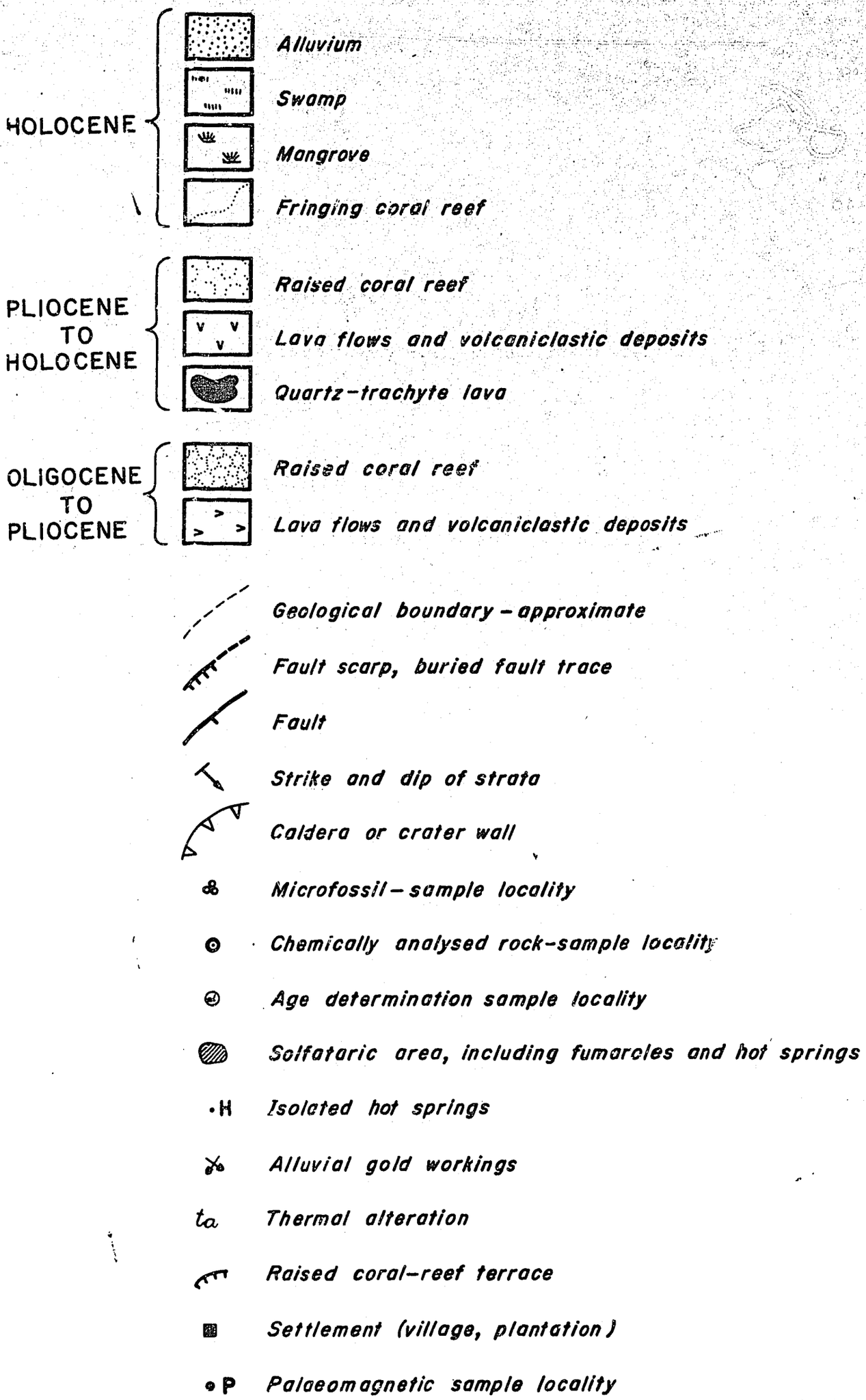

Figure 2. Legend to geological maps (Figs 4-6, 9, 12, 15).

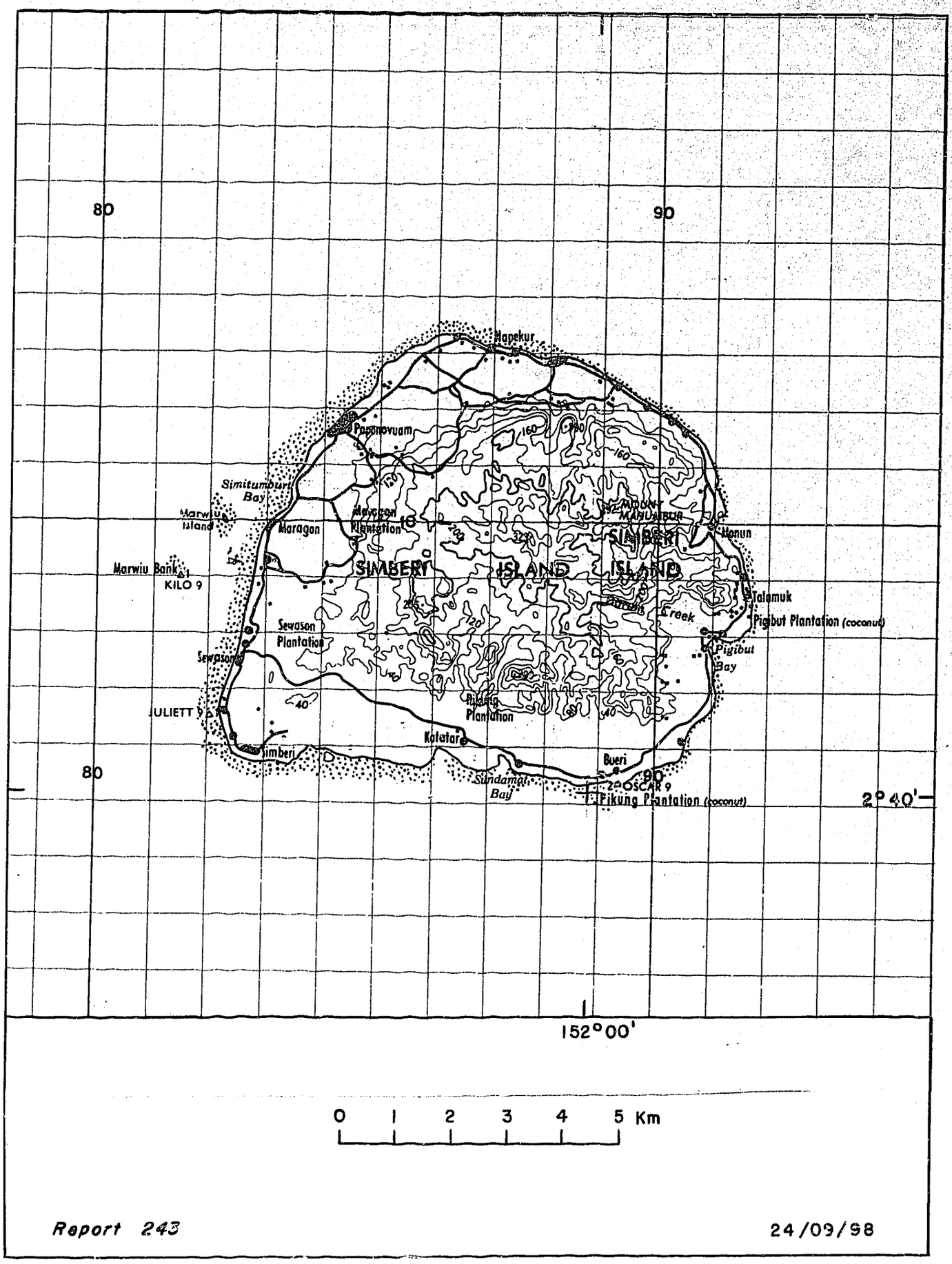

Figure 4b. Topography of Simberi Island, Tabar Islands.

Part of Sheets 9292 and 9392 (Edition 1) Series T601, Papua New Guinea 1:100 000 Topographic Survey, reproduced by permission of the Surveyor General, Department of Lands and Surveys, Papua New Guinea.

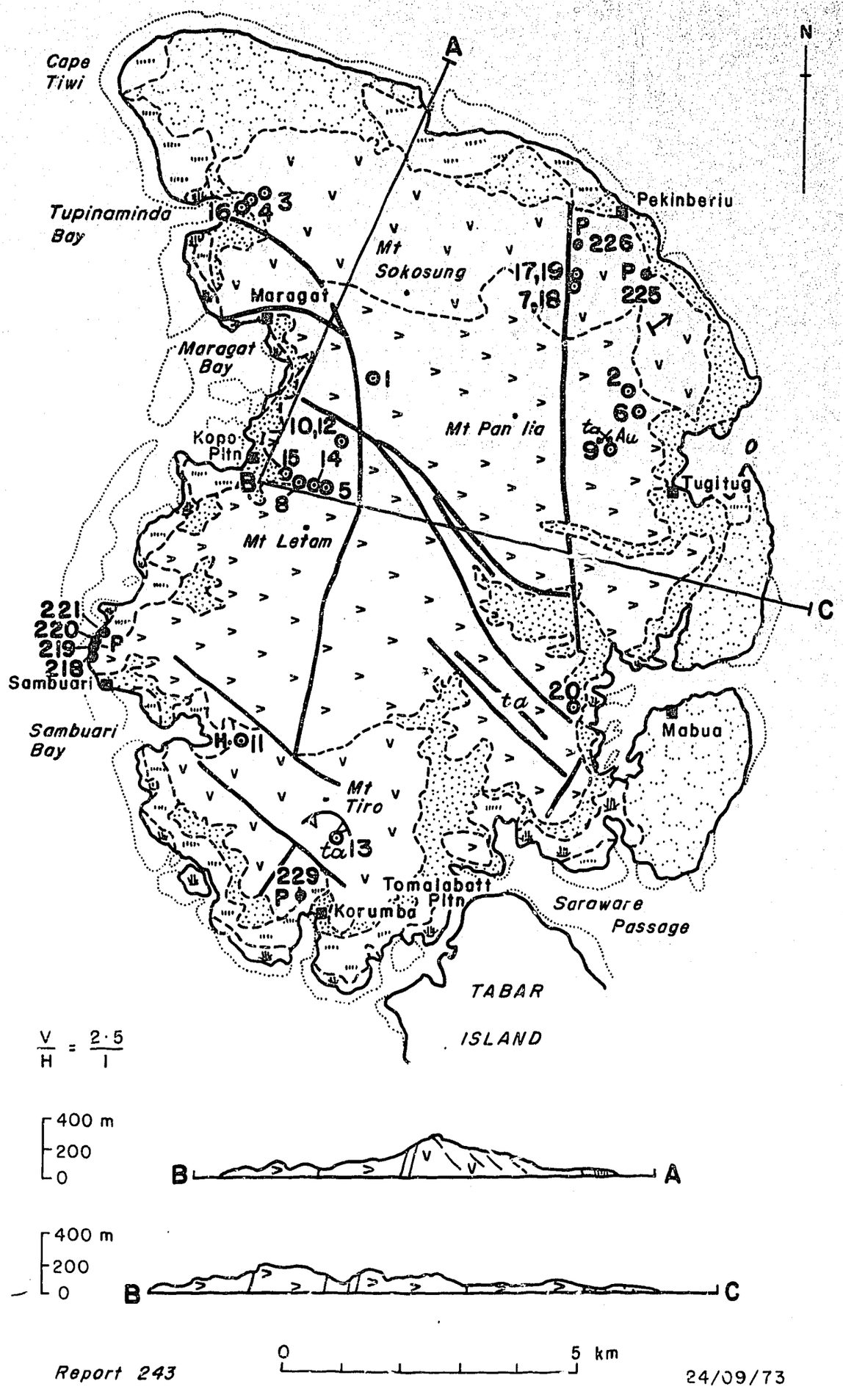

Figure 5a. Geology of Tatau Island, Tabar Islands (see legend in Fig. 2).

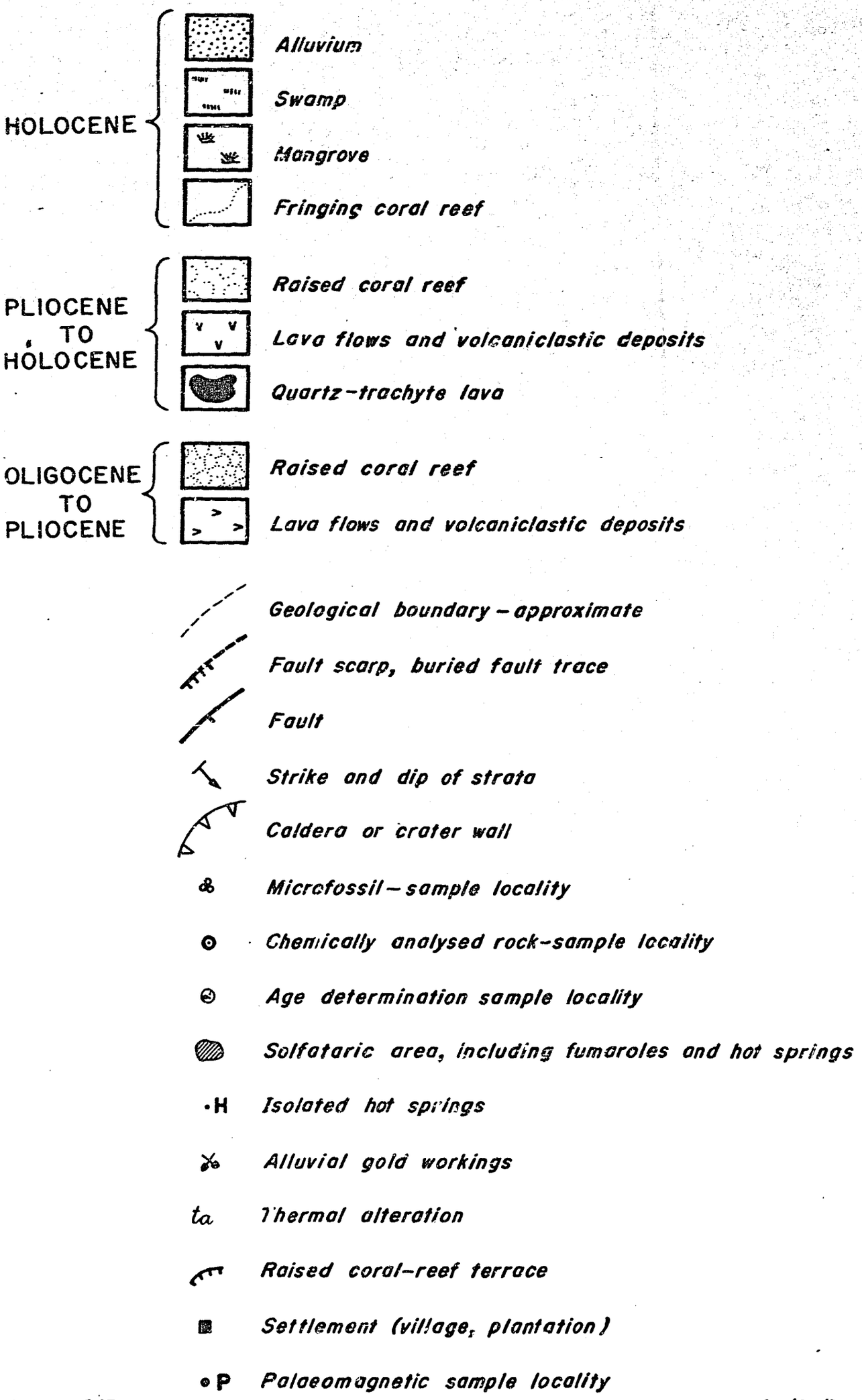

Figure 2. Legend to geological maps (Figs 4-6, 9, 12, 15).

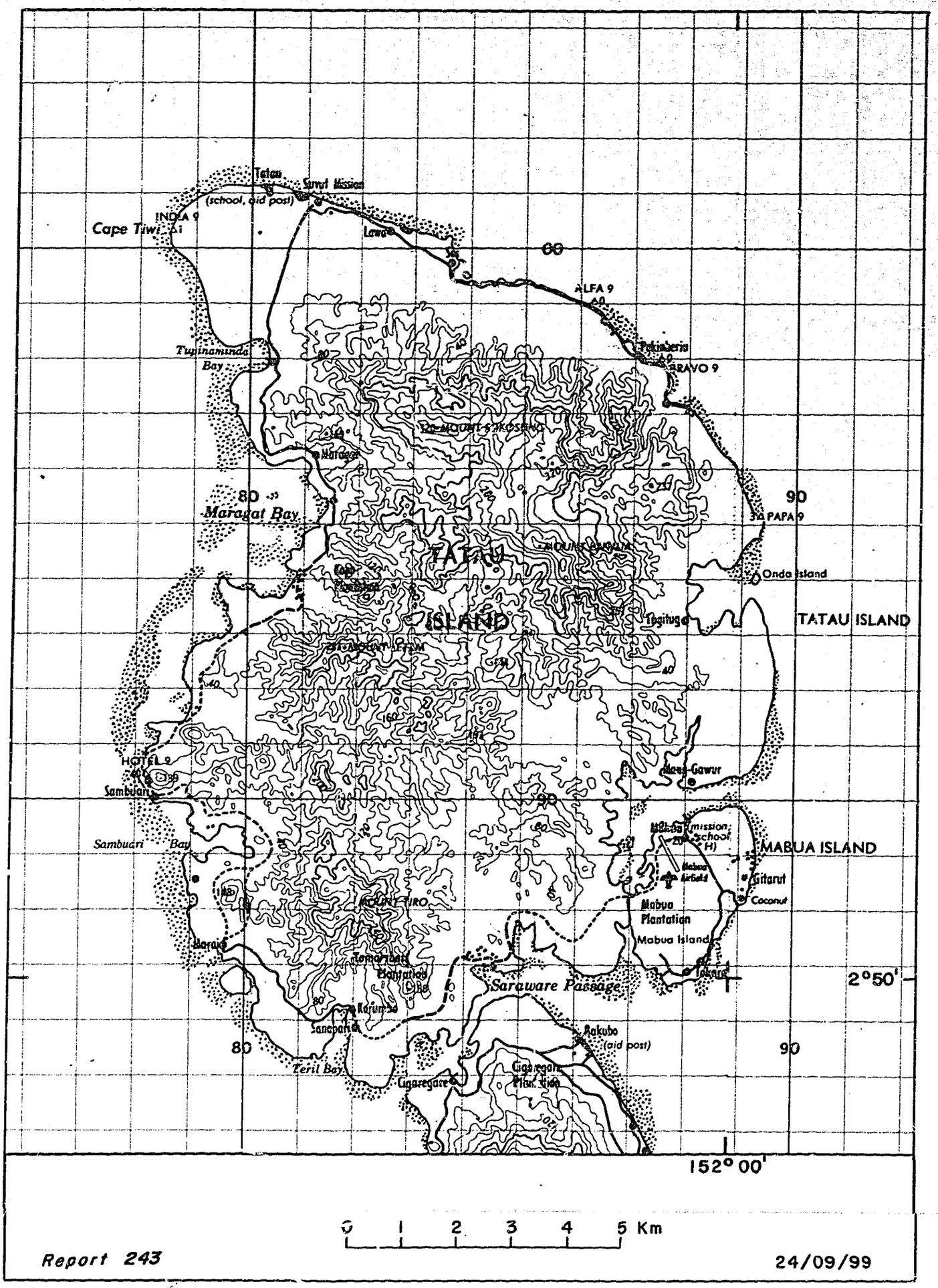

Figure 5b. Topography of Tatau Island, Tabar Islands.

Part of Sheet 9292 (Edition 1) Series T601, Papua New Guinea 1:100 000 Topographic Survey, reproduced by permission of the Surveyor General, Department of Lands and Surveys, Papua New Guinea.

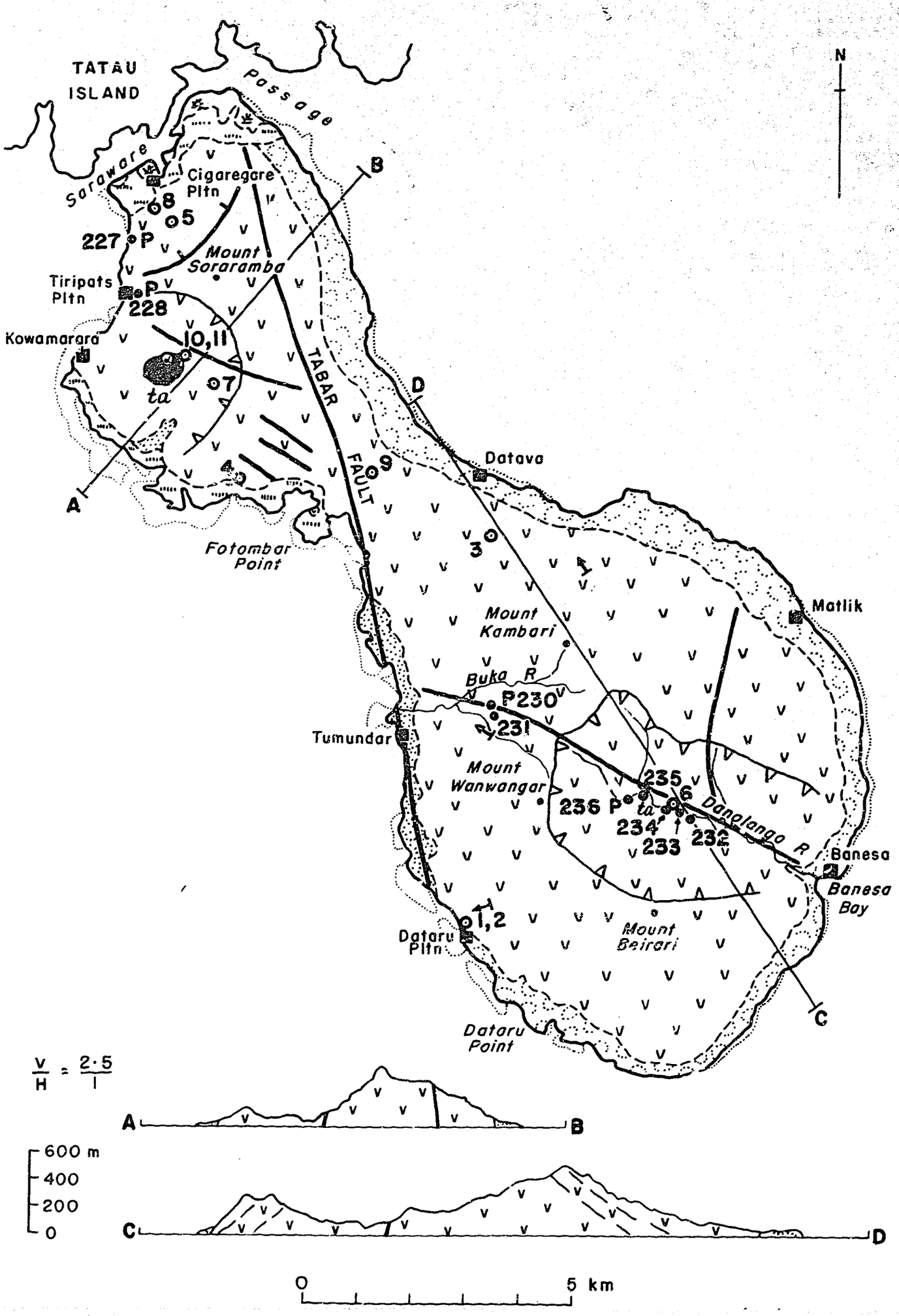

Figure 6a. Geology of Tabar Island, Tabar Islands (see legend in Fig. 2).

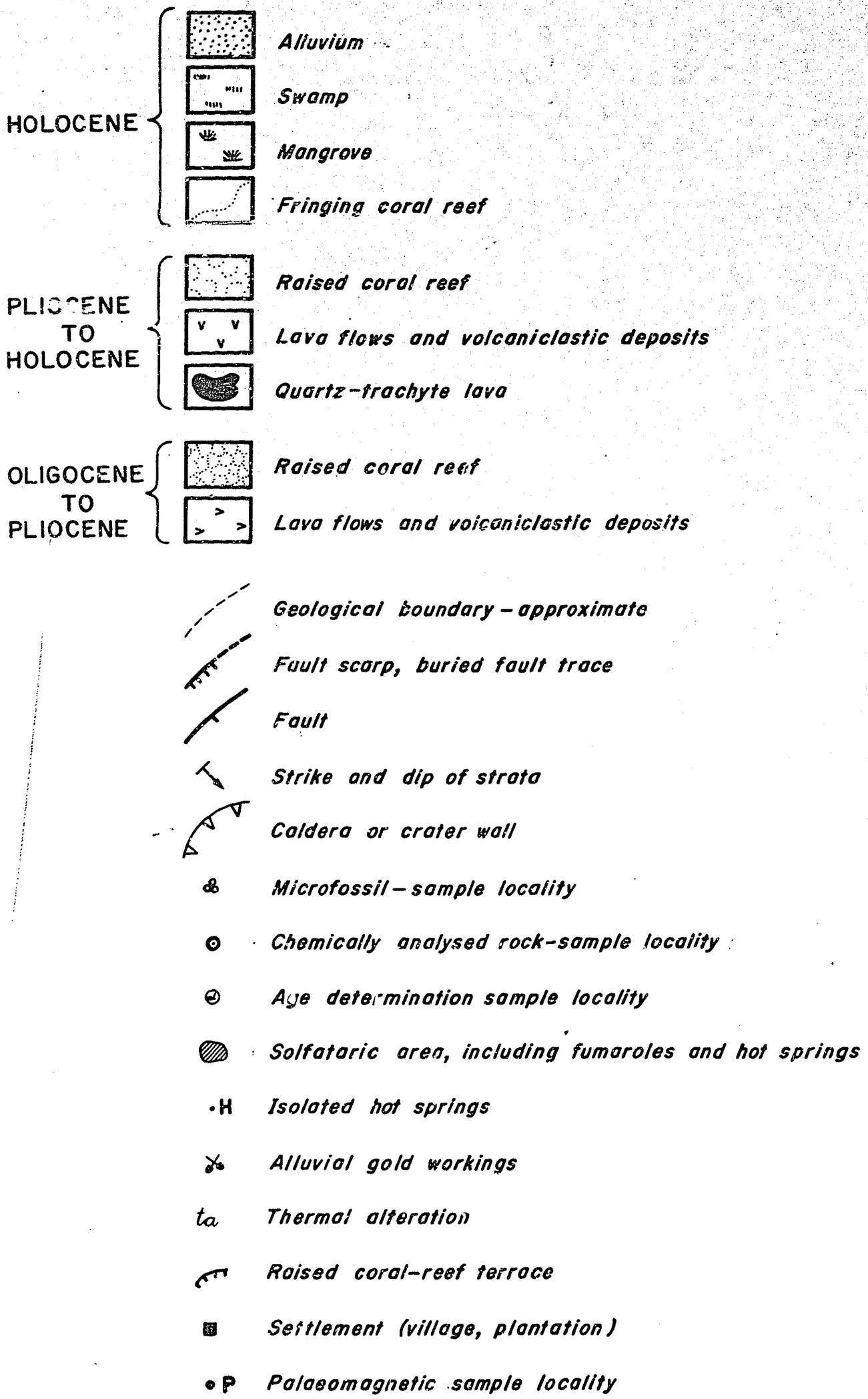

Figure 2. Legend to geological maps (Figs 4-6, 9, 12, 15).

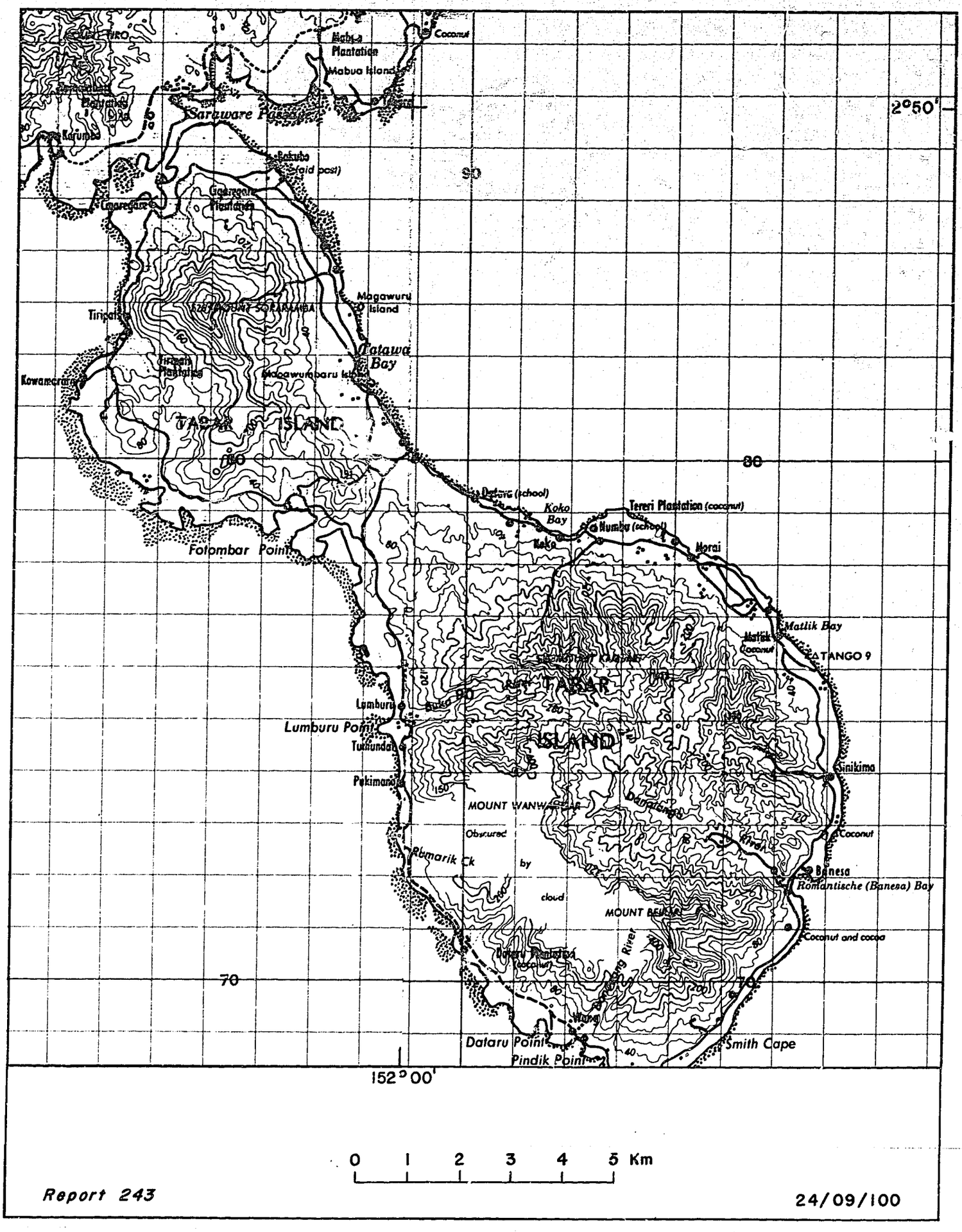

Figure 6b. Topography of Tabar Island, Tabar Islands.

Part of Sheets 9292 and 9392 (Edition 1) Series T601, Papua New Guinea 1:100 000 Topographic Survey, reproduced by permission of the Surveyor General, Department of Lands and Surveys, Papua New Guinea.

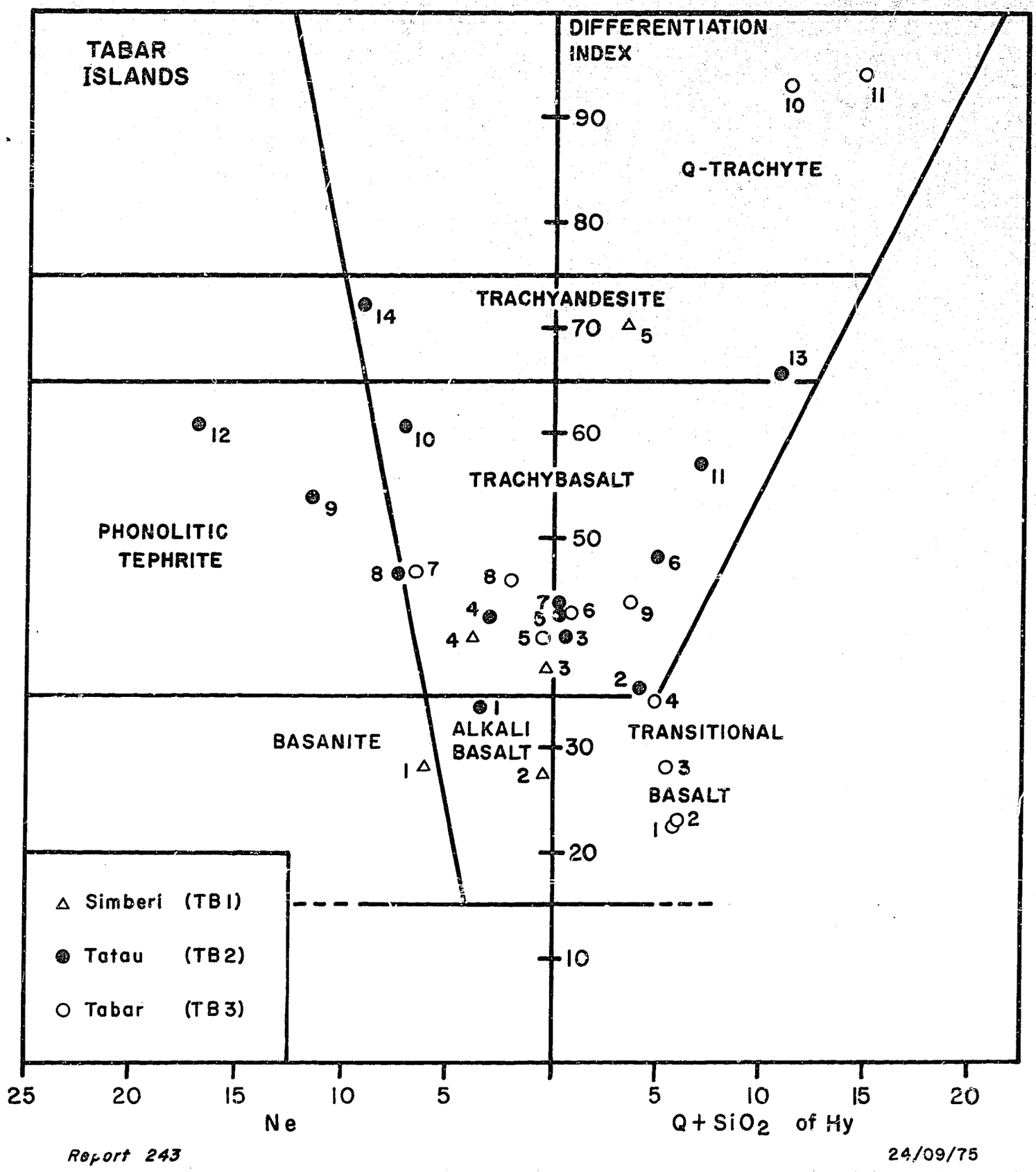

Figure 7. Rock-nomenclature diagram for rocks from the Tabar Islands (see Fig. 3). Chemical analyses listed in Tables TB1-3.

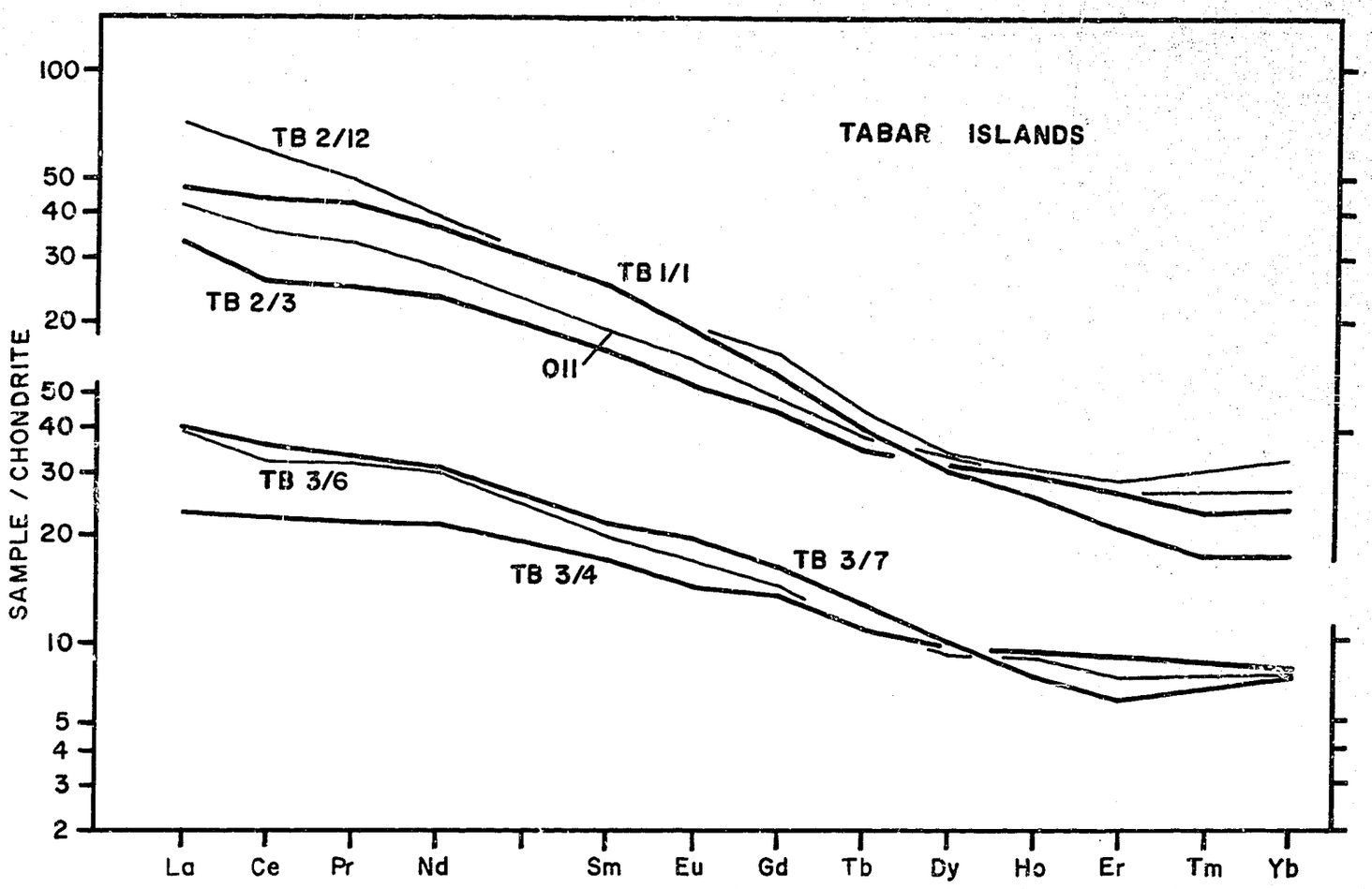

Figure 8. Chondrite-normalised REE abundances in seven rocks from the Tabar Islands (see also Fig. 18). Data listed in Table 5. Chondrite normalising values and those used in Figures 11, 14, 17, 18 are as follows: La 0.367, Ce 0.957, Pr 0.137, Nd 0.711, Sm 0.231, Eu 0.087, Gd 0.306, Tb 0.058, Dy 0.381, Ho 0.085, Er 0.249, Tm 0.036, Yb 0.248

LIHIR GROUP

Introduction

The Lihir Group of islands (152°40'E, 3°10'S) consists of the main island of Lihir, the nearby islands of Mali and Sanambiet, and the smaller islands of Masahet and Mahur to the north (Fig. 9). The group is almost midway between the Tabar and Tanga groups, and is about 50 km east of New Ireland. Lihir is the largest island in the Tabar-to-Feni chain, covering about 190 km^2, and also has the highest population (about 5000).

Lihir is triangular-shaped, and its high and varied relief is a reflection of youthful and complex volcanic landforms. Annual rainfall is high (over 2500 mm), and the island is incised by a dense, mainly consequent, drainage network. Drainage is controlled by a sinuous north-south watershed that divides the island into four main catchment areas, the largest covering most of the western half. The average height of the watershed above sea level is about 400 m, and the two highest peaks on the island rise to just over 700 m.

Lihir is mostly covered in dense, primary, tropical vegetation, except along the low-lying cultivated coastal margin, where most of the population lives. In addition to indigenous subsistence agriculture, there are several cocoa and coconut plantations, the largest of which is Londolovit Plantation in the northeast. There is a serviceable airstrip suitable for light aircraft about 3 km north of Londolovit. Masahet and Mahur, 7 and 22 km, respectively, north of Lihir, are small dome-shaped islands, each covering about 8 km^2 and about 200 m high. These islands, as well as Sanambiet and Mali, are almost fully used for the cultivation of subsistence crops.

General geology

Lihir Island is a Pliocene to Holocene volcanic complex built up from several volcanoes, the oldest of which were partly destroyed by faulting and partly buried under extrusives from younger volcanoes. Coralgal reef accreted to the margins of the complex during the Quaternary. Low-temperature (less than 100°C) fumarolic activity still takes place in small, scattered solfataras that have developed around the base of a volcanic plug inside the caldera of the youngest volcano, Luise. Masahet

and Mahur Islands are the summits of raised volcanoes that are no younger than Pleistocene, and which are entirely overlaid by terraced coralgal reef limestone. Sanambiet and Mali islands are raised Quaternary reef platforms.

Five volcanic morphological units can be recognised on Lihir: the Londolovit block, the Wurtol 'wedge', and three younger volcanoes - Kuniho, Kinami, and Luise. The oldest of the units is the Londolovit block, which is the faulted, strongly dissected, northern segment of a large, mainly Pliocene stratovolcano. The Wurtol wedge is the block-faulted western remnant of a Plio-Pleistocene volcano, and the Huniho, Kinami, and Luise volcanoes are recognisable Pleistocene cones with wholly or partly preserved summit craters.

The analysed rocks are mainly trachybasalt and alkali basalt, and rocks richer in normative nepheline and of more felsic compositions are rare or apparently absent (Table LH1, Fig. 10, Table 7). Q-trachyte samples have not been analysed, but quartz trachyte may have originally made up the altered volcanic plug at the centre of Luise volcano. Most of the analysed samples have less than 50 weight percent SiO_2, and more than 5 percent MgO.

Londolovit block

The Londolovit block is a faulted, Pliocene (possibly as old as Upper Miocene) volcanic unit covering about 20 km^2 in the north of Lihir Island (Fig. 9). The block consists of the oldest exposed strata on the island, and is unconformably bounded to the southwest and south by Huniho volcano and the Wurtol 'wedge', respectively, and to the north by a narrow fringing belt of raised Quaternary coralgal limestone.

The block is a 350-m thick sequence of northerly dipping mafic lavas and volcaniclastic rocks, overlying a poorly exposed ankaramitic basement. The block is an immaturely eroded volcanic landform, whose four main river systems have cut back deeply almost to its southern boundary, so creating a rugged, highly dissected terrain of broad headwall valleys and subsequent drainage. Several northwest-trending faults intersect the block, and a larger easterly striking fault, mostly concealed under Pleistocene volcanic rocks, defines its southeastern margin.

The upper to middle lithologies of the block are mafic lava flows, averaging about 10 m in thickness, that alternate with lithic-tuff breccias, volcarenites, lahars, and conglomerates. Primary volcanic horizons thin out northwards where they give way to a thick basal pile of laharic deposits,

bedded tuff, and conglomerate. Lahar deposits and tuff beds are best exposed within a 1-km belt of low relief between the raised Quaternary limestone and the elevated rugged terrain at the northern margin of the block. The upper parts of the Londolovit pile are transgressive to sub-littoral Lower Pliocene foraminiferal limestones. Londolovit lavas are weathered, zeolitised and, in places, lateritised, reflecting their Tertiary age. Steep waterfalls are developed in stream courses where lava flows crop out and overlie less resistant, undercut rocks.

The lahar deposits are typically an unsorted, structureless mélange of volcanolithic blocks and clasts within a highly weathered clayey matrix. In contrast, the tuff deposits are well sorted, laminated beds, consisting of winnowed, fine-grained aggregates of airfall crystal and volcanolithic particles. Some ashfall and laharic strata along the northern base of the Londolovit block underlie coralgal limestone and back-reef sediments. Calcareous volcarenites and tuffs, exposed in natural caves developed under Pleistocene limestone about 2 km east of the airstrip, include abundant Pliocene planktonic foraminiferal assemblages that provide the only positive evidence for the age of the Londolovit block (Gallasch, 1974; Appendix 1).

The ankaramitic basement of the Londolovit block is partly exposed in a stream near the western boundary of Londolovit Plantation. It consists of massive, jointed, and weathered lava, which, near the plantation boundary at least, is partly overlaid by thin, grey, pyritised, hydrothermally derived clays. Pyritised clay is also present along major joint planes, striking 240^{o} and 320^{o}, in the basement.

Wurtol wedge

Wurtol wedge is a collective term for three contiguous fault blocks that form a narrow arcuate unit extending obliquely for about 12 km across the centre of the island (Fig. 9). These blocks are lithologically related, and have morphological characteristics by which they can be identified as segments of the western flanks of a large Plio-Pleistocene volcano. This volcano was largely destroyed by faulting, and its remnant partially buried under products from the younger Luise, Kinami, and Huniho volcanoes. The Wurtol 'wedge' in the north unconformably overlies the mid-Tertiary

Londolovit block along a boundary roughly coincident with the Londolovit River.

The wedge is a 500-m thick, westerly dipping sequence of interbedded mafic lava flows, tephra, and lahars, typical of a stratovolcano. The bulk of the original structure appears to have foundered along a major north-northeast-trending fault, whose east-facing scarp forms the eastern boundary of the Wurtol 'wedge'. This fault was later cut, and the scarp discontinously offset, by two east-northeast-trending faults that segmented the wedge into the three blocks, downthrown to the south (Fig. 9).

Although deeply dissected, the present topography of the wedge retains an overall fan-shaped symmetry whose 'late-residual' stage of erosion (Kear, 1957) may be evidence that the volcano is no older than Pliocene. Taking into account the dip of the strata, the area covered by the flank remnant, and assuming a symmetrical cone shape, we judge the original structure to have been a well-developed, mature stratovolcano. Its basal diameter would have been about 15 km, and its vent would have been close to that of Luise volcano.

Kinami volcano

Kinami volcano covers about 25 km^2 in the south of Lihir, and is a strongly faulted stratovolcano that disconformably bounds the Wurtol wedge to the west and the older part of Luise volcano to the north. Kinami is cut by both north-south and east-west striking faults, which have disrupted most of original structure, except for the northern flanks and part of a summit crater. A major north-trending, east-facing fault scarp, coincident with the present-day coastline, represents the foundering of part of the eastern flank of Kinami volcano. Further north, between Libuko and Luise Harbour, this fault trace appears to be partly concealed under the eastern flank of Luise volcano, but it may continue below sea level parallel to the coastline north of Luise Harbour.

The volcano consists mainly of lava flows, tuff breccias, and agglomerates, together with minor unconsolidated tephra and derived detrital deposits. Sampled lavas include phonolitic tephrite, which, in common with many of the Lihir Island samples, is markedly rich in clinopyroxene phenocrysts, some in large cumulated aggregates. Tuff breccias and agglomerates are found most commonly as thick valley-fill deposits from which

large detached erratics have accumulated in stream beds.

The dominant landform within the strongly faulted area in the south and southeast is a sheer-sided spine, over 700 m high, which extends southwards from the crater scarp. In contrast, the undisrupted northern flanks of the volcano are radially symmetrical relative to the crater and are eroded to the planeze stage. This erosional immaturity is consistent with a volcano of Pleistocene age.

The fault scarp on the eastern side of the Wurtol 'wedge' appears to have acted as a barrier to west-flowing Kinami lava flows, causing them to build up against the scarp wall and diverting them north and south. The southern part of Luise volcano was also a barrier, and the two volcanoes coalesced, forming a prominent 450-m high saddle at their boundary.

Huniho volcano

Huniho volcano makes up the northwestern corner of Lihir. It is a 700-m high stratovolcano containing twin summit craters. A smaller adventive cone, 450 m high, rests on the flank of the main cone, 3 km southeast of the summit. Huniho volcano is similar in size to Kinami volcano, but is more completely preserved. The volcano partly overlies the Londolovit block to the northeast, and overlaps the Wurtol wedge along a boundary marked by the Londolovit and Kunidolam Rivers. The outer margins of the volcano to the north and west are overlaid by the narrow belt of Quaternary coralgal limestone that extends round the coastline of the island.

In contrast to Luise and Kinami volcanoes, which are predominantly made up of lava flows and tuffs, Huniho volcano is built up to a greater extent from poorly consolidated volcanoclastic deposits. These are laid down as a thick heterogeneous cover of tephra and lahars on the outer flanks of the cone, overlying a relatively smaller inner core of mafic lavas, indicating that the later stages of activity were primarily explosive and accompanied by little or no effusion of lava flows.

A 10-m thick semi-consolidated ash sequence at Gosmaium on the western flank of Huniho is built up from a sub-horizontal series of laminated beds, ranging from several centimetres to about one metre thick. The overall fine grain size throughout the sequence is consistent with derivation from a distant volcanic centre. Minerals identified microscopically from ash beds are feldspar, clinopyroxene, opaque oxides, green

amphibole, and biotite. The presence of amphibole and biotite may be of significance, in that these minerals are common in rocks of Luise volcano, 13 km to the southeast, which may have been source of the ash.

The flanks of the volcano are deeply incised by a pseudo-radial drainage system, where headward erosion and subsequent streams have cut back easily through the thick volcaniclastic cover. Erosion of the cone has also been accelerated by slumping of the unstable upper slopes. Despite its strong dissection, the youthfulness of the cone is indicated by the presence of small localised planezes and by the two well-defined summit craters, both of which retain well-preserved scarps. The larger crater is breached to the west, and is partially infilled by deposits from a smaller explosive centre, whose crater straddles the northern limb of the larger crater. The volcano is probably Pleistocene, judging by its morphology.

Luise volcano

Luise is a Quaternary stratovolcano. It has an elliptical breached caldera, 5.5 km across its long axis and 3.5 km across its short axis, and is open to the sea in the northeast at Luise Harbour. The caldera is the most prominent topographic feature on Lihir, and is the youngest and most distinctive volcanic structure. The immature landform of Luise volcano is also clearly emphasised by a youthful consequent drainage system in the early planeze stage of development.

Luise volcano rests within the remains of an older volcano that was mostly destroyed, either by faulting or collapse, and partially buried beneath products from the Luise and Kinami centres. A remnant of this older structure, including part of a crater or caldera scarp, is preserved as a prominent landform on the southern flank of Luise volcano.

The Luise caldera has a uniformly steep-sided wall that rises to 700 m above sea level, the highest point on the volcano, and gives way to an inclined floor sloping towards Luise Harbour. The caldera is uniformly elliptical, and does not have the cuspate outline of calderas thought to have formed by a series of collapses. By extrapolating the dip slope of the flanks, and assuming the former existence of a symmetrical cone, we estimate the height of the original volcano before cauldron subsidence to have been greater than 1000 m above present sealevel.

Luise volcano has undergone only minor post-caldera degradation, judging by its present landform. The flanks radiate from the caldera rim, are only moderately dissected, and form a distinct disconformable boundary along the Wurtol wedge fault scarp to the west. Like the flows of Kinami,

those from the Luise centre have ponded against the faults scarp of the Wurtol wedge near the middle of the island and have been diverted to the north and south. The continuation of the fault trace north of the scarp is concealed under Luise extrusives as far as the Londolovit River, north of which it reappears about 1 km upstream from the river mouth.

The volcano is made up of lava flows ranging between 5 and 20 m thick, together with interbedded ash breccia and tuffaceous horizons. Much of the sequence is well exposed in the inner caldera wall, to a lesser extent along the coast, but also along the lower reaches of the Londolovit River, where massive jointed lavas crop out as sheer-sided escarpments along the southern bank. The lavas range from dark and pyroxene-phyric to light and feldspar-rich, but virtually all of the chemically analysed rocks are trachybasalt (Figs. 9, 10).

Near the centre of the caldera, a massive felsic volcanic plug extends about 200 m inland from the shore of the harbour, where it terminates in a precipitous bluff. Thermal activity takes place along the margins of the plug within a series of small, patchily developed solfataras, from which heated water is discharged into Luise Harbour at scattered points along the strandline. The plug is massive, 120 m high, and fractured, and covers about 2 km^2. It has not been examined in detail, but it appears to be extensively, if not completely, hydrothermally altered to such an extent that its original chemical composition and mineralogy are obscure. Its 'felsic' composition is not clearly established, but, originally, it could have been quartz trachyte, similar to that on Tabar Island. The light-grey rock is fine-grained and highly indurated, and has a brittle fracture. Minerals identified by X-ray diffraction are alunite, potassium feldspar (possibly sanidine), pyrite, marcasite, and galena; Pb and Mo are present in trace amounts, and Cu is between 2000 and 3000 ppm (D. Barnes, personal communication, 1976). The central position of the plug within the caldera, together with high, but localised, heat flow concentrated along peripheral solfataras, clearly indicates that the plug fills a volcanic vent that still channels residual heat to the surface. Thermal emanations from an underlying magma body or cooling intrusive presumably heat up groundwater that reaches the surface by convection.

Small quantities of hydrothermally derived muds are being deposited in the solfataras, and older vegetated deposits up to 1 m thick are also found over a limited area. These light grey, generally pyritised muds - locally called 'simbawan' - are generated by the degradation of country rock with boiling, acidic, sulphate water. Where surface discharge is limited, pools are formed and a convective system established wherein the solid material is broken down both mechanically and by chemical reaction, eventually forming a glutinous suspension. A substantial amount of native sulphur is, in places, incorporated in the muds, as well as pyrite. Further details on the thermal areas and their water chemistry are given below.

The landform of Luise volcano and the thermal activity are consistent with a Quaternary age for the volcano whose last stages of activity may have taken place well within the Holocene. There are no records of eruption observations nor local legends consistent with modern activity, but there are no valid reasons to assume that volcanic activity could not take place again in the future.

Quaternary limestone and alluvium

Lihir is almost entirely bounded by a narrow belt of raised, Quaternary coralgal reef limestone. This belt is best developed on the north coast, between Huniho and Londolovit, where it forms a continuous 50-m high platform with prominent cliffs and headlands. The islands of Sanambiet and Mali, interconnected by shallow present-day reef, but separated from Lihir by 3 km of open sea, are a discontinuous eastern extension of this belt. Between the raised reef and the high volcanic interior is a narrow low-relief zone of mixed littoral arenaceous to rudaceous alluvial deposits. The raised reef is more discontinuous on the southwestern and northeastern sides of the island, cropping out mainly as headlands, and isolated stacks standing less than 40 m above sea level. These discontinuous areas correspond with major drainage outlets and the Luise Harbour thermal activity.

The raised-reef limestone consists of recrystallised, fore-reef bioherm and back-reef facies, which extend up to 3 km inland. Back-reef-facies deposits exposed at Gosmaium village are a chaotic assemblage of coralgal debris, molluscan fragments, and organic casts. The assemblage also includes lenses of littoral calcareous sediments and volcaniclastic

material. Identified benthonic microfossils are Operculina, Acervulina, and fragments of Carpentaria (Appendix 1).

Beds of littoral sediments, transgressive to back-reef facies, are rarely exposed. One such 3-m thick unit south of Luise Harbour is a horizontal stratiform sequence of unconsolidated calcilutites, made up mainly of fresh clinopyroxene and opaque oxides, and minor amounts of weathered clasts and carbonaceous material, including plant fragments and spores.

Thermal areas of Lihir Island

Thermal activity on Lihir Island is restricted to the area near the eastern coastline at Luise Harbour, where thermal pools, coastal seepages, and fumaroles - whose temperatures do not exceed 100°C - are found in two broadly defined fields about 1 km apart (Fig. 9). Descriptions of the thermal areas were given by Reynolds (1956) and Fisher (1957), based mainly on information supplied by Mr. Sciortino, formerly of Londolovit Plantation; and from September 1954 to August 1955, temperatures of the more active fumaroles were included in the monthly reports of the Rabaul Volcanological Observatory. The thermal areas were again visited in February 1973 (Wallace and Crick) and October 1974 (Wallace). Notation used here for the thermal areas is the same as that adopted by Reynolds and Fisher. Thermal area 'E' of Fisher (1957) is difficult to locate on aerial photographs, but may be the area southwest of area B.

Thermal Area A, adjacent to the beach, is about 25 m in diameter and contains a number of small bubbling hot pools. The most active pool (called the 'Roaring Spring' by Reynolds, 1956), on the northern margin of this area, is usually covered with stones by local people who use them in cooking shell-fish. Water from this spring has a temperature of 99°C, and froths up between the stones about every 30 seconds before subsiding again. No water was observed discharging from this pool in 1973-74. A slight smell of H_2S permeates the area, and is more noticeable around this particular spring. Temperatures of the nearby springs range from 81 to 95°C. Water is discharged from this area onto the beach, and, in October 1974, had a temperature of 39°C and a rate of discharge of about 0.5 l/sec. Sublimates of native sulphur encrust fragmented blocks of lava, which are extensively altered hydrothermally. Apart from the frothing pool, all the other pools were dry in 1974, and only wisps of vapour rose from small fissures inside

the area. Thermal waters seep into the bay below the high-tide mark and along several small water courses either side of area A. One stream, 200 m to the south of 'A' had, in 1974, a rate of discharge of 0.75 l/sec, a temperature of 37.5°C, and a pH of 3.4. Thermal quick-sands may be present in this area, as a local guide recounted an incident in which a man lost his life when he leaped from a canoe into shallow water and was sucked into hot sand. Thermal activity also takes place along and adjacent to small warm streams just inland from A.

Thermal area B is about 800 m southwest of A and is the largest thermal area. It consists of numerous small springs, mud pools, and sulphur encrusted fumaroles. Fumarolic emission is weak: minor gas ebullition takes place in the mud pools, and there is a smell of H_2S. Temperatures of the springs and pools range from 83 to 96°C, and fumarole temperatures from 95 to 99°C. No springs or hot pools of water were visible when this area was again visited in October 1974, although water could be heard bubbling beneath dried-up mud crusts in depressions where hot bubbling pools had been visible in 1973. Occasional wisps of vapour were escaping from small fissures and holes at temperatures of about 90°C. The smell of H_2S was pervasive and hydrothermal alteration of rock debris was extensive; sublimates and native sulphur were abundant, but no siliceous sinter was seen.

A small ridge separates area B from another thermal area about 200 m to the northeast, where the activity is confined to numerous small pools that have temperatures ranging from 45 to 80°C. Minor gas ebullition takes place in several of these pools.

Thermal areas C and D are about 1 km south of area B (Fig. 9). Area C is divided in two by a small stream. Thermal activity is similarly divided: the area to the northeast of the stream contains only hot pools, whereas the area to the southeast contains only small sulphur-encrusted fumaroles. The pools have temperatures ranging from 50 to 80°C, and are arranged linearly in a depression 50 m long by 20 m wide. The pools are placid and there is no gas ebullition. The fumaroles have temperatures ranging from 93 to 98°C, and emit minor quantities of vapour, which has a definite H_2S smell. Area D was not visited in 1973-74, but Reynolds (1956) reported that a temperature of 101°C had been measured from a fumarole there, and that the gas emitted had a faint H_2S smell.

Chemical analyses of thermal waters from areas A, B, and C are listed in Table 9 (see also Appendix 3). All samples have a low pH, but

have wide ranges of ionic concentrations. The role of meteoric water in these samples is probably considerable, as more than 2500 mm of rain falls on the island each year (Hart, 1970).

The two samples from area A (035) and B (036) are of the acid-sulphate-chloride type of White (1957). The Na/Cl value of the sample from area A (Table 10) is similar to sea-water but concentrations are low, apart from SO_4. Sea-water, possibly from seepage or spray from the nearby shore, may therefore have contributed to the chemical composition, and the high SO_4 and low pH may have been produced through the action of H_2S oxidising to form oxy-sulphur acids. The low overall ionic concentrations in this sample are consistent with superficial meteoric water being a major component. Sample 036 from area B, on the other hand, has higher concentrations of Na, Cl, and SO_4. Ionic ratios (Table 10) are different from those of sea-water, and the composition of this sample has probably been determined mainly by deep circulating meteroic waters that have become enriched in NaCl (possibly through wall-rock interactions) and acidified and enriched with SO_4 through near-surface oxidation of H_2S.

Thermal water flowing onto the beach from area A (sample L1) is similar in composition to the sample collected from area B, but ionic concentrations are less. Ionic ratios are different from those of sea-water, and have probably been formed in much the same way as the sample from area B, but diluted by superficial meteoric water. The SiO_2 content of thermal waters, that have circulated within a geothermal system can give an indication of subsurface temperatures (Fournier & Rowe, 1966), but in the case of sample L1 only a minimum subsurface temperature of 130°C can be given, because of probable dilution of its SiO_2 content by superficial meteoric water.

Sample 034, collected from a stagnant thermal pool in a mud-lined crater in thermal area C, is typical of the acid-sulphate type described by White (1957), characterised by a low pH and high SO_4 content. The low overall ionic concentrations of this sample, apart from SO_4, and the lack of disturbance or any apparent outflow from this pool, may be evidence that the water is almost entirely accumulated rainfall that has been acidified and enhanced in SO_4 by oxidised H_2S.

Table LH1. Lihir Island

	1	2	3	4	5	6	7	8
SiO_2	45.6	47.8	45.94	46.3	47.2	47.7	46.7	47.25
TiO_2	0.48	0.67	0.73	0.89	0.86	0.94	1.36	0.87
Al_2O_3	7.10	9.15	12.11	12.0	13.6	12.7	14.1	13.21
Fe_2O_3	4.85	5.40	5.19	6.05	4.70	4.70	5.75	5.33
FeO	4.25	3.45	5.72	4.55	5.65	6.40	5.15	5.56
MnO	0.17	0.15	0.21	0.19	0.20	0.20	0.19	0.20
MgO	13.8	11.3	9.05	8.80	8.70	7.65	7.45	7.39
CaO	17.4	17.2	14.65	15.2	12.9	13.3	12.9	12.87
Na_2O	0.80	1.73	2.79	1.39	1.67	2.15	2.60	3.02
K_2O	0.49	0.40	0.44	1.50	1.51	2.25	1.06	1.15
P_2O_5	0.19	0.23	0.35	0.37	0.28	0.43	0.41	0.45
S	0.07	0.02	<0.02	0.04	0.05	0.02	0.07	0.02
H_2O+	2.30	1.58	2.09	1.82	1.95	1.21	1.99	1.65
H_2O-	1.36	0.82	0.37	1.02	0.87	0.45	0.43	0.93
CO_2	0.90	0.15	0.18	<0.05	0.20	0.25	0.30	0.21
rest	0.30		0.29			0.31	0.27	0.30
	100.06	100.05		100.12	100.34	100.66	100.73	100.41
O=S	0.03	0.01		0.02	0.02	0.01	0.03	0.01
Total	100.03	100.04	100.11	100.10	100.32	100.65	100.70	100.40
Trace elements								
Ba	85		195			180	145	190
Rb	16.0		12.0			41.5	36.5	45.0
Sr	640		1175			1110	1050	1153
Zr	34		45			70	70	57
Nb	2.0		1.5			1.5	0.5	1.5
Y	9		15			17	18	18
La	6		13			12	12	14
Ce	18		28			31	27	32
Nd	9		16			18	17	18
Sc	58		47			39	35	36
V	229		208			313	287	306
Cr	800		110			200	107	147
Co			45					46
Ni	158		40			40	27	39
Cu	75		106			161	130	144
Zn	52		82			89	76	87
Ga	9.5		13.5			15.0	15.5	14.5

1. Ankaramite. 74400025 (also 73680030). MB584604. Lava flow in stream near western boundary of Londolovit Plantation.
2. Sodic alkali basalt. 69400361. MB477582. Sample near ridge east of Banam village.
3. Sodic basanite. 76400035. MB582599. Boulder in stream on western part of Londolovit Plantation.
4. Potassic alkali basalt. 69400363. MB477582. Sample near ridge east of Banam village.
5. Potassic transitional basalt. 74400022 (also 73680027). MB559503. Boulder in stream northeast of Wurtol village.
6. Potassic alkali basalt. 74400024 (also 73680029). MB579595. Lava flow in Londolovit River.
7. Sodic alkali basalt. 74400020 (also 73680024). MB592590. Boulder in stream south of Londolovit village.
8. Sodic alkali basalt. 76400037. MB581593. Block below lava flow in Londolovit River.

continued on next frame

Table LH1 cont. Lihir Island

	9	10	11	12	13	14	15	16
SiO_2	45.7	46.55	48.9	46.7	47.9	46.6	50.1	47.8
TiO_2	1.08	0.90	0.82	1.04	0.87	0.95	0.96	1.10
Al_2O_3	15.6	14.50	15.2	16.1	15.2	15.4	15.8	15.5
Fe_2O_3	5.85	5.45	5.40	5.40	5.70	6.30	5.45	5.50
FeO	4.75	6.38	5.05	5.50	5.00	5.40	4.35	5.50
MnO	0.23	0.23	0.19	0.21	0.22	0.22	0.18	0.21
MgO	6.65	6.14	6.00	5.85	5.85	5.80	5.75	5.65
CaO	12.2	12.49	11.5	12.1	12.0	11.8	9.85	11.5
Na_2O	2.55	3.11	2.65	3.05	3.40	3.60	2.80	2.60
K_2O	1.51	2.90	2.15	1.87	2.90	1.75	2.45	1.94
P_2O_5	0.41	0.55	0.35	0.54	0.53	0.60	0.36	0.36
S	0.03	<0.02	0.02	<0.01	0.02	0.02	0.02	0.02
H_2O+	2.35	0.57	1.36	1.19	0.12	1.30	0.91	1.75
H_2O-	0.95	0.19	0.70	0.32	0.20	0.36	0.75	0.65
CO_2	0.15	0.03	0.10	<0.05	0.10	0.05	0.10	0.20
rest	0.28	0.33		0.32	0.33	0.38		0.28
	100.29		100.39		100.34	100.53	99.83	100.56
O=S	0.01		0.01		0.01	0.01	0.01	0.01
Total	100.28	100.32	100.38	100.19	100.33	100.52	99.82	100.55
Trace elements								
Ba	230	265		265	270	390		175
Rb	44.5	57		128	59	59		40.0
Sr	1130	1360		1430	1440	1780		1140
Zr	93	57		74	67	65		82
Nb	2	1.5		2	2	2		1.5
Y	27	19		21	19	19		19
La	13	14		15	16	19		12
Ce	32	34		37	40	43		32
Nd	17	20		17	20	22		16
Sc	25	31		21	24	15		30
V	245	347		251	275	264		284
Cr	72	31		24	94	18		47
Co		50						
Ni	17	25		14	20	14		16
Cu	134	167		160	175	219		131
Zn	90	91		74	72	77		78
Ga	16.0	16.5		17.5	16.5	17.0		16.5

9. Potassic alkali basalt. 74400018 (also 73680022). MB518548. Lava flow in stream northeast of Lamboa village.

10. Potassic tephrite. 76400039. MB601536. Boulder in stream south of Putput No. 1 village.

11. Potassic ne-trachybasalt. 74400016 (also 73680020). MB582535. Lava at base of western wall of Luise caldera.

12. Potassic alkali basalt. 69400338. MB559462. Sample near Palie Mission.

13. Potassic phonolitic tephrite. 74400017 (also 73680021). MB589477. Lava flow in stream near base of escarpment west of Kinami village.

14 Sodic phonolitic tephrite. 74400042. MB582535. Boulder in stream at base of western wall of Luise caldera. This rock is classified as a sodic tephrite using the CIPW norm calculated volatile-free and standardising the oxidation state of iron according to the equation of Irvine & Baragar (1971) - see Johnson & others (1976, Table 1).

15. Potassic hy-trachybasalt. 69400371. MB586551. Sample near base of northwestern wall of Luise caldera.

16. Potassic transitional basalt. 74400021 (also 73680025). MB476570. Lava flow in stream south of Gosmaium village.

continued on next frame

Table LH1 cont. Lihir Island

	17	18	19	20	21	22	23	24
SiO_2	51.3	48.2	48.5	49.6	51.6	51.63	48.85	47.6
TiO_2	0.89	1.27	1.02	0.82	0.89	0.75	0.89	1.13
Al_2O_3	15.6	16.2	16.8	15.6	15.5	16.15	16.49	17.3
Fe_2O_3	4.95	6.00	5.70	3.30	5.00	4.59	4.88	5.55
FeO	3.90	5.10	4.95	6.80	4.05	4.19	5.29	4.65
MnO	0.17	0.20	0.20	0.18	0.17	0.18	0.20	0.21
MgO	5.60	5.55	5.50	5.50	5.45	5.37	4.91	4.80
CaO	9.85	11.0	11.1	10.4	10.4	9.80	10.17	11.0
Na_2O	3.15	3.00	3.10	2.95	3.25	3.32	3.03	3.85
K_2O	2.60	1.69	1.22	1.87	2.50	2.74	2.27	1.44
P_2O_5	0.35	0.39	0.43	0.35	0.35	0.35	0.36	0.63
S	0.02	0.03	0.04	0.02	0.05	<0.02	<0.02	0.04
H_2O+	0.99	1.00	0.98	1.27	0.23	0.66	1.49	1.16
H_2O-	0.69	0.60	0.58	0.71	0.41	0.19	0.66	0.62
CO_2	0.10	<0.05	<0.05	0.2	0.05	0.08	0.07	0.25
rest	0.24					0.25	0.27	
	100.40	100.23	100.12	99.57	99.90			100.23
O=S	0.01	0.01	0.02	0.01	0.02			0.02
Total	100.39	100.22	100.10	99.56	99.88	100.25	99.83	100.21
Trace elements								
Ba	225					225	265	
Pb	46.0					49.0	39.0	
Sr	905					950	1085	
Zr	79					66	60	
Nb	2.0					1.5	1.0	
Y	19					20	20	
La	11					11	11	
Ce	26					23	24	
Nd	14					14	13	
Sc	19					22	21	
V	196					224	266	
Cr	108					113	14	
Co						33	37	
Ni	32					32	16	
Cu	87					105	139	
Zn	66					68	78	
Ga	16.0					16.5	17.0	

17. Potassic hy-trachybasalt. 69400365B. MB594566. Sample near northern shore of Luise Harbour.

18. Potassic ne-trachybasalt. 69400356. MB477582. Sample near ridge east of Banam village.

19. Sodic transitional basalt. 69400343. MB559462. Sample near Palie Mission.

20. Potassic hy-trachybasalt. 71400512. MB574541. Sample at southwestern wall of Luise caldera.

21. Potassic hy-trachybasalt. 69400369. MB594566. Sample near northern shore of Luise Harbour.

22. Potassic hy-trachybasalt. 76400045. MB594572. Boulder at northern shore of Luise Harbour.

23. Potassic ne-trachybasalt. 76400041A. MB601536. Boulder in stream south of Putput No. 1 village.

24. Sodic ne-trachybasalt. 69400348. MB559467. Sample near Palie Mission.

continued on next frame

Table LH1 cont. Lihir Island

	25	26	27	28	29	30
SiO_2	49.64	49.55	46.7	49.9	53.5	50.6
TiO_2	0.99	0.91	0.81	0.97	0.57	0.73
Al_2O_3	16.91	16.66	16.1	18.0	18.2	18.0
Fe_2O_3	4.89	4.50	5.35	4.30	4.30	5.10
FeO	5.38	5.91	5.10	5.60	3.75	4.70
MnO	0.21	0.20	0.26	0.19	0.18	0.50
MgO	4.71	4.70	4.65	4.55	3.25	3.25
CaO	9.46	10.39	11.0	9.00	8.50	7.60
Na_2O	3.13	3.34	2.55	2.65	4.05	3.80
K_2O	2.33	2.28	2.40	2.55	2.60	2.45
P_2O_5	0.39	0.37	0.61	0.37	0.38	0.37
S	0.02	<0.02	0.04	0.01	0.02	0.06
H_2O+	0.96	0.86	1.69	1.37	0.50	1.10
H_2O-	0.54	0.25	1.27	0.71	0.40	0.70
CO_2	0.01	0.04	1.30	0.05	0.25	1.15
rest	0.27	0.27				
	99.84		99.83		100.45	100.11
O=S	0.01		0.02		0.01	0.03
Total	99.83	100.23	99.81	100.22	100.44	100.08

Trace elements

Ba	220	260
Rb	40.0	36.5
Sr	1021	1039
Zr	70	60
Nb	1.0	1.5
Y	24	20
La	10	10
Ce	28	27
Nd	17	14
Sc	22	25
V	285	297
Cr	11	18
Co	37	38
Ni	14	19
Cu	170	151
Zn	93	83
Ga	17.5	17.0

25. Potassic hy-trachybasalt. 76400038. MB601536. Boulder in stream south of Putput No. 1 village.

26. Potassic ne-trachybasalt. 76400041B. MB601536. Boulder in stream south of Putput No. 1 village.

27. Potassic hy-trachybasalt. 74400019 (also 73680023). MB585447. Lava flow in stream north of Linmel village.

28. Potassic transitional basalt. 71400514. MB574541. Sample at southwestern wall of Luise caldera.

29. Potassic hy-trachybasalt. 74400023 (also 73680028). MB616518. Boulder from small rise northwest of Libuko village.

30. Potassic hy-trachybasalt. 74400015 (also 73680019). MB585531. Lava flow at base of southwestern wall of Luise caldera.

Table 7. Additional trace-element data for 4 rocks from Lihir Group determined by spark-source mass spectrography

	LH1/9	LH1/12	LH1/13	LH1/14
Cs	0.58	1.1	0.76	1.0
Pb	31	7.1	45	8.8
La	10.3	15.4	17.1	18.8
Ce	24.4	36.0	42.4	42.5
Pr	3.14	4.71	4.94	6.04
Nd	15.5	21.4	24.1	27.7
Sm	4.18	5.46	5.22	6.36
Eu	1.37	1.73	1.66	1.97
Gd	4.76	5.40	5.20	6.24
Tb	0.71	0.76	0.68	0.77
Dy	4.17	4.26	3.38	3.39
Ho	0.93	0.83	0.64	0.73
Er	2.40	2.18	1.55	1.79
Tm[a]	0.31	0.30	0.26	0.24
Yb	2.17	2.06	1.68	1.70
Lu[a]	0.34	0.32	0.24	0.26
Th	0.79	1.37	1.35	1.43
U	0.56	0.83	0.94	0.89
Hf	1.98	1.87	1.63	1.83
Sn	1.0	1.1	1.3	1.1
Mo	0.64	1.0	1.3	1.1

a. Interpolated value.

Table 8. Summary of mineral compositional data for the Lihir Group.

Sample	Clinopyroxene	Amphibole	Olivine	Biotite
Lavas:				
LH1/3	diopside/Al-salite/salite	magnesiohastingsite	Fo_{87-56}	Mg_{74-58}
LH1/10	Al-salite/salite		Fo_{68-45}	
LH1/14	Al-salite/salite			
LH1/23	diopside/Al-salite/salite		Fo_{54-42}	
Cumulate:				
LH1/31	diopside/Al-salite/salite		Fo_{91-87}	Mg_{86}

Sample	Oxide	Feldspar	Feldspathoid	Other
Lavas:				
LH1/3	mt	An_{65-35}		analcite
LH1/10	mt	$An_{69}-Or_{20}$	haüyne, leucite	apatite, sulphide (po)
LH1/14	mt	An_{82-34}	haüyne, sodalite	apatite, sulphide (cpo)
LH1/23	mt	$An_{79}-Or_{64}$	———	apatite, zeolite
Cumulate:				
LH1/31	chromite/mt	An_{24}		calcite

Abbreviations. Fo: forsterite; mt: magnetite; An: anorthite; Or: orthoclase po: pyrrhotite; cpo: chalcopyrite.
Slash between two mineral names refers to compositional continuity (solid solution) between the minerals.

Table 9. Compositions of thermal waters from Lihir Island

Location	Area A		Area B	Area C	Average Ocean
	outflow 15 m inland	pool 20 m inland	pool 0.4 km inland	pool 0.8 km inland	
Sample no.	L1	035	036	034	
Collection date	10 Oct 1974	9 Feb 1973	10 Feb 1973	9 Feb 1973	
Temp. °C	39	90	83	50	
pH (20°C)	2.8	2.1	2.8	1.6	8.3
E.C. (Micro-s/cm)	3388	-	-	-	
Total dissolved solids (mg/l)	1698	-	-	-	
Al	6.7	-	-	-	0.01
Cu	0.01	-	-	-	0.003
Fe	8.33	-	-	-	1.3
Mn	0.41	-	-	-	0.002
Zn	0.29	-	-	-	0.01
As	0.1	-	-	-	0.003
Hg	0.0005	-	-	-	3×10^{-5}
Sr	0.35	-	-	-	8
Rb	0.43	-	-	-	0.12
Ca	31	34.3	36.1	8.8	400
Mg	14	19	12.1	9.5	1272
Na	495	90	2075	18.9	10600
K	63	6.5	250	17.0	380
Li	0.35	-	-	-	0.17
B	2.7	-	-	-	4.6
F	0.15	-	-	-	1.3
Cl	398	177.3	1489	70.9	18980
Br	<2	-	-	-	65
SO_4	695	840	1050	3220	2649
NO_3	2	-	-	-	
CO_3	n.d.	-	-	-	
HCO_3	n.d.	-	-	-	140
SiO_2	110	-	-	-	6.4

n.d.: not detected.

Analyses by Mines Division Laboratory (Port Moresby), except for sample L1 which was analysed by Amdel.

Table 10. Ionic ratios for thermal waters from Lihir Island

Location	Area A		Area B	Area C	
	outflow 15 m inland	pool 20 m inland	0.4 km inland	0.8 km inland	Average Ocean
Sample No.	L1	035	036	034	
Na/Cl	1.244	0.508	1.394	0.267	0.558
B/Cl	0.0068	-	-	-	0.0002
SO_4/Cl	1.75	4.74	0.71	45.42	0.14
Ca/Na	0.063	0.381	0.017	0.466	0.038
K/Na	0.127	0.072	0.120	0.899	0.036
Li/Na	71×10^{-5}	-	-	-	1.6×10^{-5}
Mg/Ca	0.5	0.6	0.3	1.1	3.2

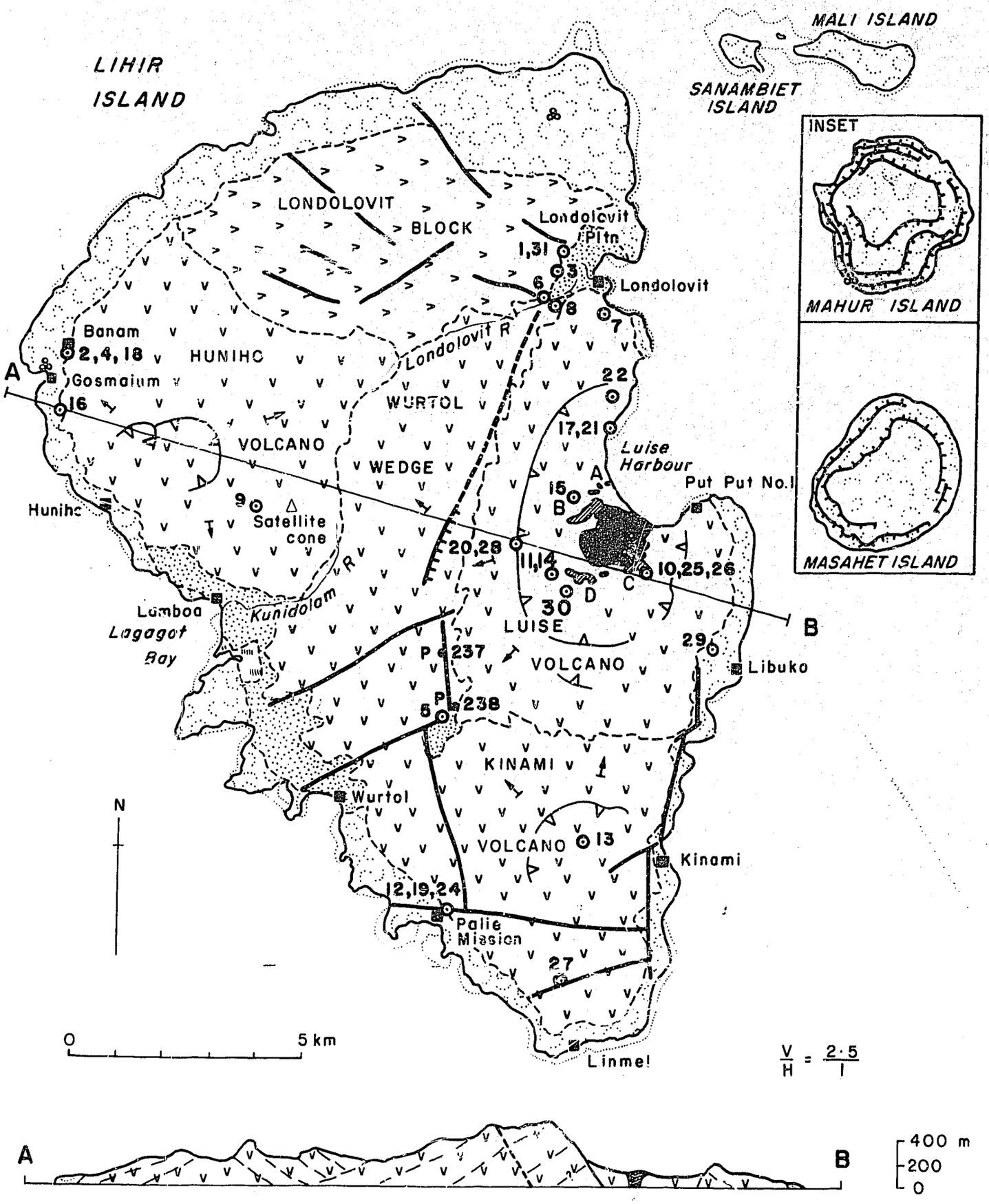

Figure 9a. Geology of the Lihir Group (see legend in Fig. 2).

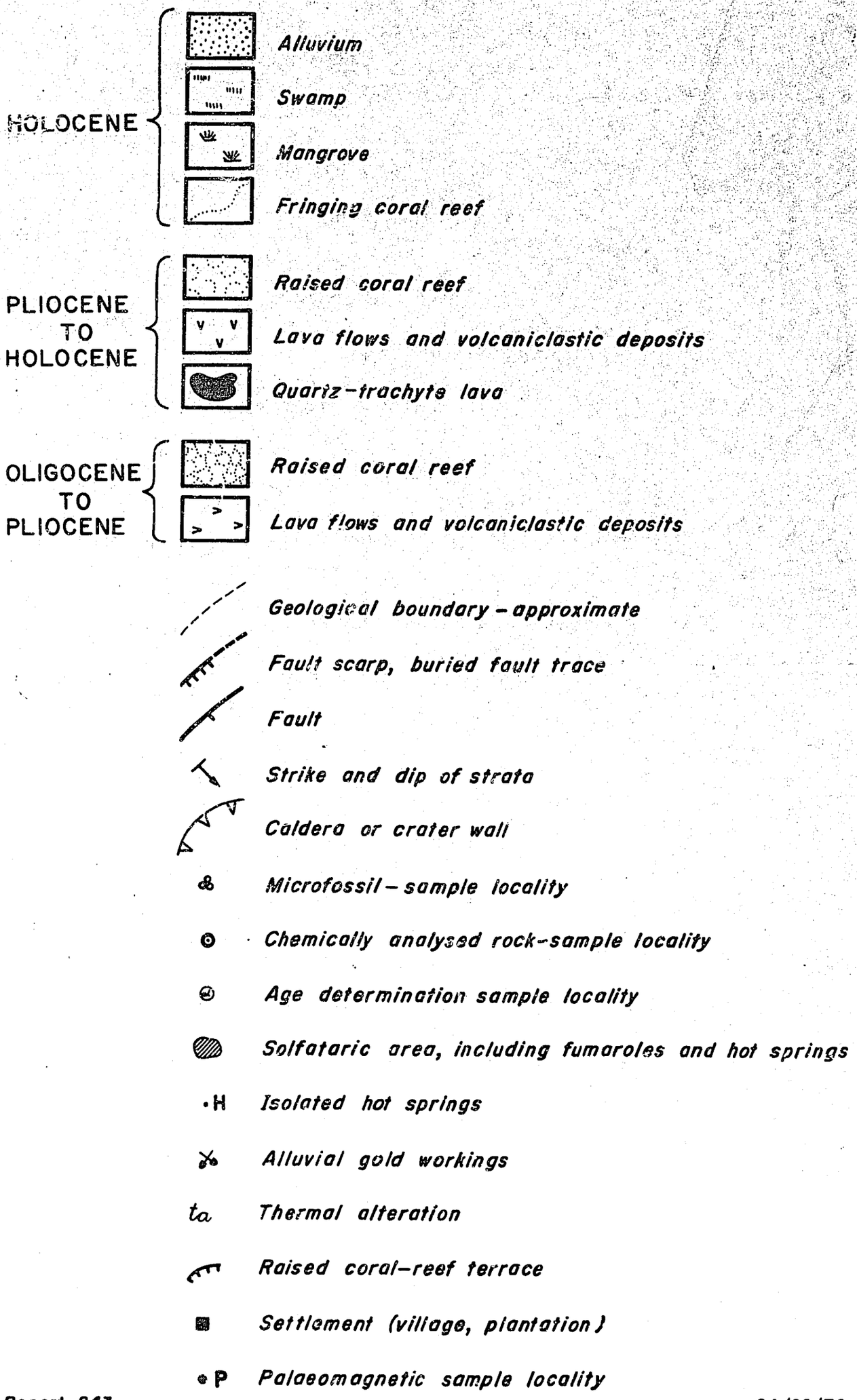

Figure 2. Legend to geological maps (Figs 4-6, 9, 12, 15).

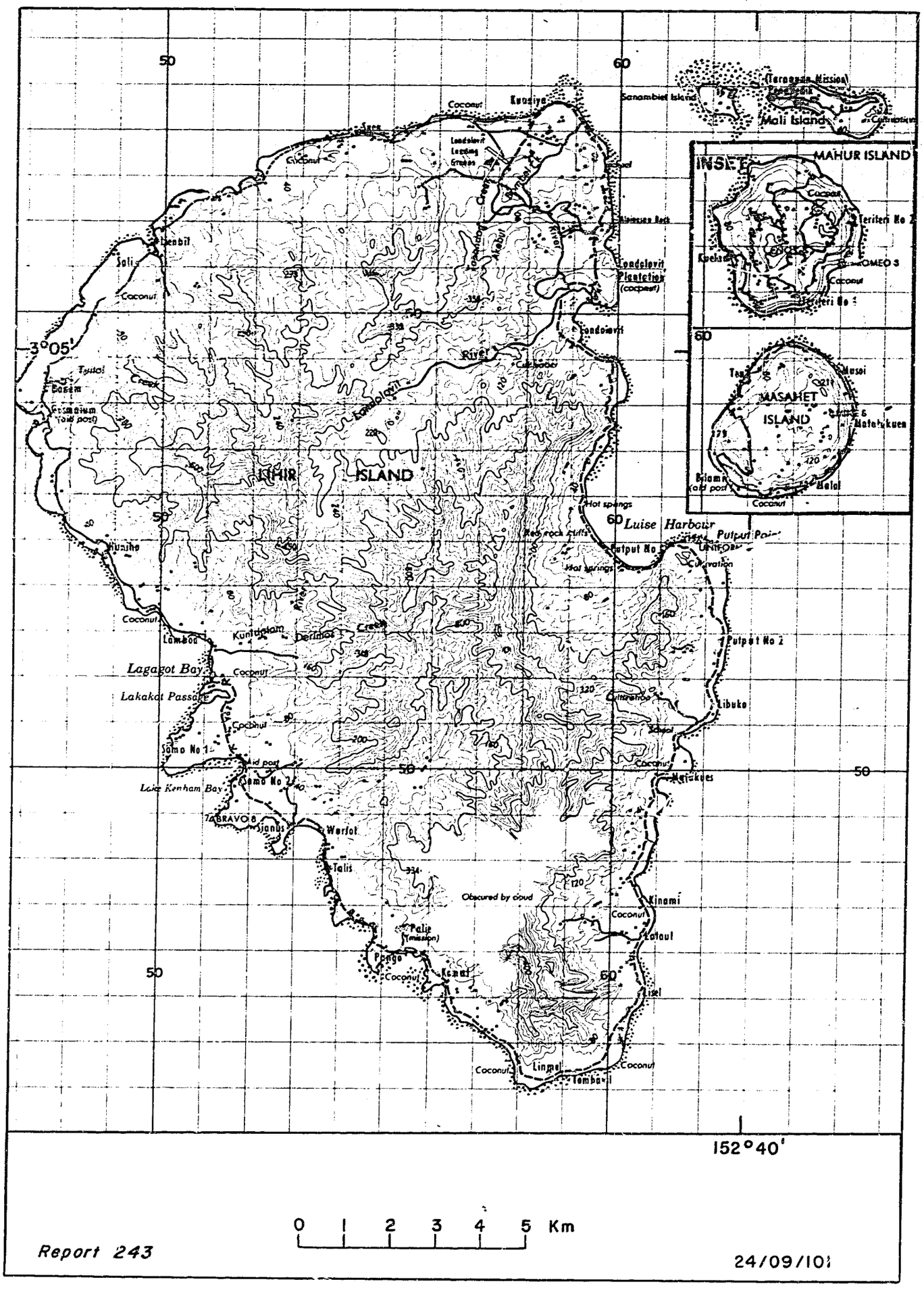

Figure 9b. Topography of the Lihir Group

Part of Sheet 9491 (Edition 1) Series T601, Papua New Guinea 1:100 000 Topographic Survey, reproduced by permission of the Surveyor General, Department of Lands and Surveys, Papua New Guinea.

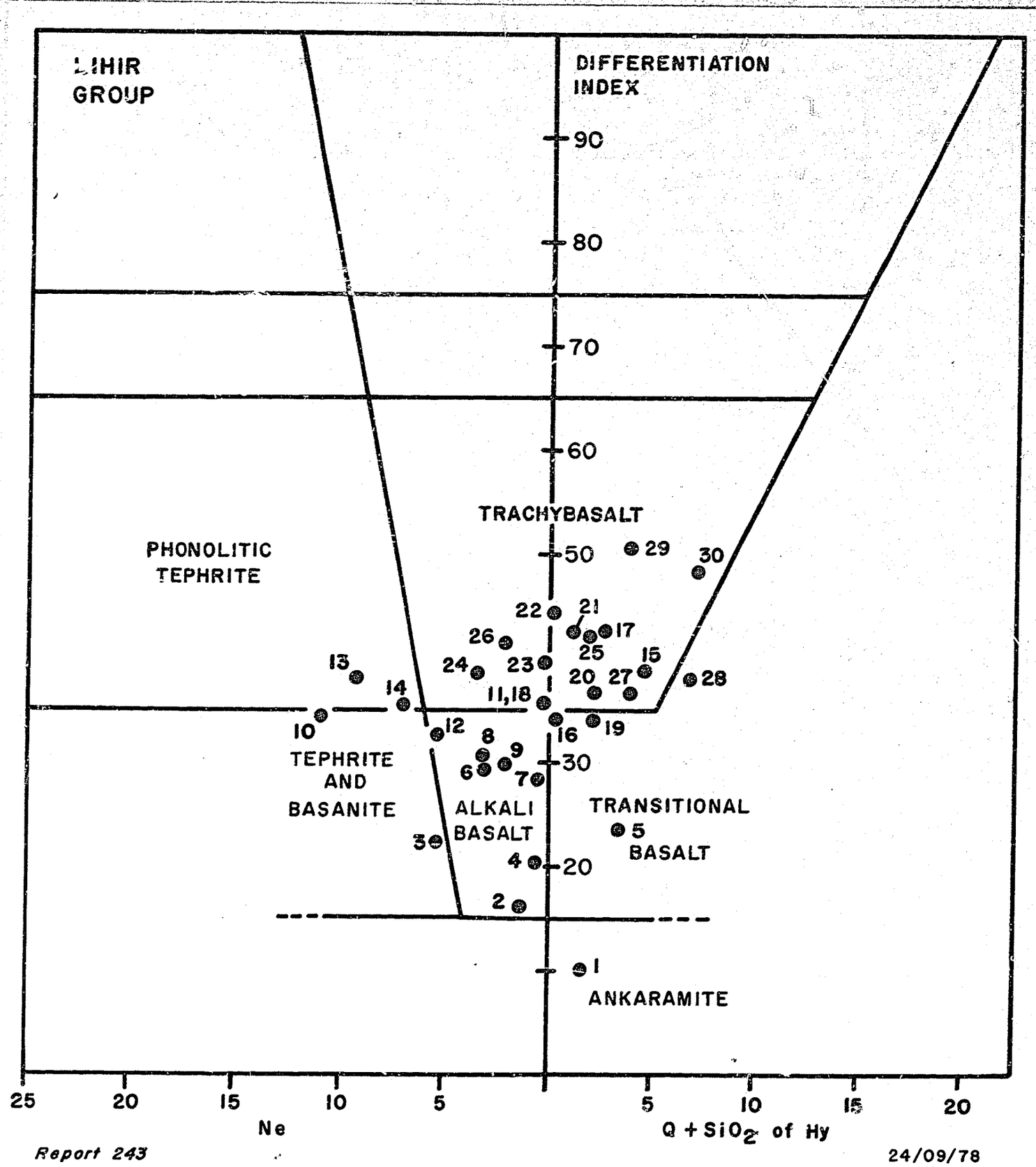

Figure 10. Rock-nomenclature diagram for rocks from Lihir Island (see Fig.3). Chemical analyses listed in Table LH1.

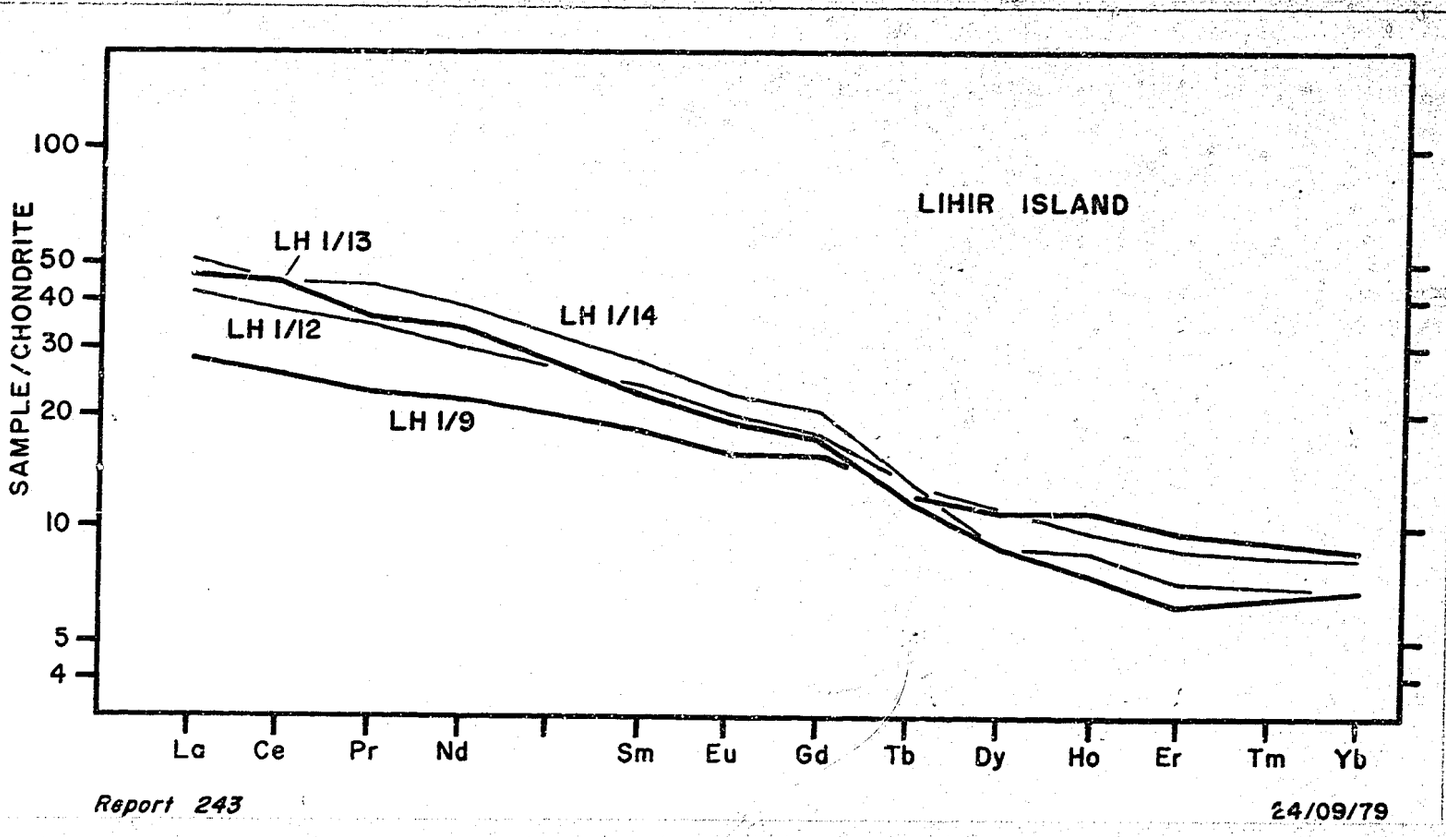

Figure 11. Chondrite-normalised REE abundances in four rocks from Lihir Island. Data listed in Table 7.

TANGA ISLANDS

Introduction

The Tanga Islands are midway between the Lihir and Feni island groups (Fig. 1), and are the smallest of the four groups in the Tabar-to-Feni chain (Fig. 12). The Tanga group is made up of four inhabited islands- Malendok, Lif, Tefa, and Boang - and two uninhabited islets, Bitlik and Bitbok. Malendok and Boang are 6 km apart, cover 30 and 25 km^2, respectively, and are the two largest islands in the group, supporting most of the population. Lif and Tefa each cover about 2 km^2, and extend in an arc southwards from Malendok. Lif is separated from Malendok by a deep 1-km wide channel, and is connected to Tefa by a shallow neck of coral reef that can be crossed on foot at low tide. Bitlik and Bitbok are midway between Tefa and Malendok, and are also connected by shallow coral reef.

Apart from small cultivated areas around scattered coastal villages, and two large plantations at Put and Nono, Malendok - the main volcanic island- is covered in dense primary rain forest. A coastal track skirts the island, but access to the interior can be gained by following stream courses and hunting tracks. The terrain in the centre and south of Malendok is deeply dissected. Peaks and ridges rising to over 400 m above sea level are bounded in the south by a steep fault escarpment, and on the west by a series of steep spurs and deep intervening stream valleys. Country towards the north and east is deeply incised, but relief decreases towards the coast.

Structure and general geology

The Tanga Islands represent the eroded remnant of a Plio-Pleistocene stratovolcano, Tanga volcano, the summit of which was largely destroyed by caldera collapse during the Lower Pleistocene, and by later complex faulting. Bitlik and Bitbok are the remains of a trachtye cumulodome built up on the caldera floor during a post-caldera phase of volcanism. Fringing coralgal limestone, which may have once girdled the original volcano, is in part preserved as a raised peripheral belt around the northern and eastern margins of Malendok. Boang Island consists entirely of limestone.

Tanga caldera is mainly below sea-level, but its arcuate outline can be partially traced as sheer fault escarpments bordering Put Bay on the south coast of Malendok, and on Lif and Tefa Islands (Fig. 12). No bathymetric data are available, but the sense of curvature of the fault scarps is

consistent with an elliptical form for a caldera centred on Bitbok and Bitlik. The distance across the widest part of the caldera between Tefa and Put village is 6 km. The caldera wall on Madendok is represented by two concentric arcuate fractures, both concave to the south, and the outermost ring fault truncates the belt of raised, fringing coralgal limestone near Kiam.

The structure of Tanga volcano has been modified by complex faulting, and the volcanic rocks are commonly strongly jointed. A major north-trending fault crosses Malendok, intersecting the caldera scarp a few hundred metres west of Put village, where the fault trace can be recognised by a narrow zone of indurated hydrothermally altered breccia projecting out from the scarp face. A break in continuity of lithologies in the west of Malendok may be evidence that another major fault passing through the caldera is part of a fault zone between Lif and Malendok, running roughly parallel to the west coast.

The volcanic rocks of Tanga volcano fall into three compositionally separate groups (Fig. 13): (a) a dominantly intermediate group consisting mainly of trachybasalt and phonolitic tephrite, which are confined to Malendok, Lif, and Tefa; (b) ne-trachyte, which is restricted to Malendok: and (c) Q-trachyte, confined to Bitbok and Bitlik in the centre of the caldera (Tables TG1-4, Tables 2, 11, Figs. 13, 14).

The intermediate lavas are invariably fine-grained, dark blue to grey, and typically studded with tiny pyroxenes, which are the only type of phenocryst. In addition to vertical joints, many individual lava flows throughout the sequence have a prominent sub-horizontal cleavage that gives the impression of an undulose pile of closely fitting slabs, each about 20 cm thick. The slab-like effect is thought to be a cooling feature of the lava flows, that was accentuated by later faulting. Spheroidal weathering is also seen in lavas cropping out along the southern coast of Malendok and in high ground near the centre of the island.

Malendok Island

Malendok is the largest subaerial remnant of the original Tanga volcano, and consists of a thick succession of lava flows and interstratified volcaniclastic deposits. The most complete section is between Put and Salkangkis villages (Fig. 12), where a 200-m thick series of lavas in the

caldera wall dips northwards towards sea-level. The lithology of the volcanic pile changes progressively northwards: the lava flows thin out and interbedded tuffs and volcanic rudites become more prominent. The northerly depositional dips of the clastic deposits range from 10 to 30°. Volcanic rocks at the coast, including deposits of fine grey tuff, are unconformably overlaid by a peripheral belt of raised coral limestone, which forms an 80-m high escarpment.

The raised reef limestone partially encircles Malendok along a belt extending around the northern and eastern margin of the island from Fangwel to Kiam (Fig. 12). The limestone between Fangwel and Nonu Plantation forms an 80-m high plateau, which, at its widest, extends just over 1 km south of Balanwaransau village and rises inland to about 120 m above sea-level. From Nonu plantation to Kiam the limestone is eroded along a sloping wave-cut platform, and has a scarp that extends up to 500 m inland, but which is discontinuous because of breaching by easterly flowing streams. Lenses of light-grey material exposed high in the cliff face near Gargaris village contrast with yellow-to-white limestone. These lenses are possibly volcanic ash deposited at the same time as the limestone, possibly towards the end of eruptive activity of Tanga volcano.

A thin cover of unconsolidated trachyte tephra on Malendok in places overlies more mafic rocks. The tephra is best exposed in a narrow zone between the two arcuate fault scarps on the south side of the island, where it crops out as a poorly sorted mixture of fine, creamy coloured lutite and coarser fragments of trachyte ranging up to angular blocks of cobble size. Welded trachyte tuff is exposed near Salkangis village, for about 100 m along the strandline, as a chaotic broken assemblage of large blocks. The beds consist of numerous layers of welded scoriae of differing sizes that form a compact, indurated unit about 4 m thick. Etching of the unit by differential weathering has highlighted individual beds that range in thickness from less than 1 cm up to several centimetres. Disruption of the unit into chaotic blocks may have resulted from faulting within the caldera, but also from subsequent wave and tidal action.

Present-day thermal activity in the Tanga Islands is minimal and confined to the south coast of Malendok. A hot spring about 1 km west of Kiam village trickles from small hole in a lava outcrop and forms a pool

near the beach. In 1974, the temperature was 35°C and the water had a pH of about 3. Rocks in contact with the spring water are stained by iron oxides and there is a faint smell of H_2S. Near Salkangis village, on the east side of Put Bay, minor amounts of H_2S gas bubble diffusely from a lava outcrop within the tidal margin. These hot springs probably derive from residual heat (possibly from a cooling intrusive) being channelled through the caldera ring faults.

Lif, Tefa, Bitlik, and Bitbok Islands

Lif and Tefa Islands each cover about 3 km^2 and represent small remnants of Tanga volcano, forming a discontinuous arc south of Malendok. The eastern side of Lif and the northern side of Tefa are curved, steep escarpments that mark the trend of the caldera fault.

Both Lif and Tefa are made up of vesicular intermediate lavas similar in composition to those of Malendok. The lava pile on Lif is over 280 m thick. Vesicles tend to form elongate flow-orientated cavities up to 12 cm long in some lavas, suggesting that the flows were more viscous than, say, those of tholeiitic composition. The orientation of the vesicles is westerly, indicating that the lavas may have flowed in this direction. Basal lavas on Tefa are overlain by poorly considated trachybasalt volcaniclastic deposits dipping about 15° south, and these are covered by weathered trachyte tephra.

Raised limestone is present on both islands as flat, eroded platforms which form apical spits up to a metre above sea-level. Younger raised beach deposits of rounded volcanic pebbles, coral fragments, and layered shelly material, unconformably overlie volcanic rocks along parts of the southern side of Tefa. Black beach sands on the south coast of Tefa contain high concentrations of ferromagnesian minerals and some magnetite, but not in economically exploitable quantities.

Bitlik and Bitbok are sparsely vegetated rock pinnacles. Bitbok is the larger - about 90 m above sea-level and about 600 m long. The Q-trachyte exposed on the islets is porphyritic and pale grey, weathering to creamy white; small, rare, angular mafic xenoliths are also found which, viewed in thin section, appear to have undergone recrystallisation. Feldspar, mostly anorthoclase, up to 6 mm long, is the main phenocryst type, together with small flakes of biotite. The groundmass in thin section is flow-banded.

Boang Island

Boang is arcuate, 10 km long, 4 km wide, and about 6 km northeast of Malendok. It is a flat-topped broken plateau of raised coralline limestone, titled a few degrees to the south, and has a maximum height of 140 m above sea-level. Boang is less densely forested than Malendok, and most of it is covered by coconut plantations. The permeable nature of the limestone terrain is reflected by immature doline development, and by the rarity of surface drainage, which is limited to two small streams flowing into the large bay on the south coast. Apart from a low-lying flat strip up to 600 m broad, extending around the southern and western margin, the coastline generally rises abruptly as a series of steep terraces and sheer cliffs. The terraces are best developed on the north coast, and may represent stages of uplift or eustatic changes in sea-level during the Pleistocene.

Geological history

Malendok, Lif, and Tefa Islands are the remnants of the summit of a stratovolcano of dominantly intermediate composition. If the original subaerial cone before cauldron subsidence was symmetrical and had a circular base and a radius of 8.5 km (the distance between Bitbok and Balanwaransau village - see Fig. 12), then it would have covered about 230 km^2. The latest stage of volcanism from this cone was mainly ne-trachytic in composition, and may have taken place at the time the caldera, or calderas formed. More than one stage of subsidence is indicated by the double caldera ring fault on Malendok Island. The final stages of activity were the formation of Bitbok and Bitlik Q-trachytes, presumably as a post-caldera cumulodome.

K/Ar dating of two biotite extracts from Bitbok trachyte samples (Appendix 2) yielded ages of 1.08 and 1.14 $\pm$ 0.08 m.y. These ages establish the time of the latest volcanism as early Pleistocene. Whole-rock K/Ar dating of a Lif trachybasalt gave a younger age of 0.187 $\pm$ 0.02 m.y., but this determination is considered to be in error (the sample is vesicular, and there may have been argon loss). Samples of limestone from the Tanga Islands submitted for palaeontological age determination were found to be either barren of fauna or to have non-diagnostic faunal assemblages. The early Pleistocene age for the Q-trachyte volcanism requires that the older, intermediate stage of volcanism for the main part of the volcano must have been Pliocene or older. However, the freshness of the lava and the immature weathering profile are indicative of an age not older than Pliocene.

The relationship between Tanga volcano and Boang Island is unclear. Boang may be a submarine extension of the same structure, or limestone may have been built either on a separate volcanic edifice or some other topographic high. No igneous rocks have been found on Boang that confirm a volcanic origin for the island.

Table TG1. Malendok Island

	1	2	3	4	5	6	7	8
SiO_2	48.73	48.32	48.60	48.9	47.4	47.8	49.6	61.46
TiO_2	0.75	0.82	0.77	0.80	0.72	0.72	0.65	0.57
Al_2O_3	14.86	15.61	15.92	15.7	15.4	15.2	17.0	18.42
Fe_2O_3	5.01	4.62	5.05	4.50	5.55	5.00	4.85	3.04
FeO	4.64	5.38	4.75	5.55	3.40	3.75	3.25	0.73
MnO	0.22	0.22	0.22	0.21	0.18	0.18	0.15	0.08
MgO	6.18	5.24	5.17	5.10	5.00	4.65	3.85	1.47
CaO	11.07	10.18	10.04	9.50	9.45	9.55	7.40	3.28
Na_2O	3.55	3.63	3.89	3.80	4.40	4.95	4.65	6.51
K_2O	3.53	3.74	4.02	3.10	2.00	3.10	4.10	3.14
P_2O_5	0.58	0.64	0.62	0.63	0.49	0.55	0.46	0.18
S	<0.02	<0.02	0.02	0.01	0.02	0.03	0.07	<0.02
H_2O+	0.57	0.53	0.54	1.67	3.90	2.20	2.65	0.58
H_2O-	0.19	0.20	0.20	0.25	1.63	0.82	1.06	0.23
CO_2	0.17	0.40	0.19	0.05	0.26	0.21	<0.02	0.14
rest	0.39	0.39	0.39			0.37	0.37	0.31
			100.39		99.80	100.18	100.11	
O=S			0.01		0.01	0.01	0.03	
Total	100.44	99.92	100.38	99.77	99.79	100.17	100.08	100.14
Trace elements								
Ba	310	325	345			340	385	530
Pb	70	97	88			17.2	57	59
Sr	1725	1720	1785			1780	1890	1534
Zr	71	74	72			75	88	147
Nb	2.5	3.5	2.0			2	3	6.5
Y	18	20	19			18	15	11
La	18	19	19			19	19	15
Ce	42	44	45			43	44	33
Nd	23	23	23			23	18	14
Sc	26	23	22			15	12	6
V	284	307	291			261	203	134
Cr	107	33	47			54	12	1
Co	43	39	39					9
Ni	24	13	17			17	10	3
Cu	190	209	195			158	155	14
Zn	89	95	85			88	73	47
Ga	15.5	16.5	16.5			16.0	18.5	22.0

1. Potassic phonolitic tephrite. 76400048. NB239145. Lava flow half way up fault scarp near Put village.
2. Potassic phonolitic tephrite. 76400051. NB242142. Block on track from fault-scarp rim to shore.
3. Potassic phonolitic tephrite. 76400049. NB242142. Boulder on track from fault-scarp rim to shore.
4. Potassic ne-trachybasalt. 71400488. NB234145. Sample at base of fault scarp near Put village.
5. Sodic ne-trachybasalt. 69400295. NB225200. Sample in stream near Fang village.
6. Potassic phonolitic tephrite. 69400286. NB255134. Sample near track on south coast west of Kiam village.
7. Potassic phonolitic tephrite. 69400292. NB208162. Sample on ridge near coast south of Sinaudo village.
8. Sodic Q-trachyte. 76400050. NB242142. Boulder on rim of fault scarp near Put village.

continued on next frame

Table TG1 cont. Malendok Island

	9	10	11
SiO_2	55.0	55.3	54.9
TiO_2	0.41	0.44	0.39
Al_2O_3	21.1	21.7	21.1
Fe_2O_3	2.85	2.40	2.40
FeO	1.36	1.81	1.71
MnO	0.17	0.18	0.18
MgO	1.07	1.05	1.01
CaO	3.55	3.15	3.15
Na_2O	4.85	5.45	4.85
K_2O	6.35	6.50	6.65
P_2O_5	0.22	0.23	0.19
S	0.01	0.04	0.15
H_2O+	2.15	0.85	1.50
H_2O-	0.65	0.45	1.44
CO_2	<0.05	0.10	0.05
rest			0.39
		99.65	100.06
O=S		0.02	0.07
Total	99.74	99.63	99.99
Trace elements			
Ba			465
Rb			114
Sr			2080
Zr			113
Nb			4
Y			17
La			23
Ce			48
Nd			19
Sc			2
V			123
Cr			25
Co			
Ni			2
Cu			74
Zn			94
Ga			20.5

9. Potassic ne-trachyte. 71400490. NB240146. Sample at fault scarp near Put village.

10. Potassic ne-trachyte. 71400552. NB260167. Sample near coast at Nonu Plantation.

11. Potassic ne-trachyte. 74400012 (also 73680013). NB234151. Lava flow at summit of fault scarp north of Put village.

Table TG2. Lif Island

	1	2	3	4	5
SiO_2	48.5	49.0	48.0	48.83	46.2
TiO_2	0.71	0.79	0.80	0.76	0.93
Al_2O_3	13.7	15.0	15.0	15.42	15.4
Fe_2O_3	6.05	5.10	4.95	5.03	5.75
FeO	4.30	5.25	5.10	4.99	4.75
MnO	0.18	0.21	0.21	0.21	0.21
MgO	6.80	5.55	5.45	5.27	4.70
CaO	11.6	10.9	10.1	10.15	11.3
Na_2O	3.30	3.85	3.85	4.04	1.89
K_2O	1.70	3.35	3.95	3.98	2.45
P_2O_5	0.44	0.54	0.51	0.54	0.60
S	0.01	0.02	0.02	<0.02	0.04
H_2O+	1.93	0.13	1.37	0.29	3.50
H_2O-	0.55	0.15	0.40	0.09	1.68
CO_2	0.1	0.10	0.02	0.17	0.4
rest			0.36	0.36	
		99.94	100.09		99.80
O=S		0.01	0.01		0.02
Total	99.87	99.93	100.08	100.13	99.78
Trace elements					
Ba			350	325	
Rb			127	63	
Sr			1650	1552	
Zr			74	69	
Nb			2	2.0	
Y			17	18	
La			19	18	
Ce			43	39	
Nd			22	21	
Sc			19	25	
V			275	297	
Cr			28	23	
Co				37	
Ni			17	17	
Cu			178	211	
Zn			82	91	
Ga			17.0	16.5	

1. Potassic ne-trachybasalt. 71400479. NB202117. Sample on ridge northwest of Lubun village.
2. Potassic phonolitic tephrite. 74400014. NB204126. Boulder below cliff on northern coast.
3. Potassic phonolitic tephrite. 69400267. NB201127. Sample at cliff on northern coast.
4. Potassic phonolitic tephrite. 76400056. NB204126. Boulder below cliff on northern coast.
5. Potassic transitional basalt. 71400486. NB206119. Sample on eastern coast.

Table TG3. Tefa Island

	1	2	3	4
SiO_2	47.7	47.2	48.21	51.1
TiO_2	0.73	0.74	0.90	0.72
Al_2O_3	14.2	15.3	15.64	17.3
Fe_2O_3	5.30	5.85	5.03	4.50
FeO	3.20	3.55	5.67	4.10
MnO	0.20	0.15	0.24	0.18
MgO	6.25	5.45	5.07	3.60
CaO	11.1	9.60	10.55	7.25
Na_2O	3.35	3.90	3.63	4.55
K_2O	3.60	2.45	2.46	4.10
P_2O_5	0.45	0.58	0.69	0.56
S	0.02	0.03	<0.02	0.03
H_2O+	1.28	3.05	1.13	1.24
H_2O-	0.41	1.33	0.36	0.38
CO_2	0.02	0.37	0.39	0.05
rest	0.36		0.39	
	100.17	99.55		99.66
O=S	0.01	0.01		0.01
Total	100.16	99.54	100.36	99.65
Trace elements				
Ba	365		325	
Rb	94		20.5	
Sr	1600		1829	
Zr	61		76	
Nb	2		2.5	
Y	16		22	
La	18		19	
Ce	40		47	
Nd	20		26	
Sc	25		21	
V	258		326	
Cr	66		20	
Co			41	
Ni	21		14	
Cu	190		214	
Zn	85		95	
Ga	16.0		17.5	

---

1. Potassic phonolitic tephrite. 69400271. NB219091. Sample at or near fault scarp on northern coast.
2. Potassic ne-trachybasalt. 69400275. NB219091. Sample at or near fault scarp on northern coast.
3. Potassic ne-trachybasalt. 76400054. NB216085. Lava flow at southwestern coast.
4. Potassic ne-trachybasalt. 71400475. NB219091. Sample at or near fault scarp on northern coast.

Table TG4. Bitlik and Bitbok Islands

	1	2	3	4
SiO_2	63.6	63.2	63.2	62.8
TiO_2	0.45	0.49	0.48	0.42
Al_2O_3	18.5	18.7	18.8	18.9
Fe_2O_3	2.95	2.90	2.55	2.70
FeO	0.31	0.40	0.54	0.09
MnO	0.03	0.03	0.03	0.02
MgO	0.75	0.74	0.58	0.15
CaO	2.40	2.10	2.05	1.69
Na_2O	6.80	6.10	6.05	6.35
K_2O	2.55	2.65	2.65	2.60
P_2O_5	0.15	0.19	0.10	0.10
S	0.07	0.11	0.35	0.81
H_2O+	0.57	1.50	1.53	2.15
H_2O-	0.59	0.49	0.48	0.32
CO_2	0.05	<0.05	0.05	<0.05
rest				
	99.77	99.60	99.44	99.10
O=S	0.03	0.05	0.17	0.40
Total	99.74	99.55	99.27	98.70
Trace elements				
Ba				
Rb				
Sr				
Zr				
Nb				
Y				
La				
Ce				
Nd				
Sc				
V				
Cr				
Co				
Ni				
Cu				
Zn				
Ga				

1. Sodic Q-trachyte. 74400013 (also 73680017). NB232121. Lava on north coast of Bitbok Island.
2. Sodic Q-trachyte. 71400503. NB233123. Lava making up Bitlik Island.
3. Sodic Q-trachyte. 71400501. NB233123. Lava making up Bitlik Island.
4. Sodic Q-trachyte. 71400496. NB233118. Lava at eastern end of Bitbok Island.

Table 11. Additional trace-element data for 7 rocks from Tanga Islands determined by spark-source mass spectrography

	TG1/1	TG1/6	TG1/7	TG1/8	TG1/11	TG2/3	TG3/1
Cs	0.91	1.0	1.6	0.32	3.8	0.83	1.1
Rb	9.8	7.9	8.9	6.6	21	6.3	6.6
La	18.2	17.0	23.3	14.0	28.5	17.1	17.9
Ce	41.9	39.7	52.8	27.8	48.3	38.0	45.7
Pr	4.78	4.95	6.89	3.72	6.14	4.16	5.05
Nd	20.7	22.9	30.7	15.0	23.8	17.7	22.1
Sm	4.77	5.94	6.22	3.07	5.05	4.62	5.58
Eu	1.43	1.82	1.96	0.89	1.63	1.41	1.80
Gd	4.48	4.45	5.33	2.60	4.45	4.15	4.88
Tb	0.61	0.70	0.70	0.42	0.60	0.59	0.65
Dy	3.42	4.01	3.83	2.40	3.29	3.20	3.26
Ho	0.60	0.71	0.60	0.36	0.61	0.55	0.62
Er	1.50	1.90	1.30	0.94	1.70	1.33	1.55
Tm	0.21	0.27[a]	0.21[a]	0.13	0.28[a]	0.20[a]	0.23[a]
Yb	1.43	1.86	1.42	0.91	1.92	1.42	1.62
Lu	0.22	0.29	0.22	0.14	0.31	0.22	0.25
Th	1.75	1.79	2.04	1.83	3.80	1.67	1.56
U	0.98	0.85	1.42	1.12	2.30	0.97	1.02
Hf	1.9	2.19	2.17	3.9	2.46	1.66	1.6
Sn	0.91	1.3	1.1	0.92	2.6	0.95	1.2
Mo	n.d.[b]	1.4	2.5	n.d.	1.5	1.6	1.4

a. Interpolated value.

b. n.d.: not determined.

Table 12. Summary of mineral compositional data for the Tanga Islands.

	TG1/1	TG1/8
Clinopyroxene	Al-salite/salite	diopside/salite
Amphibole		magnesiohastingsite
Olivine	Fo_{75-47}	
Biotite		Mg_{74}
Oxide	mt	exsolved mt
Feldspar	An_{74}-Or_{74}	An_{29}-Or_{35}
Feldspathoid	leucite, sodalite	
Others	apatite	opx (Mg_{83})

Abbreviations. Fo: forsterite; mt: magnetite; An: anorthite; Or: orthoclase; opx: orthopyroxene. Slash between two mineral names refers to compositional continuity (solid solution) between the minerals.

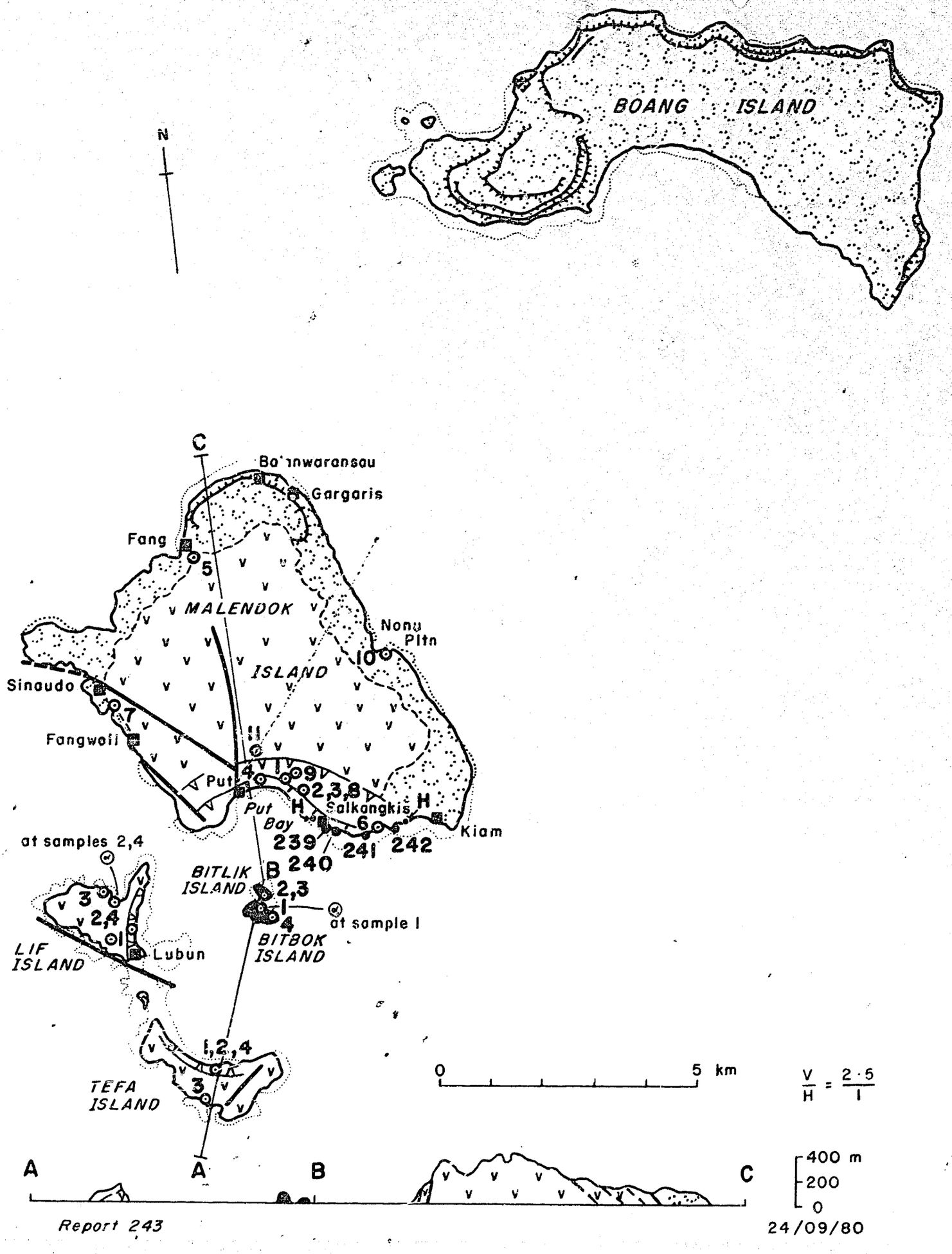

Figure 12a. Geology of the Tanga Islands (see legend in Fig. 2).

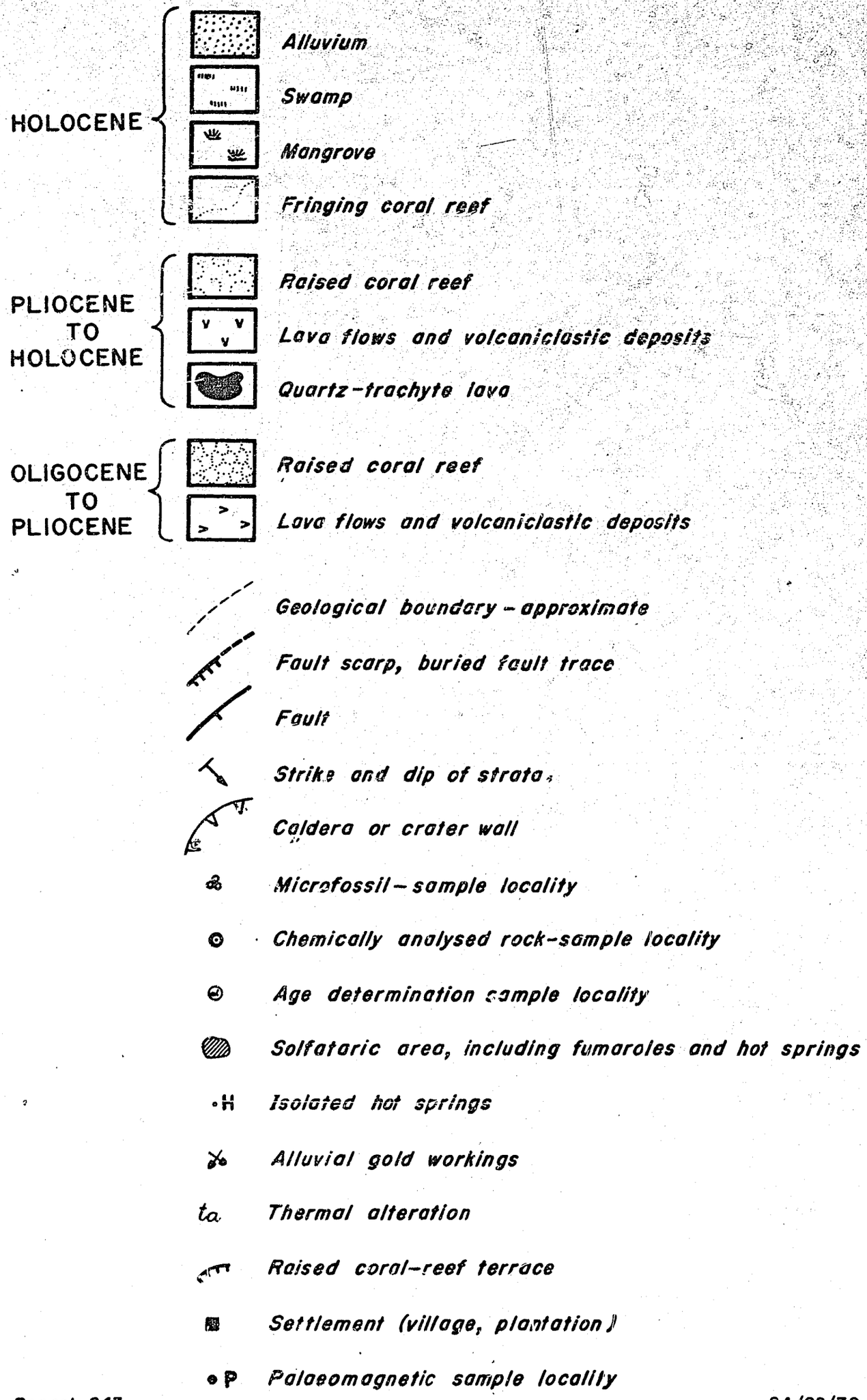

Figure 2. Legend to geological maps (Figs 4-6, 9, 12, 15).

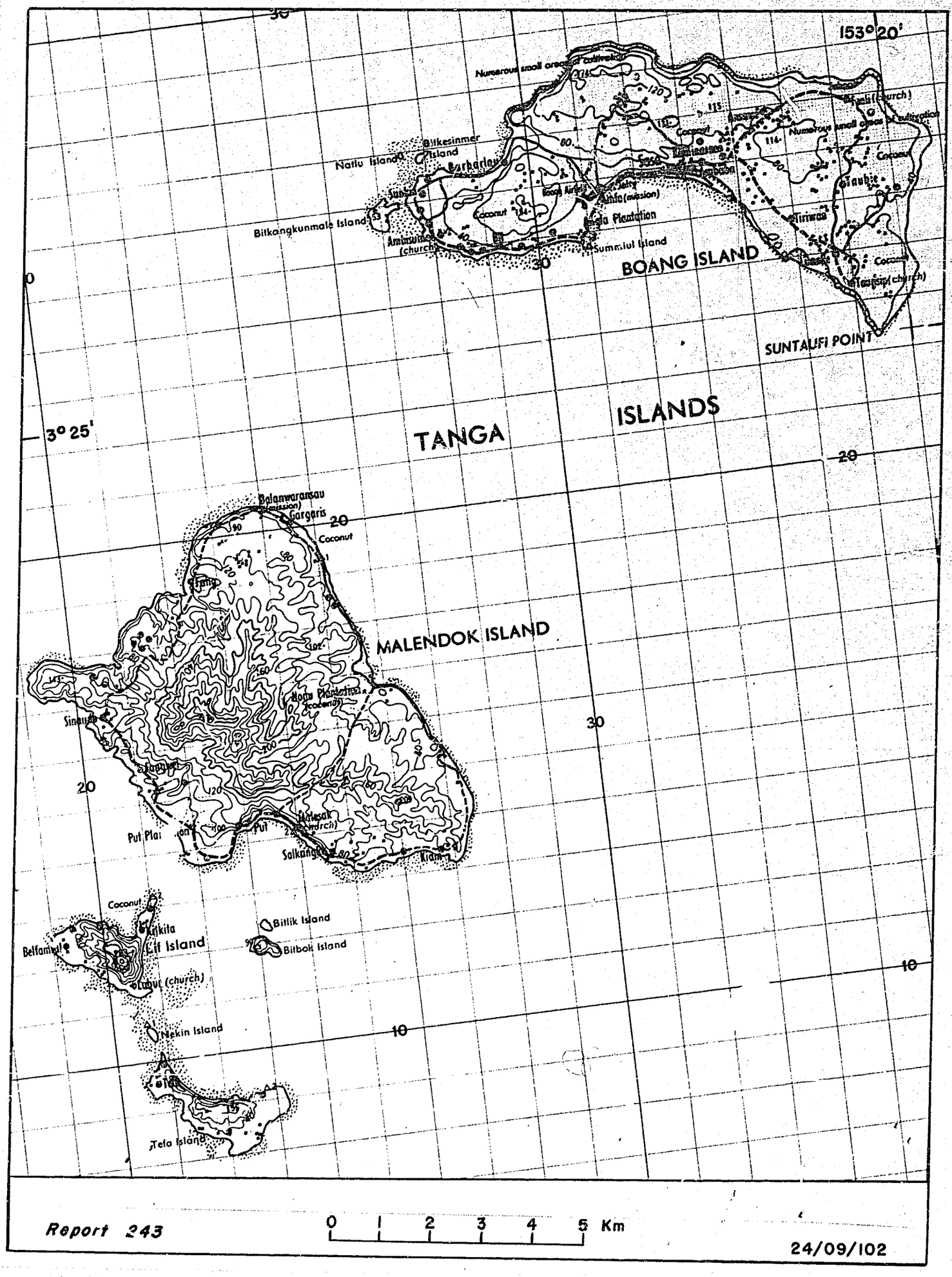

Figure 12b. Topography of the Tanga Islands.

Part of Sheet 9591 (Edition 1) Series T501, Papua New Guinea 1:100 000 Topographic Survey, reproduced by permission of the Surveyor General, Department of Lands and Surveys, Papua New Guinea.

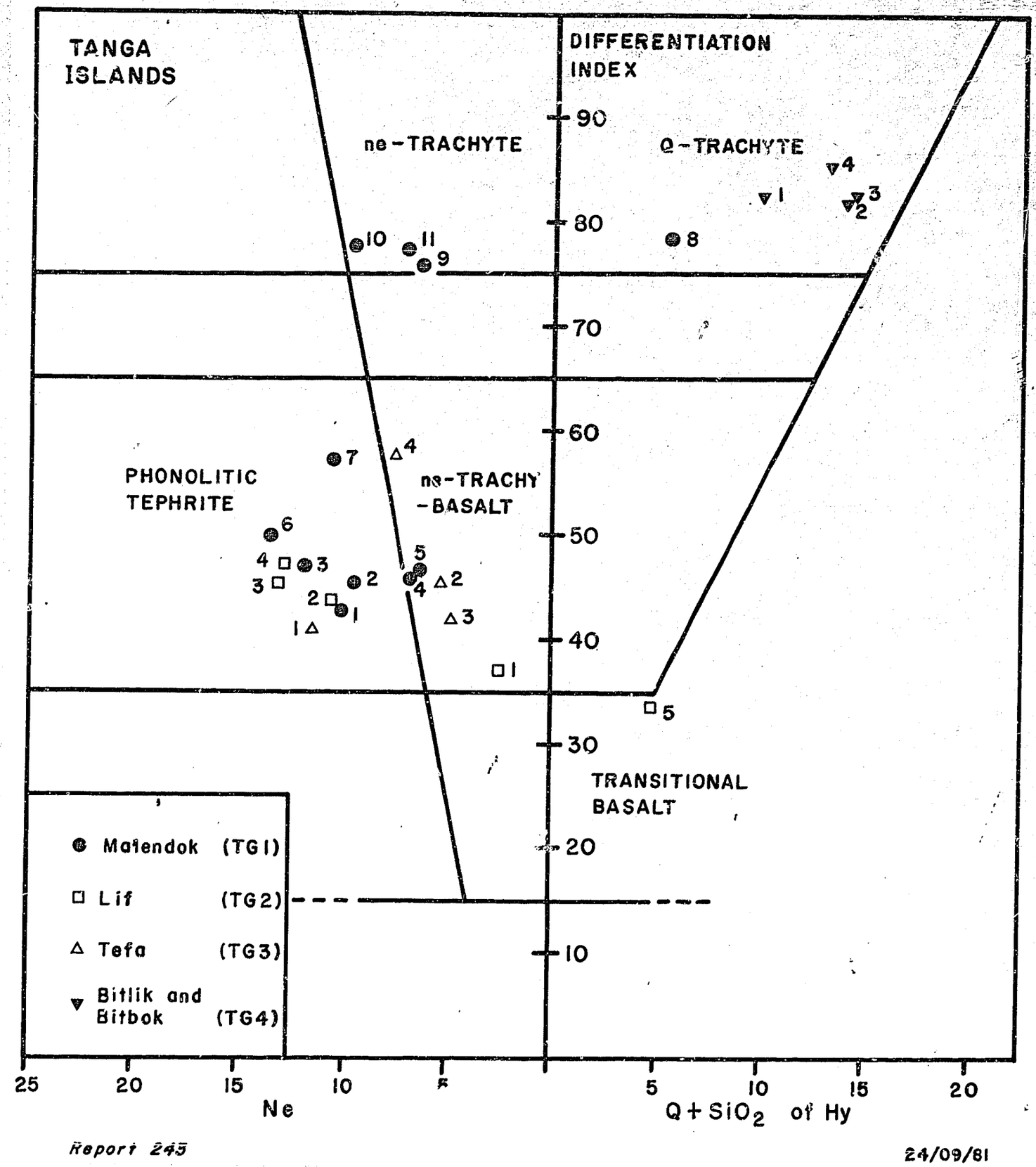

Figure 13. Rock-nomenclature diagram for rocks from the Tanga Islands (see Fig. 3). Chemical analyses listed in Tables TG1-4.

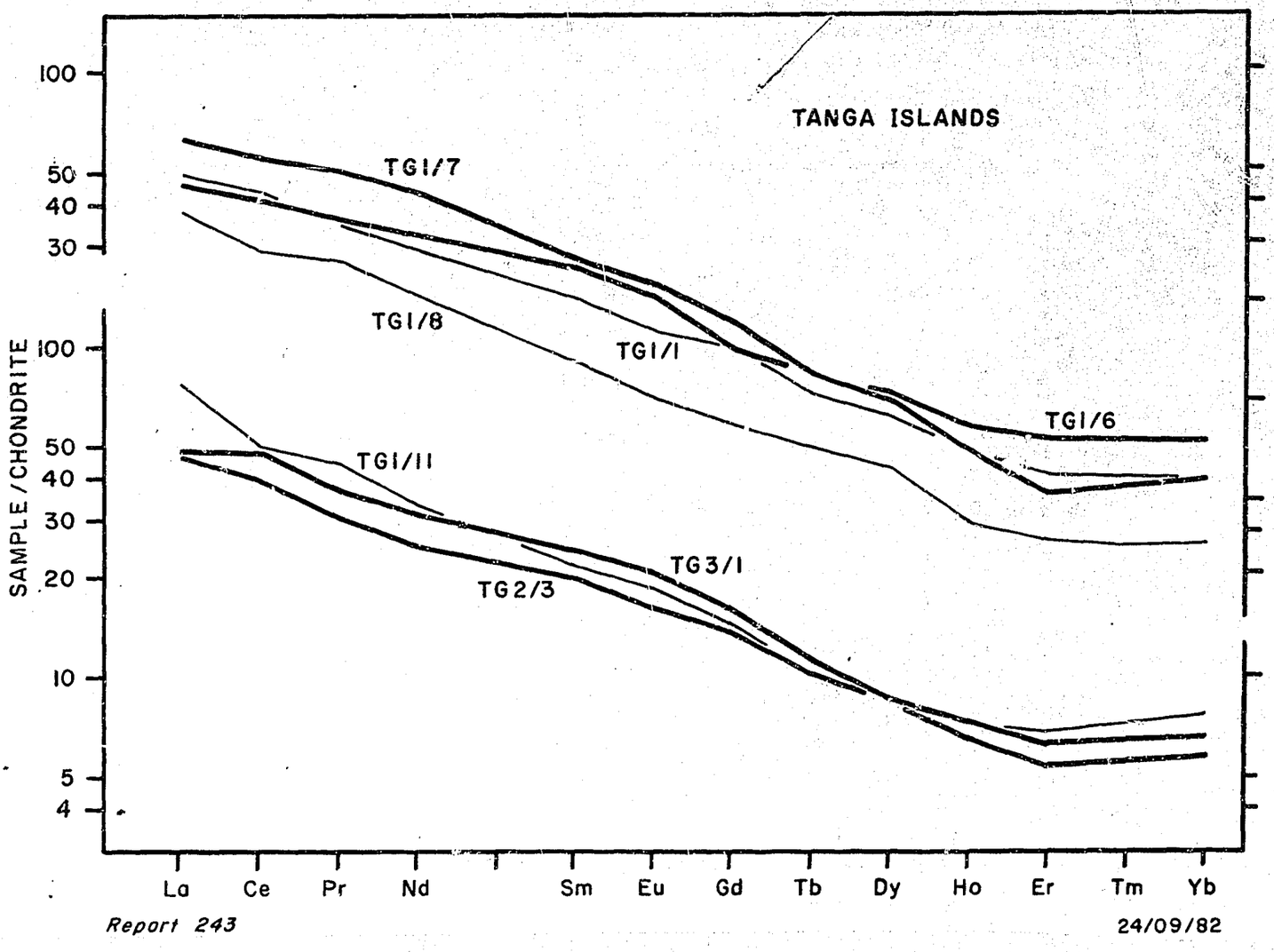

Figure 14. Chondrite-normalised REE abundances in seven rocks from the Tanga Islands. Data listed in Table II.

FENI ISLANDS

Introduction

The Feni Islands is a collective name for two adjacent islands, Ambitle and Babase, separated by a shallow 400-m wide passage known as Salat Strait (Fig. 15). The islands are at the southeastern end of the Tabar-to-Feni chain, about 70 km from the Tanga Islands and 60 km east of New Ireland (Fig. 1). Both islands are dissected Late Tertiary to Quaternary volcanoes whose vestigial, but topographically recognisable, volcanic landforms include traces of small satellite centres and the remains of an eroded central caldera and crater. Active thermal areas on Ambitle are probably an indication that volcanic activity continued well into the Quaternary and that the volcano may not be extinct. Ambitle, the larger island (also known as Anir or Feni Island), covers about 87 km^2. Babase covers about 23 km^2.

Ambitle is mantled by thick rain forest, and apart from some exploitation of cleared ground along the lower reaches of the three main rivers - the Nanum, Olu, and Niffin - cultivation is confined to the narrow alluvial coastal margin. Cultivation on Babase is more general, except on the upper slopes of a volcano in the east of the island and in its swampy interior. The Feni Islands support a population of just over 1000, who live by subsistence agriculture, supplemented by fishing and cash cropping of cocoa and copra. There are several large cocoa and coconut plantations throughout the islands, and a well-maintained airstrip at Malekolen on the western tip of Babase is suitable for light aircraft.

Geology of Ambitle Island

Ambitle is a truncated Plio-Pleistocene stratovolcano built on a poorly exposed tilted basement of middle-to-upper Oligocene marine limestone (Fig. 15). The volcano is a typical, composite, central-vent structure consisting of a thick succession of interbedded lavas, lahar deposits, tuffs and scoriae. The volcano includes the remnant of a small eroded caldera, about 3 km in diameter, that lies west of the centre of the

island and whose wall is breached in the west and southwest. The floor of the caldera is almost wholly covered by a younger, low-angle, Q-trachyte cumulodome, capped by a shallow summit crater. Raised, Lower Pleistocene, fringing coralgal reef crops out at the northern tip of the island as an isolated circular massif, 20 m high and 1500 m across its base. West of this massif, almost to Fatkarson, and eastwards to Balenkolen, the reef limestone is found as a narrow, poorly exposed platform, eroded down to sea-level, and mostly covered by alluvium. A narrow continuous belt of present-day fringing reef girdles the island, extending locally in the north and south up to 500 m offshore.

Scattered, low-temperature (less than 100°C) thermal areas in the caldera and on the western flank of the volcano are evidence that heat and gases - perhaps from a cooling intrusive - are being channelled to the surface through the conduit system of the volcano. These thermal phenomena consist of a small solfatara field on the western rim of the caldera, boiling springs within the caldera, and further scattered boiling springs and mud pools along the shore and on low-lying ground between Waramung and Danlam (see below).

The island has rugged relief, resulting from collapse of the central part of the structure, breaching of the central caldera, and radial dissection of the flanks of the volcano by a well-developed consequent drainage network. The maturity of the drainage system is particularly evident on the northern and eastern flanks of the volcano where several of the larger rivers have cut to depths of over 200 m. The extent to which the centre of the structure has been modified, leaving a truncated residual profile, is illustrated by the cross section in Figure 15. Overall relief decreases uniformly from the central caldera towards the coastal margin, and the volcano is best preserved north of a line between Fatkarson and Nalula villages. The highest peaks on the island rise to almost 500 m and are mostly adjacent to the caldera and to two fault scarps bounding the Niffin River catchment area. These two scarps define the limits of a northwest-southeast, 2-km wide graben on the southeastern flank of the volcano. Another fault, trending northeast from Nanum Bay, intersects the crater in the south.

The volcano of Ambitle consists of an older succession of mainly mafic and intermediate lava flows and pyroclastic deposits, overlaid by a younger, relatively thin mantle of trachyte tephra, and by the trachyte cumulodome. The mafic and intermediate lava flows crop out along the coast

in many places throughout the island, but are best exposed along the western coast between Tanambia and Matoff Bay. Inland lava flows are invariably concealed under thick tephra and are best exposed as bedrock in streams. Between Tanambia and Danlam several thin flows extend to the foreshore, but between Waranguspik and Nanum Bay composite lava units crop out as massive steep bluffs rising to several hundred metres.

The analysed volcanic-rock samples from Ambitle cover a wider compositional range than those from any of the other island groups. Most of the samples are strongly undersaturated and intermediate in composition (phonolitic tephrite and tephritic phonolite), but alkali basalt, tephrite, and basanite are also represented, as well as trachybasalt and trachyandesite (Table FN1, Tables 13, 14, Figs 16-18). Heming (1979) presented 10 Ambitle rock analyses, one of which was of a Q-trachyte. The other nine were said to be tephrite and basanite, but, as shown in Figure 16, none of Heming's samples are tephrite and basanite in the sense used throughout this report. Rather, they are trachybasalt, phonolitic tephrite, and tephritic phonolite. The strongly silica-undersaturated character of Ambitle Island rocks was first recognised by Glaessner (1915), and prominent, strikingly blue phenocrysts of the feldspathoid haüyne are seen in the thin sections of many Ambitle samples.

The lavas in the field range in texture from fine-grained to porphyritic and from light grey through to dark blue and dark green. Many lavas are zeolitised. In common with rocks from the other islands, pyroxene-phyric lavas are ubiquitous throughout Ambitle, although some, believed to be generally older than the rest, include a larger amount of olivine. Clinopyroxene phenocrysts are found both as large crystals, up to 2 cm in length, and as cognate cumulate clots; some pyroxenes have a bright iridescence in hand specimen. Inclusions made up almost entirely of clinopyroxene, as distinct from the cognate glomeroporphyritic pyroxenes, are common to several lavas cropping out along the west coast between Fatkarson and Waramung. These pyroxenite samples are rare in some of the lavas, but they can make up to 10 percent of some rock outcrops. One collected pyroxenite sample weighed over 30 kg. The pyroxenites are dense cumulates incorporating only a small fraction of intercumulus plagioclase which, in the larger nodules, imparts a faint pseudolayering to the rock.

Beds partly filling the Nanum and Niffin fault valleys consist of trachyte tephra. They unconformably overlie intermediate lavas, and were

apparently emplaced after disruption of the central part of the volcano. There may, therefore, have been a significant time-break between the periods of intermediate and trachytic volcanism on Ambitle. The Niffin River trachyte tephra crops out as a sheer, 20-m high escarpment about 2 km up-river from Niffin Bay. The bed is a creamy coloured, graded, arenaceous tuff breccia, containing a small fraction of mafic clasts. Near the base of the tuff bed are two thin beds, a 50-cm thick layer of weathered red clay (thought to be a former soil horizon), and a 10-cm thick layer of grey mudstone similar in texture and composition to the muds currently being generated in the thermal area behind Waramung Plantation on the west coast. The Nanam River tephra is an extensive, valley-fill mélange of trachyte tuff breccia similar in composition and thickness to the Niffin River breccia. The unit underlies Nis Nis plantation, where it is 600 m wide and 1.5 km long, and where it slopes towards the present river bed in a series of terraces, probably resulting from westward migration of the river course by lateral corrasion.

The oldest exposed lithological unit in the Feni group - also the oldest datable strata found in any part of the Tabar-to-Feni island chain - is a small inlier of bedded Oligocene calcilutites cropping out at the base of volcano on the northwestern part of Ambitle. The inlier is overlaid by reworked tephra and lahar deposits, and is exposed along a 50-m stream section about 1 km east of Kurkur village (see sample site on Fig. 15). The calcilutites are an unconsolidated, banded series of planktonic marine oozes, each band distinctively coloured in shades of green, brown, or yellow. The beds are tilted towards the north and have an average dip of 25°. Examination of the abundant microfaunal assemblage by D.J. Belford (Appendix 1) yielded a middle-late Oligocene age (planktonic zone N1-N3). The limestone appears to be limited to this particular locality; no further exposures were found either in adjacent steams or elsewhere on the island.

The youngest rock type on Ambitle is a discontinuous, horizontal bed of Holocene beach conglomerate that is exposed along the foreshore between Nanum Bay and Waramung. The conglomerate is about 1 m thick, and consists of a moderate to poorly sorted graded assemblage of trachyte pebbles, a small proportion of mafic-lava pebbles, and mixed coral and molluscan fragments, all cemented by micrite. Slabs of coralline limestone are incorporated in its upper part. Most voids in fossil tests are incompletely filled by sparry

calcite. Interstitial minerals derived from trachyte - notably oligoclase, anorthoclase, and biotite - are mostly fresh and unaltered. The conglomerate is thought to represent a post-trachyte strandline sediment that was raised about 1 m above present sea level in the Holocene.

Thermal areas of Ambitle Island

Most thermal areas on Ambitle Island are near the western coast and on the western part of the caldera floor near the breaches in the caldera wall, and near the western edge of the central trachyte cumulodome (Fig. 15). The areas on the outer slopes are close to streams in two deeply incised valleys. Thermal activity consists mainly of hot to boiling mud pools and springs, and a few small low-temperature fumaroles. Reynolds (1956; see also Fisher, 1957) identified and described three thermal areas and referred to them as areas A, B and C (Fig. 15). Reynolds was also aware of a discharge of hot water into the Nanum River, but was unable to locate the source area, which is in the headwaters of the river and labelled D in Figure 15. The thermal areas were investigated again in January 1973 and in October 1974.

Thermal area A is partly within Waramung Plantation and extends from the coast inland for about 1.6 km, in a narrow belt adjacent to a small stream. Thermal activity consists mainly of warm to hot springs and mud pools, which have temperatures ranging from 67 to 99°C, scattered in patches along almost the entire length of the stream that runs along the northwestern edge of the plantation. Minor geyser activity is present in one of two, adjacent, clear-water pools, 2m in diameter, about 200 m from the coast. Water (temperature of 100°C) is ejected spasmodically about 0.5m above its surface. Two nearby mud pools are inactive, but have temperatures of 84°C and 87°C. A crust of siliceous sinter covers most of this area, indicating that the pools can overflow. No overflow was observed at the time of both investigations in 1973 and 1974, but the springs may discharge underground at a nearby beach, where minor ebullition was observed from small fissures in a lava flow cropping out below the high-tide mark. Some of the mud pools farther inland are within craters up to 5 m across and 3 m deep. One area near the south-eastern boundary of the plantation contains three mud pools that had temperatures ranging from 67 to 99°C. The area is about 40 m in diameter, and is devoid of vegetation apart from clumps of grass, bracken, and bamboo. Minor gas ebullition takes place in one of the pools, and a small mud-spatter cone had been developed on the edge of another, through which water vapour at a temperature of 98°C and having a slight H_2S smell, was being emitted. Another area nearby in a swampy region contains numerous small, hot to boiling mud pools.

A small boiling spring ejects water up to a height of 30 cm about every 30 seconds, and discharges at less than 1 litre per minute into a small stream. A slight smell of H_2S was evident in this area.

Thermal area B is an adjacent valley to the north of A. Several hot to boiling mud pools and springs are within an area 120 m in diameter, which is mostly covered with thick bracken, apart from smaller areas covered by sinter. Water temperatures ranged from 95 to 99°C. An H_2S smell is noticeable, especially near a boiling spring in a small cavernous opening, which has a temperature of 99°C. One large pool has a temperature of 95°C, is surrounded by sinter, and wells up and overflows into a nearby stream every five to ten minutes.

Thermal area C is the largest on the island, and is 2 km inland east of area B. It consists of one, large, irregularly shaped area denuded of vegetation and straddling a saddle in the caldera wall. Isolated peripheral smaller areas are found mainly to the east within the caldera. A large elongated crater about 20 m wide and 40 m long is present on the summit of the saddle. Several small thermal pools are on the northern boundary (their temperatures range from 46 to 96°C), and minor gas ebullition takes place in one of them. The northwestern section of the large thermal area is inaccessible without the aid of ropes or ladders. Several hot to boiling pools, and springs and fumaroles, are within the large thermal area and give rise to a warm mineralised stream that has a temperature of 45°C 200 m downstream from this area. A small stream that joins the Nanum River drains the southern part of the main thermal area, and several small springs and mud pools (temperatures ranging from 77 to 87°C) are found near its banks. Several other isolated, steep-sided craters containing hot mud pools (surrounded by thick rain forest) are present to the west and southwest of the main area. The largest one observed had a diameter of about 25 m. A temperature of 96°C was measured from one such mud pool which was vigorously bubbling, on the northern edge of a sinter-covered area about 30 m in diameter. Nearby, a small mud-spatter cone shaped like a tree trunk emitted minor but variable amounts of vapour smelling of H_2S at a temperature of 98°C.

Thermal area D is on the upper reaches of the Namum River, and consists of numerous, small, hot springs with temperatures ranging up to 99°C. One such spring discharged water with a temperature of 99°C at less than

1 litre per second from a fissure at the base of the trachyte cumulodome. The rocks over which it flows are stained red and brown, and a smell of H_2S is weak but noticeable.

The compositions of the thermal waters on Ambitle Island (Tables 15, 16; see also Appendix 3) fall into two distinct groups: (1) those having pH values ranging from 8.1 to 9.1, and enriched in NaCl; (2) those having low pH values between 1.9 and 3.0, and having low, overall, ionic concentrations, but relatively high SO_4 concentrations. Sample F1, collected from a small thermal spring issuing from a fissure in the central trachyte cumulodome, and sample F2, from another small thermal spring about 1 km inland in area A, are in the first group and are similar in composition to the NaCl-type thermal waters discussed by White (1957). Some NaCl-type waters have been analysed for stable isotopes, and have been shown to derive from cold, local, meteoric water modified by wall-rock interactions (White, Barnes, & O'Neill, 1973). Ionic ratios of the two samples from Ambitle Island are different from those of seawater, suggesting that the compositions of these waters too have been derived from meteoric waters that have interacted with subsurface wall rocks.

Two samples (F3,029) collected from the same spring near the beach in area A, but at different times, and sample 031 from area B, 0.9 km inland, could be classified as NaCl-type waters. However, their concentrations of Na, K, and Cl are high, and although their ionic ratios are dissimilar to seawater, some contamination by seawater, which may have been modified by wall-rock interactions, is suspected. Minimum subsurface temperatures of 140°C are indicated by the SiO_2 contents of some of these samples.

Samples in the low-pH group are of the acid-sulphate type. Three of these samples came from bubbling mud pools that had no apparent out-flow (samples 030, 031, 033) and a fourth was collected from a stream flowing to the west and draining part of area C (sample 032). One sample from this group (028) was collected from a bubbling mud pool in area A, within 100 m of a small spring where sample F2, which is typically NaCl type, was collected. Samples from the second group have low overall ionic concentrations, but relatively high SO_4 values, indicating that the waters are predominately superficial and meteoric and have been acidified by oxidised H_2S.

Geology of Babase Island

Babase is a club-shaped island, 10 km long, consisting of two Plio-Pleistocene volcanoes connected by a narrow isthmus of coral reef and alluvium (Fig. 16). A platform of fringing coral reef girdles the entire island. The larger of the two volcanoes forms most of the eastern part of the island, and is a near-circular cone containing an eroded summit crater. The smaller volcano, on the western tip of the island, is a Q-trachyte cumulodome completely overlaid by a 20 m thick cap of coralgal limestone. Micropalaeontological dating of a sample from the limestone yielded a Pleistocene age (Appendix 1).

The eastern volcano on Babase is a relatively small, but topographically well-defined, youthful Pleistocene landform, made up mainly of basaltic and trachybasaltic lava flows and minor interbedded scoria deposits that radiate steeply and uniformly from the central crater. The flanks of the volcano rise steeply from a narrow reef-fringed base to the crater rim, which is about 200m high in several places. The steep-walled crater is breached in the southwest along a narrow, mangrove-filled tidal inlet, and is poorly drained, swampy, and quite thickly vegetated. Hot springs are reputed to exist in the crater, but these could not be located, as a guide was reluctant to enter the crater because of its spiritual significance to local people (in Pidgin English, 'plez massalai' - spirits' place). Three analysed rocks from the eastern volcano are two trachybasalts and a transitional basalt (Table FN2, Fig. 16).

The Q-trachyte cumulodome in the west of Babase (sample FN2/4) crops out as the 'core' of a raised block of coralgal limestone similar in size to the nearby raised limestone block on Ambitle Island (Fig. 16). The cumulodome is best exposed in section at the base of a sheer escarpment about 40 m high, bordering the beach on the south side of the island. There, the trachyte is layered, and dips away on either side of a breccia-filled volcanic vent. The nearby raised limestone block on Ambitle is similar in size and shape to the Babase trachyte and limestone cap, and possibly it may be underlaid by trachyte. However, the trachyte is not exposed.

Samples of both the Ambitle and Babase trachytes have been dated radiometrically (Appendix 2). Hornblende concentrates from Babase yielded a Pleistocene age of 1.53 $\pm$0.15 million years and determinations on biotite

extracted from the Ambitle trachyte gave ages of 0.68 $\pm$ 0.10 and 0.49 $\pm$ 0.10 million years. Paleontological examination of limestone overlying the Babase trachyte yielded a microfaunal assemblage not older than Pleistocene (Appendix 1). On the basis of these age determinations, supplemented by age estimates based on geomorphological characteristics, the Babase trachyte and the mafic and intermediate rocks of Ambitle are believed to have been formed in the Upper Pliocene to Lower Pleistocene, separated by a significant time span from the later Ambitle Q-trachyte volcanism.

Table FNI. Ambitle Island

	1	2	3	4	5	6	7	8
SiO_2	43.0	45.1	46.8	46.2	45.8	45.9	50.79	46.33
TiO_2	1.21	0.72	0.77	0.78	0.67	0.80	0.56	0.83
Al_2O_3	6.35	11.0	10.4	10.7	10.2	12.1	16.16	12.33
Fe_2O_3	11.5	4.70	5.25	5.75	5.60	5.80	3.57	5.87
FeO	4.90	5.55	5.05	5.55	4.90	5.00	3.41	5.20
MnO	0.19	0.20	0.17	0.18	0.20	0.20	0.16	0.20
MgO	12.3	12.0	9.10	9.10	9.05	8.30	7.73	7.56
CaO	18.5	12.3	15.4	14.6	14.7	14.4	6.85	13.50
Na_2O	0.80	2.80	2.75	2.65	2.85	3.65	5.66	3.82
K_2O	0.13	1.16	0.75	0.90	2.15	2.15	3.36	2.94
P_2O_5	0.07	0.47	0.51	0.53	0.58	0.53	0.29	0.62
S	<0.01	0.01	0.03	0.05	<0.01	0.01	0.19	<0.02
H_2O+	0.71	2.75	2.00	2.25	1.54	1.29	0.42	0.41
H_2O-	0.23	0.71	0.37	0.41	1.70	0.03	0.13	0.10
CO_2	0.15	0.25	0.45	0.15	0.05	0.05	0.24	0.08
rest	0.19				0.32	0.35	0.40	0.35
			99.80	99.80			100.00	
O=S			0.01	0.02			0.09	
Total	100.23	99.72	99.79	99.78	100.31	100.56	99.91	100.16
Trace elements								
Ba	35				155	215	380	180
Rb	1.8				30.5	56	53	58
Sr	329				1280	1570	1439	1473
Zr	51				76	66	76	69
Nb	<0.5				2.0	2	4.5	2.5
Y	13				12	15	13	16
La	3				19	22	14	18
Ce	13				44	51	29	43
Nd	13				24	26	14	26
Sc	67				34	24	12	34
V	454				281	289	227	345
Cr	90				147	84	342	80
Co							36	48
Ni	55				54	45	220	54
Cu	92				160	164	165	170
Zn	62				87	84	69	91
Ga	15.0				15.0	15.5	21.5	17.5

1. Clinopyroxene-rich cumulate. 74400006 (also 73680006). NA640498. Inclusion in lava flow (represented by sample FNI-6) north of Waramumg Bay.

2. Sodic basanite. 74400001 (also 73680001). NA699499. Lava flow in stream southwest of Balankolon village.

3. Sodic alkali basalt. 71400547. NA647464. Sample on or near roadside east of Waranguspik village.

4. Sodic alkali basalt. 71400541. NA647464. Sample on or near roadside east of Waranguspik village.

5. Potassic tephrite. 74400007 (also 73680007). NA643462. Lava flow in road cutting east of Waranguspik village. This rock is classified as an olivine nephelinite (normative leucite) using the CIPW norm calculated volatile-free and standardising the oxidation of iron according to the equation of Irvine and Baragar (1971) - see Johnson & others (1976, Table 1).

6. Potassic tephrite. 74400047. NA640498. Lava flow by roadside north of Waramung Bay. Above comment for sample FNI-5 also applies to this sample.

7. Potassic phonolitic tephrite. 76400061. NA644498. Boulder in stream north of Waramung Bay.

8. Potassic phonolitic tephrite. 76400085. NA647464. Boulder in stream near road cutting east of Waranguspik village.

continued on next frame

Table FN1 cont. Ambitle Island

	9	10	11	12	13	14	15	16
SiO_2	51.05	45.58	51.3	45.6	47.32	46.6	46.0	48.91
TiO_2	0.64	0.92	0.63	0.92	0.85	0.79	0.70	0.77
Al_2O_3	16.63	13.96	17.0	14.0	15.73	15.3	17.4	16.83
Fe_2O_3	3.62	5.31	3.75	7.05	5.46	6.30	5.65	5.04
FeO	3.21	6.62	3.05	4.75	4.48	4.65	4.15	4.36
MnO	0.15	0.23	0.16	0.21	0.20	0.21	0.24	0.20
MgO	6.95	6.16	5.70	5.55	5.24	5.00	4.40	4.26
CaO	6.65	12.15	6.85	10.8	10.24	11.1	11.1	8.96
Na_2O	6.04	4.16	6.15	4.20	5.26	2.30	3.50	4.76
K_2O	3.46	3.21	3.55	3.05	3.84	2.95	3.35	3.01
P_2O_5	0.31	0.71	0.34	0.66	0.58	0.66	0.64	0.60
S	0.20	<0.02	0.18	0.14	<0.02	<0.01	0.03	<0.02
H_2O+	0.36	0.42	0.54	2.05	0.47	1.91	2.25	1.89
H_2O-	0.09	0.12	0.34	0.28	0.11	1.93	0.59	0.20
CO_2	0.38	0.13	0.10	0.30	0.27	0.25	0.15	0.17
rest	0.40	0.38			0.37			0.31
	100.14		99.64	99.56			100.15	
O=S	0.10		0.09	0.07			0.01	
Total	100.04	100.06	99.55	99.49	100.42	99.95	100.14	100.27
Trace elements								
Ba	405	205			290			235
Rb	56	61			70			48.0
Sr	1506	1709			1622			1555
Zr	78	76			78			68
Nb	5.0	2.5			3.0			2.5
Y	13	19			17			17
La	15	23			20			16
Ce	31	50			47			40
Nd	14	28			23			20
Sc	11	26			19			16
V	225	376			327			294
Cr	292	16			21			11
Co	38	48			38			34
Ni	191	31			28			21
Cu	174	209			198			11
Zn	67	109			88			84
Ga	21.5	18.5			20.5			18.0

9. Potassic phonolitic tephrite. 76400063. NA644498. Boulder in stream north of Waramung Bay.

10. Potassic phonolitic tephrite. 76400077. NA647464. Boulder in stream near road cutting east of Waranguspik village.

11. Potassic phonolitic tephrite. 74400011 (also 73680012). NA664513. Boulder in stream south of Fatkarson village.

12. Potassic phonolitic tephrite. 71400539. NA664477. Sample from Nanum River at northwestern edge of Nanum Plantation.

13. Potassic phonolitic tephrite. 76400082. NA633467. Boulder on beach near Tabulam village.

14. Potassic ne-trachybasalt. 74400003 (also 73680003). NA666483. Lava flow in Nanum River north of Nanum Plantation.

15. Potassic phonolitic tephrite. 74400009 (also 73680010). NA699464. Lava flow in Niffin River.

16. Potassic phonolitic tephrite. 76400065. NA640498. Boulder in stream near roadside north of Waramung Bay.

continued on next frame

Table FN1 cont. Ambitle Island

	17	18	19	20	21	22	23	24
SiO_2	55.40	47.2	54.0	48.8	54.5	49.21	53.3	55.8
TiO_2	0.57	0.86	0.68	0.69	0.80	0.78	0.70	0.68
Al_2O_3	16.51	17.1	16.8	18.0	17.9	18.63	18.4	17.7
Fe_2O_3	4.31	5.70	4.50	4.65	4.35	4.35	3.75	3.90
FeO	2.96	3.10	2.20	3.00	2.50	3.05	2.60	2.20
MnO	0.15	0.19	0.11	0.18	0.13	0.19	0.14	0.12
MgO	4.20	3.75	3.20	3.20	3.05	3.02	2.70	2.70
CaO	7.08	8.55	5.65	6.65	5.75	7.20	5.45	5.30
Na_2O	5.39	3.25	6.25	5.80	6.55	6.79	6.85	6.85
K_2O	2.66	3.95	3.55	4.95	3.40	4.48	3.95	3.35
P_2O_5	0.36	0.67	0.5[illegible]	0.45	0.43	0.64	0.44	0.40
S	<0.02	0.02	0.05	0.05	0.03	0.29	0.10	0.05
H_2O+	0.27	3.25	1.70	2.20	0.25	0.55	0.59	0.15
H_2O-	0.13	1.03	0.44	0.68	0.09	0.15	0.43	0.13
CO_2	0.06	1.20	0.02	0.08	<0.05	0.09	0.05	0.05
rest	0.34		0.35		0.36	0.45	0.37	
		99.82	99.89	99.38	100.09	99.87	99.82	99.38
O=S		0.01	0.02	0.02	0.01	0.14	0.05	0.02
Total	100.39	99.81	99.87	99.36	100.08	99.73	99.77	99.36
Trace elements								
Ba	400		450		440	365	445	
Rb	48.0		54		61	73	53	
Sr	1635		1780		1830	2195	1920	
Zr	88		87		90	103	91	
Nb	3.5		4		4	5.0	4	
Y	14		11		12	18	12	
La	13		12		14	22	14	
Ce	32		29		34	54	32	
Nd	16		13		15	26	15	
Sc	14		10		9	9	7	
V	204		217		217	319	224	
Cr	47		15		11	3	10	
Co	26					26		
Ni	31		10		5	8	6	
Cu	80		103		131	266	136	
Zn	63		42		51	86	51	
Ga	18.5		22.0		22.5	24.5	22.0	

17. Sodic ne-trachybasalt. 76400067. NA636496. Lava flow by roadside north of Waramung Bay.

18. Potassic ne-trachybasalt. 71400545. NA647464. Sample on or near roadside east of Waranguspik village.

19. Potassic ne-trachyandesite. 69400312. NA670469. Sample on ridge east of Nanum Plantation.

20. Potassic phonolitic tephrite. 69400334. NA641482. Sample from near hot springs in Waramung Plantation.

21. Potassic tephritic phonolite. 74400048. NA655456. Boulder near roadside south of Nanum Bay.

22. Potassic phonolitic tephrite. 76400089. NA655456. Boulder near roadside south of Nanum Bay.

23. Potassic tephritic phonolite. 69400314. NA670469. Sample from ridge east of Nanum Plantation.

24. Sodic ne-trachyandesite. 74400010 (also 73680011). NA656452. Boulder in roadcut on southern side of Nanum Bay.

continued on next frame

Table 1N1 cont. Ambitle Island

	25	26	27	28
SiO_2	55.93	57.3	55.29	69.0
TiO_2	0.67	0.60	0.61	0.17
Al_2O_3	17.95	18.2	19.26	15.9
Fe_2O_3	3.74	5.50	3.37	0.84
FeO	2.09	0.67	1.99	0.51
MnO	0.11	0.13	0.13	0.03
MgO	2.64	2.20	2.14	1.02
CaO	5.14	5.35	5.22	0.30
Na_2O	7.00	5.60	6.61	7.85
K_2O	3.38	3.30	3.76	2.50
P_2O_5	0.38	0.35	0.41	0.08
S	0.09	<0.01	0.09	0.02
H_2O+	0.18	0.50	0.46	1.13
H_2O-	0.12	0.30	0.17	0.23
CO_2	0.20	<0.05	0.26	0.05
rest	0.35		0.39	0.20
	99.97		100.16	99.82
O=S	0.04		0.04	0.01
Total	99.93	100.00	100.12	99.81
Trace elements				
Ba	420		395	450
Rb	57		57	44.5
Sr	1773		2016	935
Zr	86		93	68
Nb	4.0		4.0	3
Y	11		13	1
La	12		17	2
Ce	28		38	3
Nd	13		17	<1
Sc	9		8	2
V	217		202	27
Cr	4		3	55
Co	17		15	
Ni	8		5	16
Cu	110		163	30
Zn	46		55	36
Ga	22.5		22.5	18.5

25. Sodic ne-trachyandesite. 76400090. NA656452. Lava flow in roadcut on southern side of Nanum Bay.

26. Potassic hy-trachyandesite. 74400008 (also 75680008). NA644505. Lava flow near roadside north of Waramung Bay.

27. Potassic ne-trachyandesite. 76400058. NA643502. Boulder in stream north of Waramung Bay.

28. Sodic Q-trachyte. 74400004 (also 73680004). NA696489. Volcanic rudite on western rim of the central crater.

Table FN2. Babase Island

	1	2	3	4
SiO_2	48.6	50.3	53.4	64.7
TiO_2	1.03	0.75	0.77	0.39
Al_2O_3	17.9	18.7	19.0	18.9
Fe_2O_3	4.75	4.95	4.70	1.85
FeO	5.15	3.20	2.75	0.99
MnO	0.19	0.26	0.20	0.06
MgO	5.10	2.85	2.80	0.92
CaO	9.65	9.55	7.55	3.25
Na_2O	2.70	4.60	4.15	5.60
K_2O	1.87	2.75	3.00	2.25
P_2O_5	0.37	0.48	0.38	0.13
S	0.03	0.02	0.03	0.01
H_2O+	1.48	0.67	0.73	0.87
H_2O-	0.66	0.67	0.52	0.29
CO_2	0.20	0.20	<0.05	0.05
rest				
	99.68	99.95	99.99	
O=S	0.01	0.01	0.01	
Total	99.67	99.94	99.98	100.26
Trace elements				
Ba				
Rb				
Sr				
Zr				
Nb				
Y				
La				
Ce				
Nd				
Sc				
V				
Cr				
Co				
Ni				
Cu				
Zn				
Ga				

1. Potassic transitional basalt. 71400517. NA776552 (approximate). Exact locality uncertain.

2. Potassic ne-trachybasalt. 74400005 (also 73680005). NA776557. Lava flow on western flank of Babase volcano. This rock is classified as a potassic phonolitic tephrite using the CIPW norm calculated volatile-free and standardising the oxidation state of iron according to the equation of Irvine & Baragar (1971) - see Johnson & others (1976, Table 1).

3. Potassic hy-trachybasalt. 71400516. NA776552 (approximate). Exact locality uncertain.

4. Sodic Q-trachyte. 71400522. NA776552 (approximate). Exact locality uncertain. This sample is the most silica-saturated of all the analysed Q-trachytes from the Tabar-to-Feni Islands, and because its Fe_2O_3/FeO value has not been adjusted, it plots just to the right of the field of Q-trachytes in Figure 16 Strictly speaking it is an alkali-rich dacite, but for convenience it is here called a trachyte.

Table 13. Additional trace-element data for 8 rocks from Feni Islands determined by spark-source mass spectrography

	FN1/6	FN1/10	FN1/13	FN1/19	FN1/21	FN1/23	FN1/27	FN1/28
Cs	0.66	0.77	1.43	0.89	1.0	1.03	1.4	1.8
Pb	16	10	14	12	14	14	12	14
La	20.6	20.3	22.9	12.6	14.4	15.6	19.8	0.78
Ce	50.1	50.0	56.1	27.0	31.5	35.4	43.9	1.90
Pr	6.60	6.85	6.47	3.68	4.06	4.42	4.89	0.24
Nd	30.6	31.2	28.2	16.3	18.1	18.8	21.0	1.11
Sm	6.65	7.26	6.17	3.61	3.70	3.91	4.34	0.34
Eu	1.93	2.12	1.78	1.15	1.13	1.19	1.29	0.12
Gd	5.60	6.34	4.82	3.30	3.40	3.32	3.60	0.30
Tb	0.65	0.80	0.66	0.42	0.41	0.46	0.51	0.05
Dy	3.26	4.16	3.44	2.40	2.17	2.57	2.86	0.30
Ho	0.57	0.68	0.62	0.42	0.41	0.42	0.49	0.06
Er	1.28	1.69	1.58	1.01	1.00	1.03	1.35	0.18
Tm	0.17[a]	0.19	0.18	0.15[a]	0.15[a]	0.16[a]	0.18	0.04[a]
Yb	1.20	1.42	1.37	1.06	0.99	1.02	1.25	0.25
Lu[a]	0.19	0.22	0.21	0.17	0.16	0.18	0.20	0.04
Th	1.29	1.69	2.16	1.67	1.58	1.59	2.07	0.29
U	0.81	1.01	1.28	1.46	1.24	1.22	1.33	0.53
Hf	1.74	2.3	2.1	2.68	2.28	2.07	3.0	1.60
Sn	0.92	1.2	1.2	0.89	1.0	0.88	1.1	0.81
Mo	1.6	n.d.[b]	n.d.	2.1	3.5	2.6	n.d.	0.74

a. Interpolated value.

b. n.d.: not determined.

Table 14. Summary of mineral compositional data for the Feni Islands.

Sample	Clinopyroxene	Amphibole	Olivine	Biotite
Lavas:				
FN1/6	diopside/Al-salite		Fo_{87-43}	
FN1/9	diopside/salite		Fo_{93-74}	
FN1/10	diopside/Al-salite	tschermakitic hornblende		
FN1/13	diopside/salite		Fo_{90-47}	
FN1/15	salite/Al-salite	magnesiohastingsite		
FN1/21	salite		Fo_{80}	
FN1/22	salite	magnesiohastingsite		
FN1/24	salite	magnesiohastingsite	Fo_{86-84}	
Cumulates:				
FN1/1	salite		Fo_{84-81}	
FN1/32	diopside			
FN1/33	diopside/salite	magnesiohastingsite	Fo_{85-83}	
FN1/34	diopside/salite		Fo_{81-79}	Mg_{66}
FN1/35	diopside		Fo_{87-81}	Mg_{85-82}

	Oxide	Feldspar	Feldspathoid	Other
Lavas:				
FN1/6	mt	An_{57-17}	leucite, sodalite	
FN1/9	mt	An_{26}-Or_{56}	leucite, haüyne/sodalite	apatite
FN1/10	mt	Or_{34-42}	leucite	
FN1/13	mt	An_{62-35}	leucite	apatite
FN1/15	mt	An_{88-72}, Or_{66}		analcite, zeolite
FN1/21	mt	An_{57}-Or_{33}	haüyne/sodalite	apatite
FN1/22	mt	An_{49-21}	haüyne	apatite
FN1/24	mt	An_{42}-Or_{54}	haüyne, sodalite	apatite
Cumulates:				
FN1/1	mt			
FN1/32	mt	An_{23}-Or_{52}	leucite, sodalite	apatite
FN1/33				zeolite, glass
FN1/34	mt	An_{78}-Or_{86}	haüyne, sodalite	apatite
FN1/35	chromian-mt/mt	An_{41}-Or_{48}	haüyne	apatite

Abbreviations. Fo: forsterite; mt: magnetite; An: anorthite; Or: orthoclase. Slash between two mineral names refers to compositional continuity (solid solution) between the minerals.

Table 15. Compositions of thermal waters from Ambitle Island

Location	Area A				Area B
	0.1 km inland	0.1 km inland	1 km inland	1 km inland	0.9 km inland
Sample no.	F3	029	F2	028	031
Collection date	22 Oct 1974	10 Jan 1973	22 Oct 1974	10 Jan 1973	11 Jan 1973
Temp. ^{o}C	99	99	99	99	95
pH (20^{o})	9.1	8.8	8.3	3.0	8.2
E.C. micro··s/cm	31086	-	2766	-	-
Total dis..olved solids (mg/l)	35968	-	1576	-	-
Al	0.04	-	0.22	-	-
Cu	<0.01	-	<0.01	-	-
Fe	0.255	-	0.045	-	-
Mn	0.025	-	<0.005	-	-
Zn	0.02	-	<0.005	-	-
As	5.9	-	0.6	-	-
Hg	<0.0001	-	<0.0001	-	-
Sr	2.7	-	0.08	-	-
Rb	2.62	-	0.46	-	-
Ca	10	9.6	2	37.4	5.5
Mg	n.d.	0.4	n.d.	56.0	0.9
Na	11975	>5000	528	8.1	>5000
K	1820	2025	63	8.5	1525
Li	5.20	-	0.45	-	-
B	50	-	4.3	-	-
F	6.55	-	3.0	-	-
Cl	14465	14640	464	-	11486
Br	36	-	<2	-	-
SO_4	7501	8900	477	650	6120
NO_3	<1	-	<1	-	-
CO_3	118	-	n.d.	-	-
HCO_3	147	-	80	-	-
SiO_2	145	-	121	-	-

n.d.: not detected

continued on next frame

Table 15 cont.

Location	Area C				Average Ocean
	Main area 2.0 km inland	Stream from main area	Midpool	Base of dome 2.1 km inland	
Sample no.	030	032	033	F1	
Collection date	11 Jan 1973	11 Jan 1973	11 Jan 1973	22 Oct 1974	
Temp. ^{o}C	73	45	77	99	
pH (20^{o})	1.9	2.5	1.9	8.1	8.3
E.C. micro-s/cm	-	-	-	6454	
Total dissolved solids (mg/l)	-	-	-	4342	
Al	-	-	-	0.02	0.01
Cu	-	-	-	< 0.01	0.003
Fe	-	-	-	0.125	1.3
Mn	-	-	-	0.055	0.002
Zn	-	-	-	0.01	0.01
As	-	-	-	5.6	0.003
Hg	-	-	-	< 0.0001	3×10^{-5}
Sr	-	-	-	0.75	8
Rb	-	-	-	0.49	0.12
Ca	1.3	5.2	1.2	3	400
Mg	2.5	10.0	1.4	n.d.	1272
Na	29.2	34.1	54.5	1550	10600
K	2.8	18.8	3.7	130	380
Li	-	-	-	1.80	0.17
B	-	-	-	13.5	4.6
F	-	-	-	3.25	1.3
Cl	284	70.9	31.9	1769	18980
Br	-	-	-	6	65
SO_4	1200	310	1000	782	2649
NO_3	-	-	-	< 1	-
CO_3	-	-	-	n.d.	-
HCO_3	-	-	-	214	140
SiO_2	-	-	-	131	6.4

Analyses by Mines Division Laboratory (Port Moresby), except for samples F1, F2, and F3 which were analysed by Amdel.

Table 16. Ionic ratios for thermal waters from Ambitle Island.

	Area A				Area B
Location	0.1 km inland	0.1 km inland	1 km inland	1 km inland	0.9 km inland
Sample no.	F3	029	F2	028	031
Na/Cl	0.828	>0.342	1.138	-	>0.435
B/Cl	0.0035	-	0.0093	-	-
SO_4/Cl	0.52	0.46	1.03	-	0.53
Ca/Na	0.001	<0.002	0.004	4.617	0.001
K/Na	0.152	<0.405	0.119	1.049	<0.305
Li/Na	43×10^{-5}	-	85×10^{-5}	-	-
Mg/Ca	-	0.042	-	1.5	0.2

	Area C				
Location	Main area 2.0 km inland	Stream from main area	Mudpool	Base of dome 2.1 km inland	Average Ocean
Sample no.	030	032	033	F1	
Na/Cl	0.103	0.481	1.71	0.876	0.558
B/Cl	-	-	-	0.0076	0.0002
SO_4/Cl	4.23	4.37	31.4	0.44	0.14
Ca/Na	0.045	0.152	0.022	0.002	0.038
K/Na	0.099	0.551	0.068	0.084	0.036
Li/Na	-	-	-	116×10^{-5}	1.6×10^{-5}
Mg/Ca	1.9	1.9	1.2	-	3.2

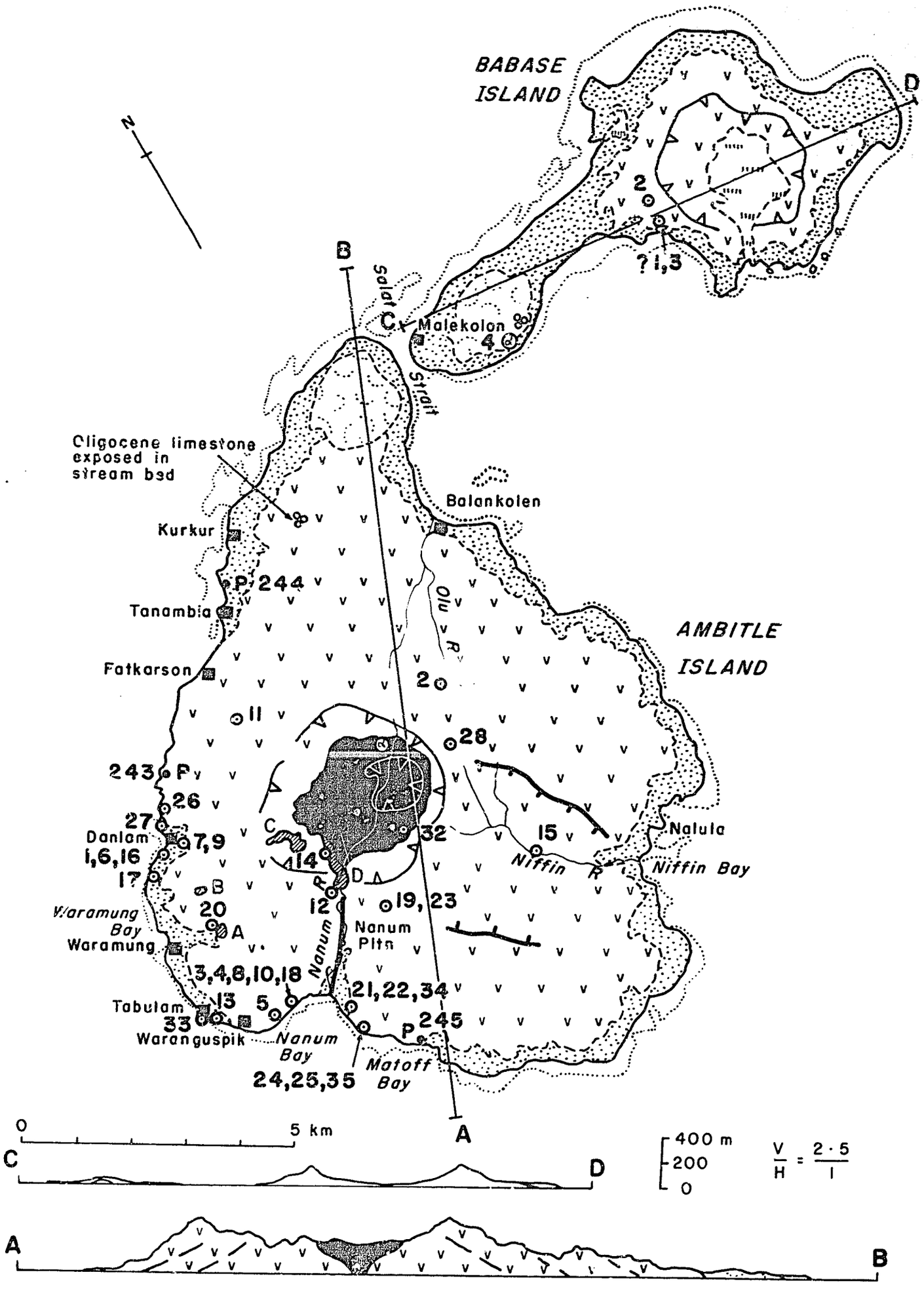

Figure 15a. Geology of the Feni Islands (see legend in Fig. 2).

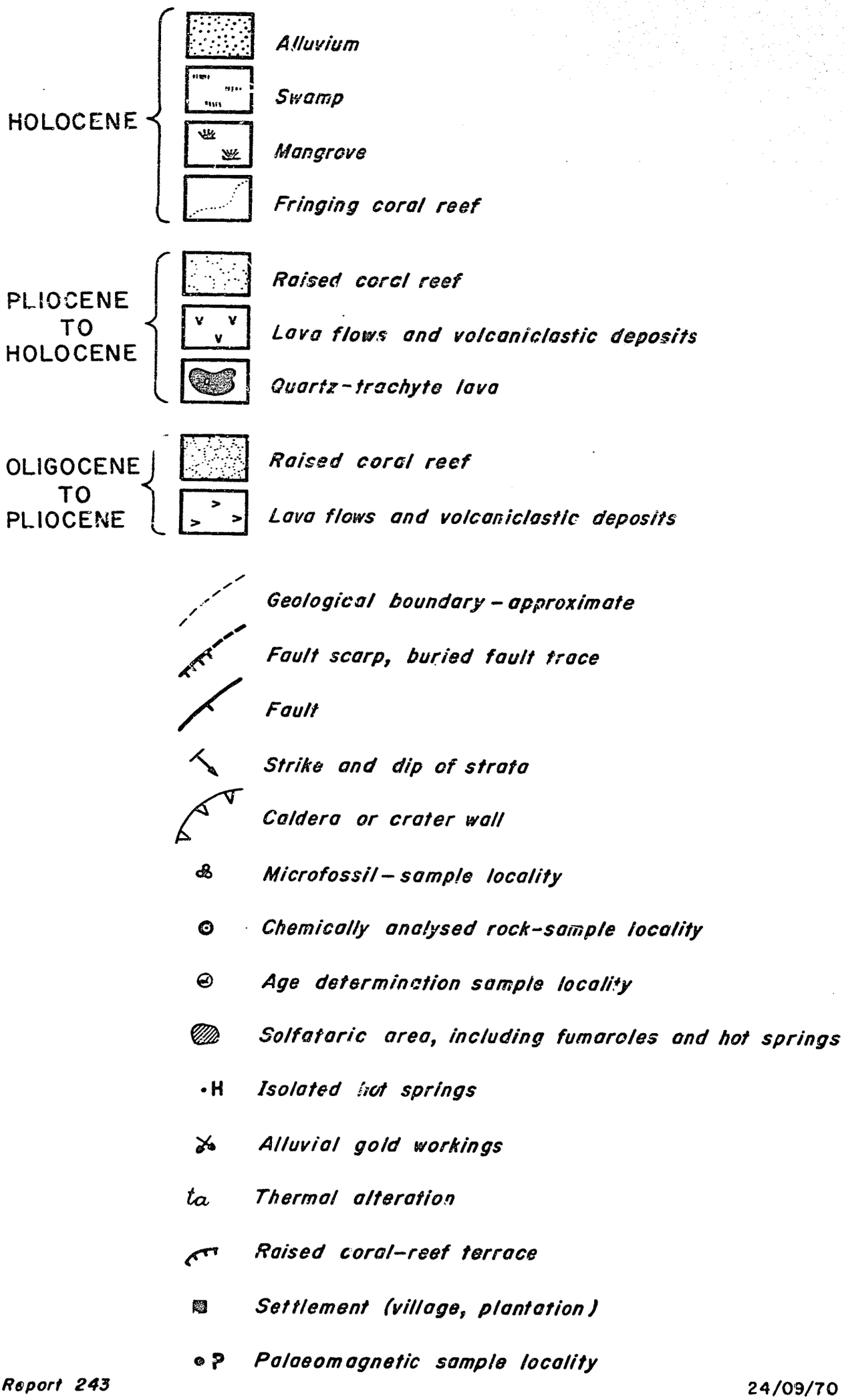

Figure 2. Legend to geological maps (Figs 4-6, 9, 12, 15).

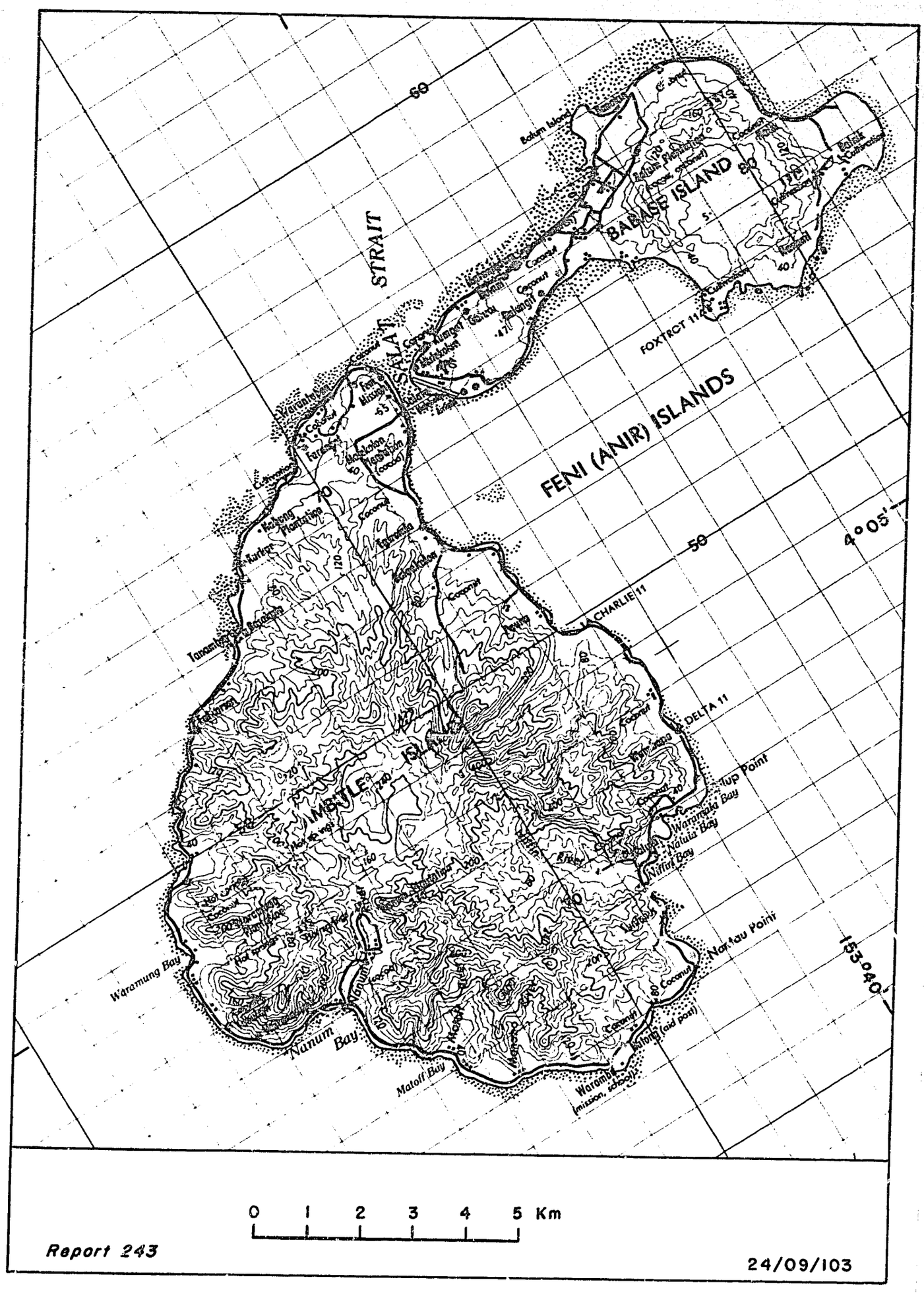

Figure 15b. Topography of Feni Islands.

Part of Sheet 9689 (Edition 1) Series T601, Papua New Guinea 1:100 000 Topographic Survey, reproduced by permission of the Surveyor General, Department of Lands and Surveys, Papua New Guinea.

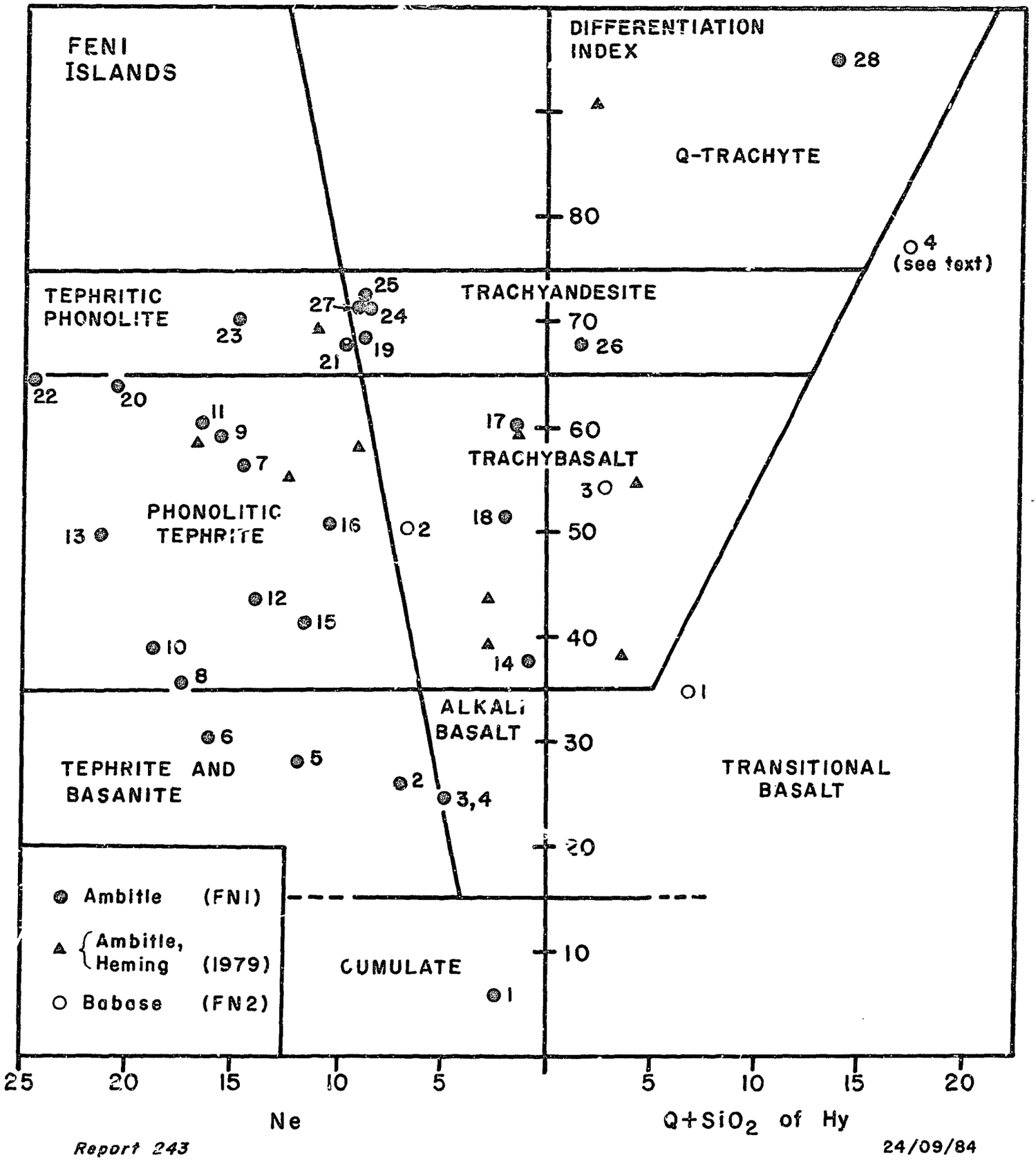

Figure 16. Rock-nomenclature diagram for rocks from the Feni Islands (see Fig. 3). Chemical analyses listed in Tables FN1-2.

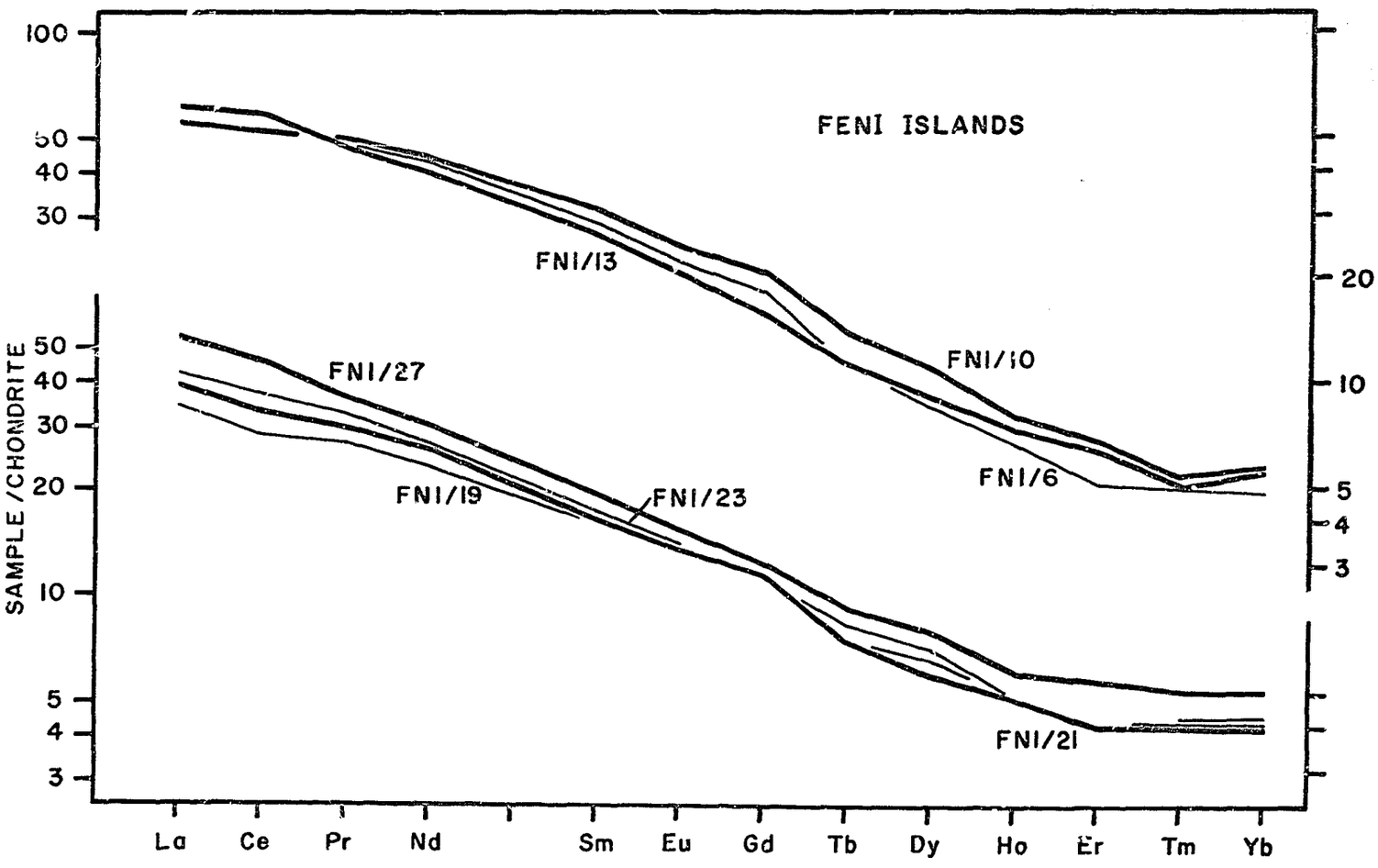

Figure 17. Chondrite-normalised REE abundances in seven rocks from the Feni Islands (see also Fig. 18). Data listed in Table 13.

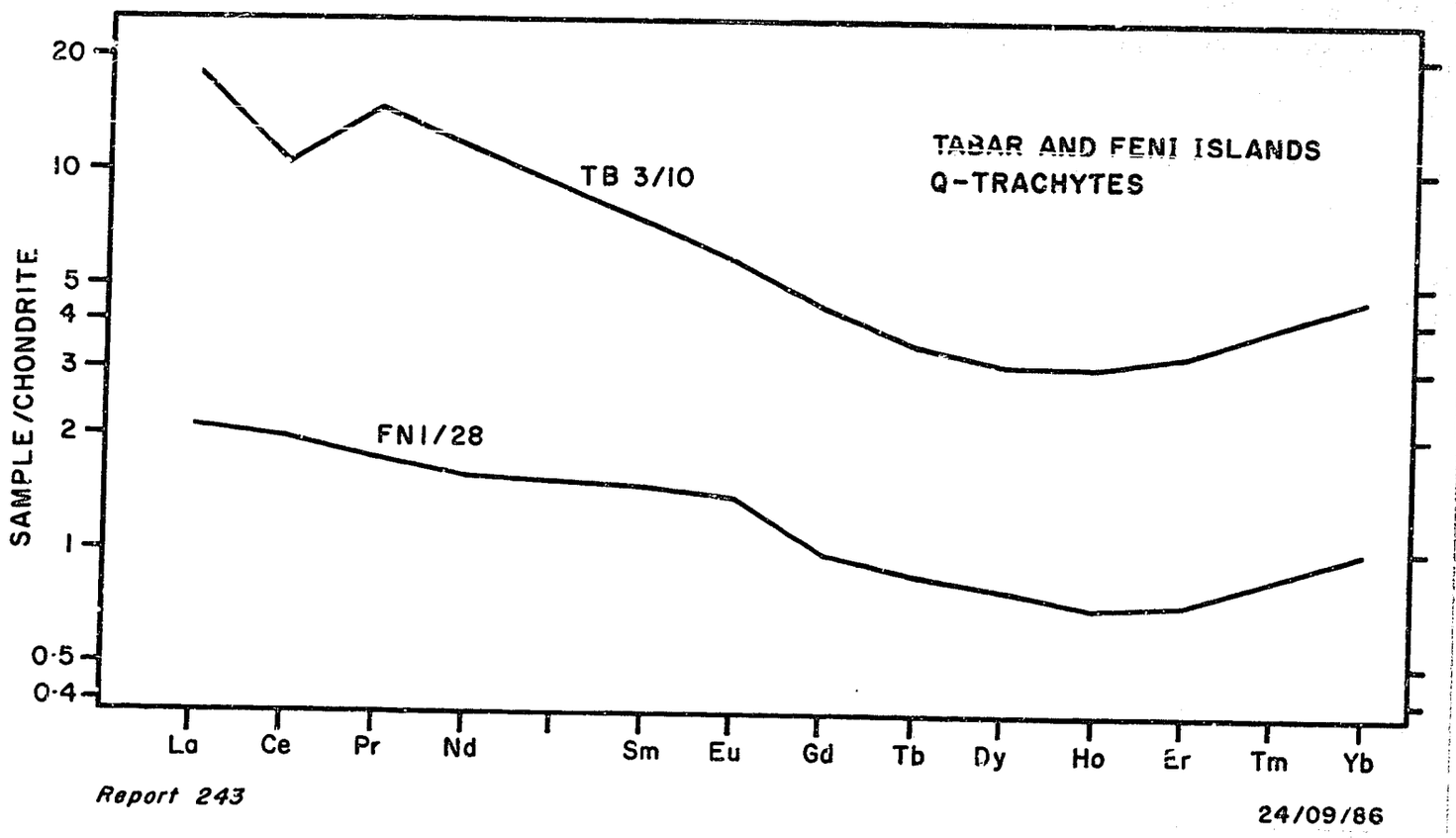

Figure 18. Chondrite-normalised REE abundances for two Q-trachytes from Tabar and Feni Islands. Data listed in Tables 5, 13.

ASPECTS OF REGIONAL GEOLOGY AND STRUCTURE

Some aspects of the regional, largely submarine geology of the Tabar-to-Feni chain are especially pertinent in evaluating the significance of the subaerial geology described above. These will not be dealt with here in detail, but opportunity is taken to present some of the regional information that is not readily available to the general reader, and to update previous interpretations of regional structure (Johnson & others, 1976; Johnson, 1979).

Bathymetry

The Tabar-to-Feni Islands rise from a shelf that extends from the northeastern coast of New Ireland northeastwards to the Lyra-Kilinailau Trough (Fig. 19). Tanga volcano and the Ambitle-Babase complex are both slightly elliptical cones whose basal diameters on the shelf floor are about 25 km, whereas the Tabar and Lihir complexes are less symmetrical and are elongated roughly north-south.

Striking morphological features of the shelf between New Ireland and the Lyra-Kilinailau Trough are: (1) a step-like increase in depth towards the southeast; (2) the siting of each island group on one of the 'steps'. The Tabar and Lihir complexes rise from seafloor about 1200m and 1600m deep, respectively, and the Tanga and Feni complexes rise from seafloor about 2000 m and 2400m deep, respectively (Fig. 19).

Seismicity

The New Britain, southern New Ireland, and Bougainville Island region represents one of the most seismically active areas anywhere in the world. In contrast, the Tabar-to-Feni chain has much less seismicity (Fig. 20). However, two seismological features of interest are shown on the epicentre map for earthquakes recorded in 1960-1979: (1) a linear zone of shallow (less than 70 km deep) earthquakes that trends north-northeastwards through Lihir, Mahur, and Masahet Islands, and which

extends southwestwards towards the Ramat Fault (Hohnen, 1978) on New Ireland; (2) a cluster of deep (342-476 km) earthquakes between Babase Island (Feni Islands) and the Lyra-Kilianailau Trough. The shallow earthquakes of the linear zone (1) are thought to represent movement along an active fault zone, members of which crop out on Lihir Island. The cluster of deep seismicity, on the other hand probably represents the deeper, more northerly parts of the Solomon Sea lithospheric plate that is being subducted northeastwards beneath Bougainville Island. The Feni Islands therefore overlie the deep parts of this downgoing slab, but not the Tabar, Lihir, and Tanga Islands.

Seismic-reflection profiles

The most systematic and comprehensive marine seismic survey to date of the area east and north of New Ireland, was that carried out by the Gulf oil company as part of a world-wide study (Gulf Oil Research and Development, 1973; see also, however: Murauchi, Ludwig, Den, Hotta, Asanuma, Yoshi , Kubotesa, & Hagiwara, 1973; Furumoto, Webb, Odegard, & Hussong, 1976; De Broin, Aubertin, & Ravenne, 1977). The Gulf seismic-reflection data were obtained using an Aquapulse (oxygen-propane) multi-channel system, and seismic profiles were run from the St Matthias Islands in the northwest to the southern tip of New Ireland, including the shelf between New Ireland and the Lyra-Kilinailau Trough (Figs 20, 21). A general interpretation of the zone east of New Ireland given by Gulf (page 42-43) is as follows:

'This sector is occupied by a deep sedimentary trough partially filled by a layered sequence which appears subdivided into two major units. The break between these units may be correlative with eastward tilting of New Ireland during the lower Miocene. The lower unit is tentatively correlated with the lower Miocene massive limestones that rest on the basement. In spite of some thickening of the lower portions of the trough, this unit generally parallels the inferred gross morphology of the basement from side to side of the depression and perhaps contributes to the building of the topographic high which represents the northern shoulder of the trough. The seismic appearance of the layer is indicative of a rather monotonous lithology possibly lacking major velocity discontinuities both within itself and at the contact with the basement. This partially accounts for the frequent failure of the data to resolve the basement topography. The overall

structural attitude and relatively constant thickness (up to 1.5 seconds or about 10,000 feet) of this lower unit suggests that it was deposited on a relatively planar surface and that the diastrophic process began towards the end of the deposition phase.

'The building of the upper unit was evidently subsequent to the main diastrophic episode, as shown by various diagnostic characteristics (Profile NI-20 and Profile NI-22). This upper unit shows evidence of a number of rock units or sedimentary aprons, that are derived largely from the uplifted New Ireland. Each of these sub-units rest [sic] at an unconformity surface. This upper unit is probably composed primarily of clastic rocks which were deposited in an environment dominated by variable sedimentological regimes, including slumping of semi-consolidated and unstable layers'.

The Gulf survey recognised a prominent, faulted, volcanic-basement ridge between the St Matthias Group and the Tabar Islands (Fig 20I-N), which is presumbly the northwestern end of the 'North Eastern Ridge' identified by De Broin & others (1977). This ridge is said to extend southeastwards, according to De Broin & others (1976), and to be offset by two or three, dextral, transcurrent faults before breaking sea-level and following the main axis of Bougainville Island. However, the ridge southeast of the Tabar Islands is not shown on the bathymetric map of Mammerickx, Chase, Smith & Taylor (1971; Fig.19). Ridge-like outlines seen on many of the Gulf reflection profiles run close to the Tabar-to-Feni Islands (Figs. 21A-C,E,F), but these may be individual diapir-like structures related to the Tabar-to-Feni volcanoes rather than parts of a continuous ridge.

A notable feature of the northwest basement ridge is that the overlying lower sedimentary cover appears to be deformed by the basement and to conform to its topographic profile (Figs 21I-N). Basement is not so clearly recognised from the Tabar Islands to the Feni Islands (Figs. 21A-G), but a similar style of localised deformation of basal sediments may be indicative of diapir-like processes. The Tabar-to-Feni volcanoes therefore appear to lie on a narrow zone of structural weakness which, at least in the northwest, may have a horst-like form and along which igneous diapirs may have been sufficiently forceful to breach the ocean-floor sedimentary pile and produce magma at the surface. Other diapirs or horsts may exist off the main structural axis (see,

for example, Fig. 21B).

Diapirically deformed sediments apparently mantling an igneous core are seen in Fig. 21A, a profile through the northern flank of the Feni-Babase complex (see also Furumoto & others, 1976, Fig. 11), and the upwarped sedimentary cover appears to correlate with the inlier of middle Oligocene, formainiferal calcilutite exposed in the north of Ambitle Island. However, this age conflicts with the early Miocene age tentatively proposed by Gulf (see above) for the lower sedimentary unit which is therefore not equivalent to the Lelet Limestone on New Ireland (Hohnen, 1978) but older. Possibly it is a time-stratigraphic equivalent of middle Eocene to upper Oligocene limestone (Hohnen, 1978) found within the adjacent Jaulu Volcanics of New Ireland. Determining the age of the deformed sediments may in future studies, provide an important means of dating the onset of the Tabar-to-Feni volcanism. The onset of volcanism was post-Oligocene in the case of the Feni Islands, and other minimum ages could be determined elsewhere in the chain by obtaining palaeontological dates from other parts of the deformed-sedimentary sequence off-shore from the Tabar-to-Feni Islands.

The evidence for a series of dextral transcurrent faults between Lihir and Feni (De Broin & others, 1977) is not compelling, as these presumed faults offset neither the Tabar-to-Feni chain nor New Ireland. Any submarine fractures are more likely to be normal faults that have caused the apparent southeastward downstepping of the seafloor on which the Tabar-to-Feni volcanism seems to have taken place.

Tectonic provenance

Coleman & Packham (1976) suggested that a major tectonic boundary runs between New Ireland and the Tabar-to-Feni chain - that is, between the Bismarck Archipelago to the west and a 'Solomon Block' to the east. There is, however, little direct support for this concept. Neither the seismic-reflection profiles (see above) nor the deep-seismic refraction studies of the region (Murauchi & others, 1973; Finlayson & Cull, 1973; Furumoto & others, 1976) provide any evidence for major dislocations between New Ireland and the Tabar-to-Feni chain. The chain is parallel to and colinear with New Ireland, and the available evidence, albeit incomplete, is consistent with both the volcanic chain and New Ireland having been part of the same tectonic unit for most, if not all, of the Cainozoic.

DISCUSSION

Geological history

The Tabar-to-Feni volcanoes were probably created in the mid-Tertiary, and they continued to be active certainly until the late Pleistocene and possibly into the Holocene. Middle Oligocene basal limestone unconformably underlies the volcanic rocks of Ambitle Island in the Feni Islands, and volcanic rocks underlie lower-to-upper Miocene reef limestone on Simberi Island (Tabar Islands), but these are the only constraints on the time that volcanism began in the island chain. Most of the volcanism may have taken place during the Pliocene and Pleistocene, but this is based mainly on qualitative comparisons of relative degrees of dissection, rather than on a comprehensive set of radiometric and palaeonotological dates. There is a clear need for a systematic geochronological study of the Tabar-to-Feni Islands.

The duration and time of volcanic activity may be more or less the same in each of the four island groups, and there is no evidence, so far, of volcanism having migrated along the island chain. The oldest known subaerial volcanic rocks are in the Tabar and Lihir groups, but the youngest rocks in all four island groups appear to have similar Quaternary ages. Furthermore, low-temperature (less than 100°C) thermal activity is found in all four island groups (especially on Lihir and Ambitle Islands), signifying that a high geothermal gradient persists throughout the volcanic chain, and that some of the volcanoes should be regarded as dormant.

Subsidence and uplift of the volcanoes took place throughout the Tabar-to-Feni province, as shown by raised limestone cappings and platforms on the subaerial volcanic rocks on many of the islands; up to three phases of uplift are indicated by terraced limestone on Boang, Mahur and Masahet Islands. The orientations of the raised limestone are consistent with a general tilting towards the south and southwest in each of the four island groups during the Pleistocene; there is no clear evidence for any pre-Quaternary phases of tilting. The southerly sense of tilt in the Tabar-to-Feni Islands is almost opposite to that of the New Ireland horst, where northeasterly tilting accompanied uplift after the upper Pliocene (Hohnen, 1978). This southerly tilt may relate to the apparent step-faulting that resulted in the segmentation of the New Ireland/

Lyra-Kilinailau shelf into fault blocks downthrown progressively to the southeast (see previous section).

The timing of these events appears to be similar to that of the later tectonic history of New Ireland outlined by Hohnen (1978). New Ireland was built up as a volcanic pile in the lower and middle Oligocene, and this was followed by erosion, submergence, and accretion of onlapping fringing reef in the Miocene. The area was then intruded by the last phases of the Lemau Intrusive Complex, and the submerged ridge became separated by a postulated graben. Volcanic activity took place within the graben from the upper Miocene to the lower Pliocene, together with general subsidence, and the present island was raised during the upper Pliocene and onwards as a fault-bounded horst, and progressively tilted to the northeast. The younger part of this history closely follows that thought to have taken place in the Tabar-to-Feni Islands - that is, block faulting, graben and horst formation, volcanism (and possibly attendant diapirism), and tilting of fault blocks.

The quartz trachytes of the Tabar-to-Feni Islands represent one of the more striking igneous features of the islands as they are in marked compositional contrast to the mainly alkaline mafic and intermediate rocks in the remainder of the chain. Quartz trachytes from the Tabar, Tanga, and Feni Islands have been chemically analysed, and the altered central plug of Luise caldera on Lihir Island was probably originally quartz trachyte in composition. The quartz trachytes appear to represent the youngest extrusions in each of the four island groups, and all are probably as young as Middle to Upper Pleistocene. They may therefore represent a dramatic and synchronous change in magma composition throughout the island chain, possibly even marking the final stages of volcanism throughout the Tabar-to-Feni chain.

An active Benioff zone is absent beneath the length of the Tabar-to-Feni chain, although a downgoing slab could have existed in the Tertiary. The relationship between the composition of the Tabar-to-Feni magmas and this postulated subduction system is still uncertain, but the extensive Pliocene and Pleistocene volcanism represented on the islands may have been triggered by normal faulting related to the Pliocene opening of the Manus Basin west of New Ireland (Johnson, Mutter & Arculus, 1979).

Summary of geochemical results

The range of rock types in the Tabar-to-Feni chain is exceptionally wide - from basalt (ankaramite, transitional and alkali basalt, tephrite, and basanite), to voluminous intermediate types (both nepheline and quartz normative). Most of the analysed rocks are nepheline normative, and some of them strongly so (greater than 10 percent). There is a considerable overlap of rock compositions between the four island groups, but those of the Tabar and Lihir groups are generally more mafic and less undersaturated than are those from Tanga and Feni (Figs. 7,10,13,16; Table 2).

Most analysed rocks from the Tabar-to-Feni Islands have high total-alkali contents (mainly 5.5-11.0 weight percent), and K_2O/Na_2O values between 0.5 and 1.1. $FeO+Fe_2O_3$ values are less than 12 weight percent and in most samples Fe_2O_3 is greater than FeO. There is no trend of iron-enrichment as degrees of differentiation increases. Low TiO_2 (less than 1.2 weight percent), high Al_2O_3, low Th/U, and high Zr/Nb are typical island-arc features of these rocks. Zr, Ba, Ga, Al, Na, and K correlate positively with SiO_2 whereas Cr, Ni, Sc, V, Mg, Fe, Ca, Ti, Mn, Cu, Zn, and P_2O_5 correlate inversely with SiO_2. Sulphur values are relatively high (most between 0.3 and 0.4 weight percent), but there are no systematic differences. CaO/Al_2O_3 values decrease markedly as Mg/Fe values decrease. Low abundances of Zr, Hf, and Nb, and enrichments in some large-ion-lithophile (LIL) elements, relative to the light rare-earth elements (REE), are all typical island-arc features of these rocks. The enrichments in incompatible elements are similar to those in alkaline mafic rocks from other island arcs, but the high abundances of Sr (about 1400-2195 ppm), Pb (up to 45 ppm), and K_2O (greater than 4.5 weight percent) are unusual for island-arc volcanic rocks. Tabar-to-Feni volcanic rocks have moderate light-REE to heavy-REE fractionation (La_N/Yb_N = 2.8-11.6, where N represents chondrite-normalised value) which is not as extreme as in intraplate or continental-rift alkalic suites. The degree of light-REE enrichment correlates with increases in the contents of P_2O_5, Sr, and K_2O.

Tabar-to-Feni rocks can be divided into four groups on the basis of normative mineralogy and geochemistry: (1) silica-saturated to slightly undersaturated transitional basalts and alkali basalts, together with associated trachybasalts and trachyandesites; (2) strongly undersaturated tephrites, ne-trachybasalts, ne-trachytes, and phonolitic tephrites; (3) rarer basanites and

potassic tephrites; and (4) quartz trachytes. Rocks of group 1 (found mainly on the Tabar and Lihir island groups) are characterised by lower total-alkali contents, lower LIL-element abundances, higher CaO/Al_2O_3 and higher Zr/Nb (20-70) values, and by less fractionated chondrite-normalised REE patterns (Fig. 22), compared with rocks from groups 2 and 3. Group 2 rocks (particularly abundant in the Tanga and Feni Islands) have higher contents of alkali and LIL elements (especially Sr), lower CaO/Al_2O_3 and lower Zr/Nb (20-30) values, and more fractionated REE patterns (Fig. 22) than do the alkali and transitional basalts of group 1. Rocks of the third group appear to be uncommon, but have been found in all but the Tanga Islands. They have total-alkali contents and CaO/Al_2O_3 values similar to those of the transitional basalts (group 1), but have more fractionated REE patterns (Fig. 22) and greater depletions in heavy REE. Group 3 rocks have higher LIL-element contents, yet lower LIL-element/light-REE values than do rocks in the other two groups (Ba_N/La_N values of about 1). The quartz trachytes are found in all four island groups and may represent young crustal melts. They are extremely depleted in P_2O_5 and REE (Fig. 22), and have exceptionally high LIL-element/REE values.

The results of least-squares-mixing calculations do not support the interpretation that the three alkalic rock groups are related by crystal fractionation. However, the chemical evolution within suites 1,2 and 3 can be modelled satisfactorily by crystal fractionation of different proportions of clinopyroxene + olivine $\pm$ amphibole $\pm$ magnetite. This interpretation is supported by the differences in trace-element contents.

The $^{87}Sr/^{86}Sr$ values for 28 samples range from 0.70365 to 0.70452 (Table 3). These values do not correlate with differences in major-element compositions, except that the quartz-trachytes have Sr-isotopic ratios in the upper part of the range. $^{143}Nd/^{144}Nd$ values for seven samples (M.T. McCullough, unpublished data) range from ε_{Nd} = 8.6 to 5.4 and roughly correspond to increasing $^{87}Sr/^{86}Sr$ values. The ε_{Nd} values fall within the range (8.6-5.3) of a variety of other volcanic rock types from west Melanesian island arcs (Perfit, McCullough, & Johnson, 1982). Tabar-to-Feni isotopic data plot within, and slightly to the right of, the 'mantle array', in common with those for other intraoceanic island-arc suites. Samples with the least fractionated REE (group 1) generally have the highest ε_{Nd} values, and those with more fractionated REE patterns (group 3) have lower ε_{Nd} values. One quartz-trachyte from Tabar Island has Sr and Nd ratios

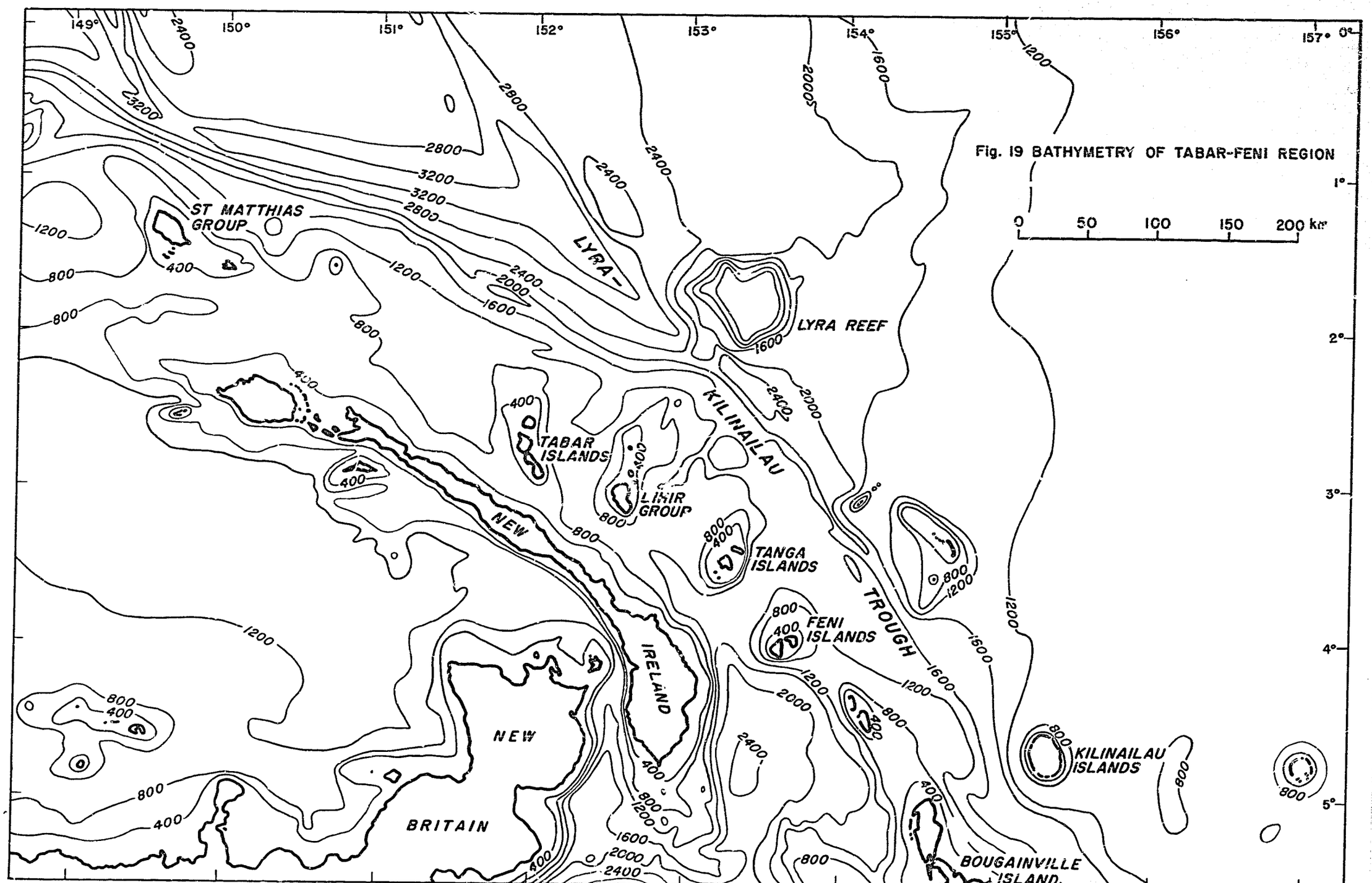

Figure 19. Bathymetry of Tabar-to-Feni region (adapted from Mammerickx & others, 1971; isobaths in fathoms).

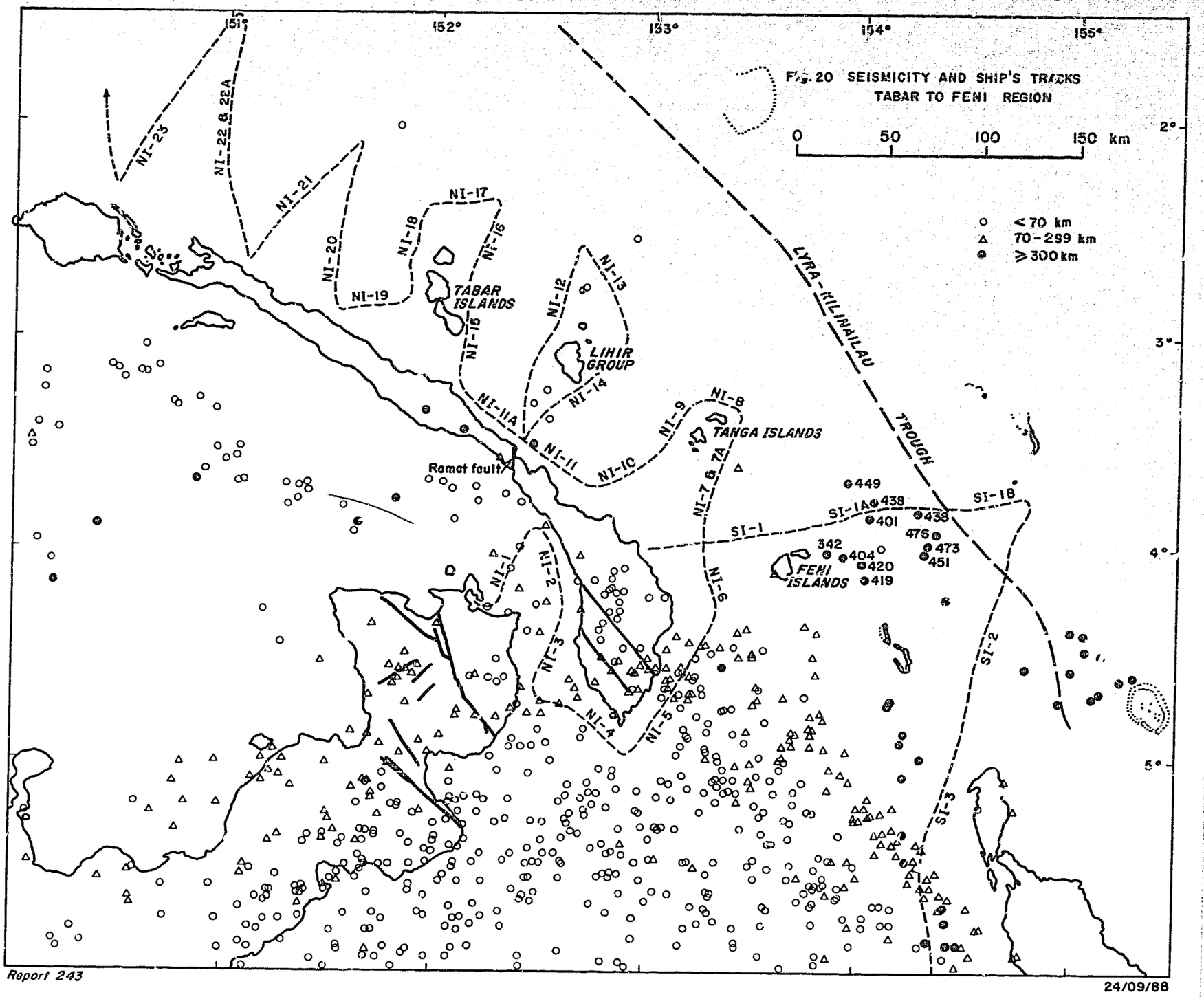

Figure 20. Epicentres of earthquakes recorded by 20 or more stations between January 1960 and December 1979 (BMR Earthquake Data File), and ship's tracks of seismic-reflection profiles given in Figure 21.

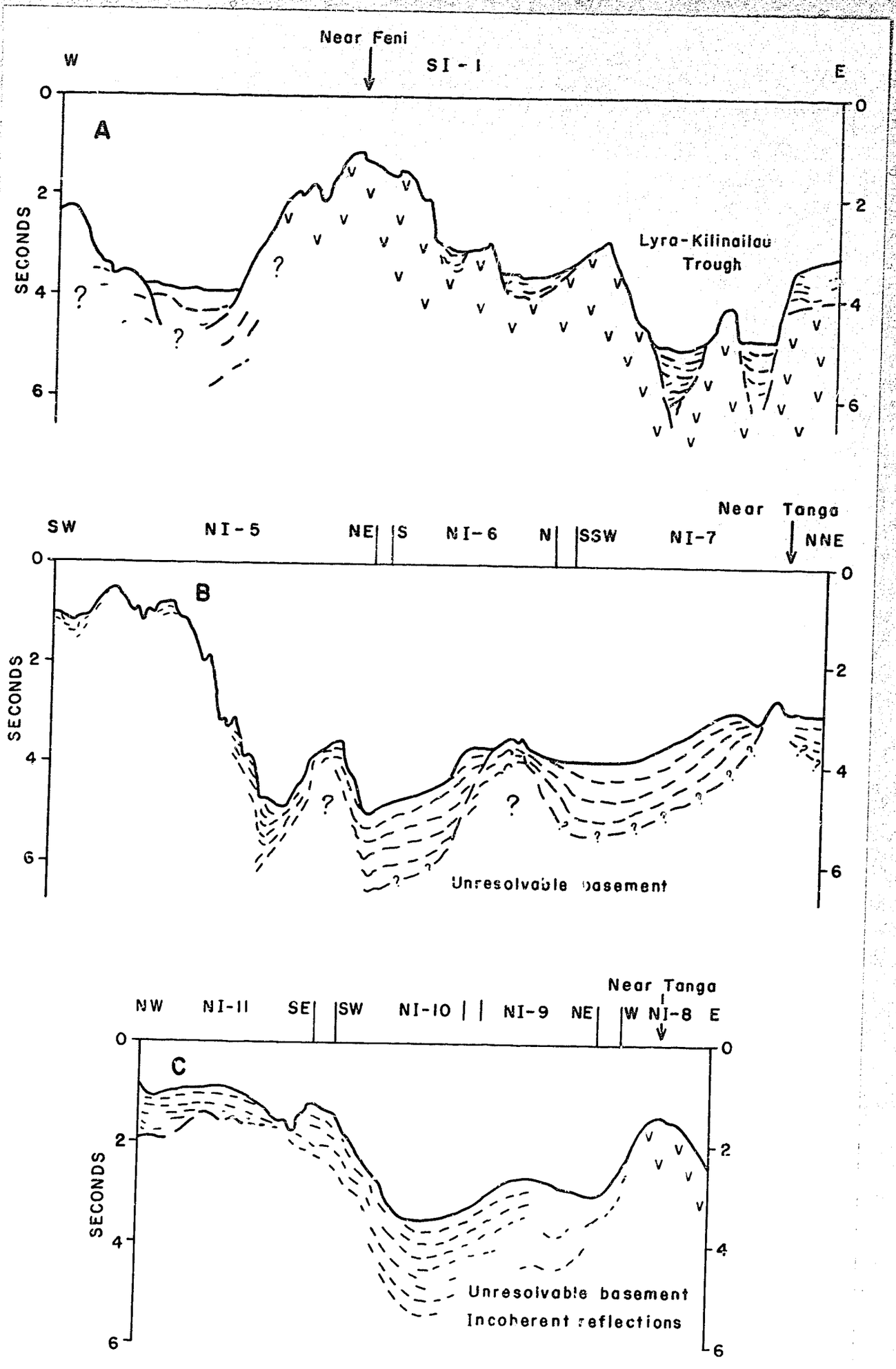

Figure 21. Interpretations of seismic-reflection profiles run in the Tabar-to-Feni region of Gulf Oil Research and Development (1973). Ship's tracks given in Fig. 20.

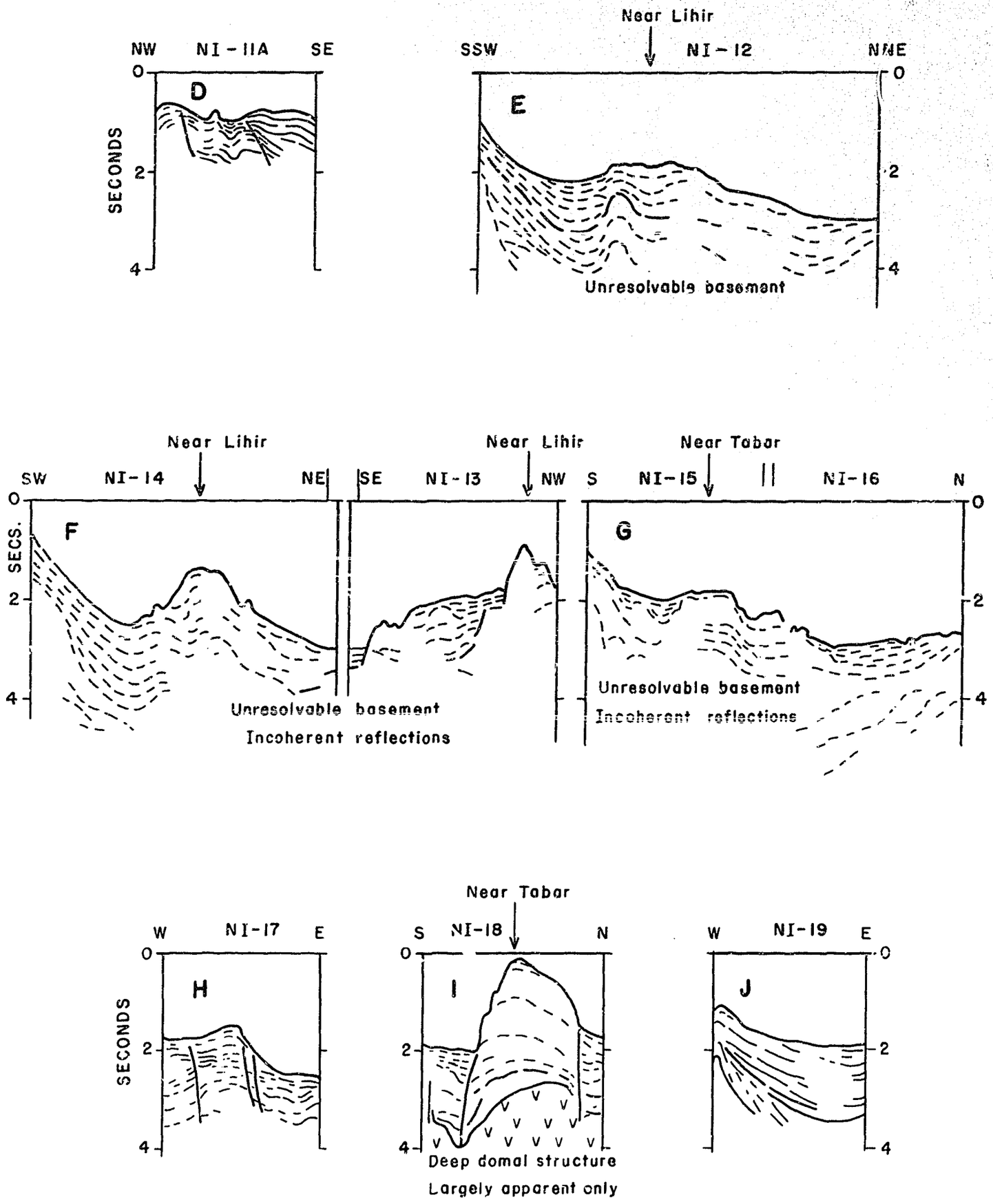

Figure 21. (continued) Interpretations of seismic-reflection profiles run in the Tabar-to-Feni region of Gulf Oil Research and Development (1973). Ship's tracks given in Fig. 20.

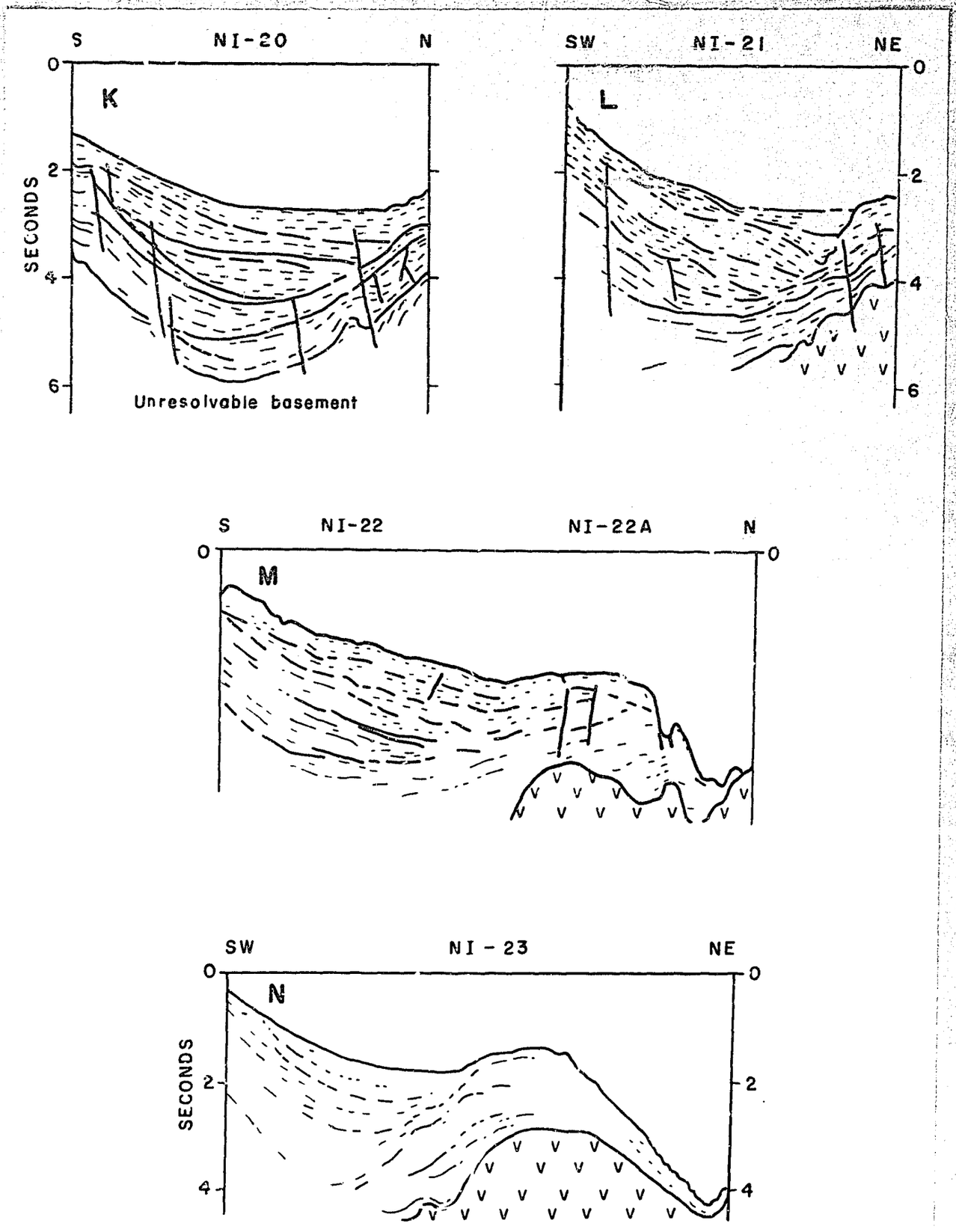

Figure 21. (continued) Interpretations of seismic-reflection profiles run in the Tabar-to-Feni region of Gulf Oil Research and Development (1973). Ship's tracks given in Fig. 20.

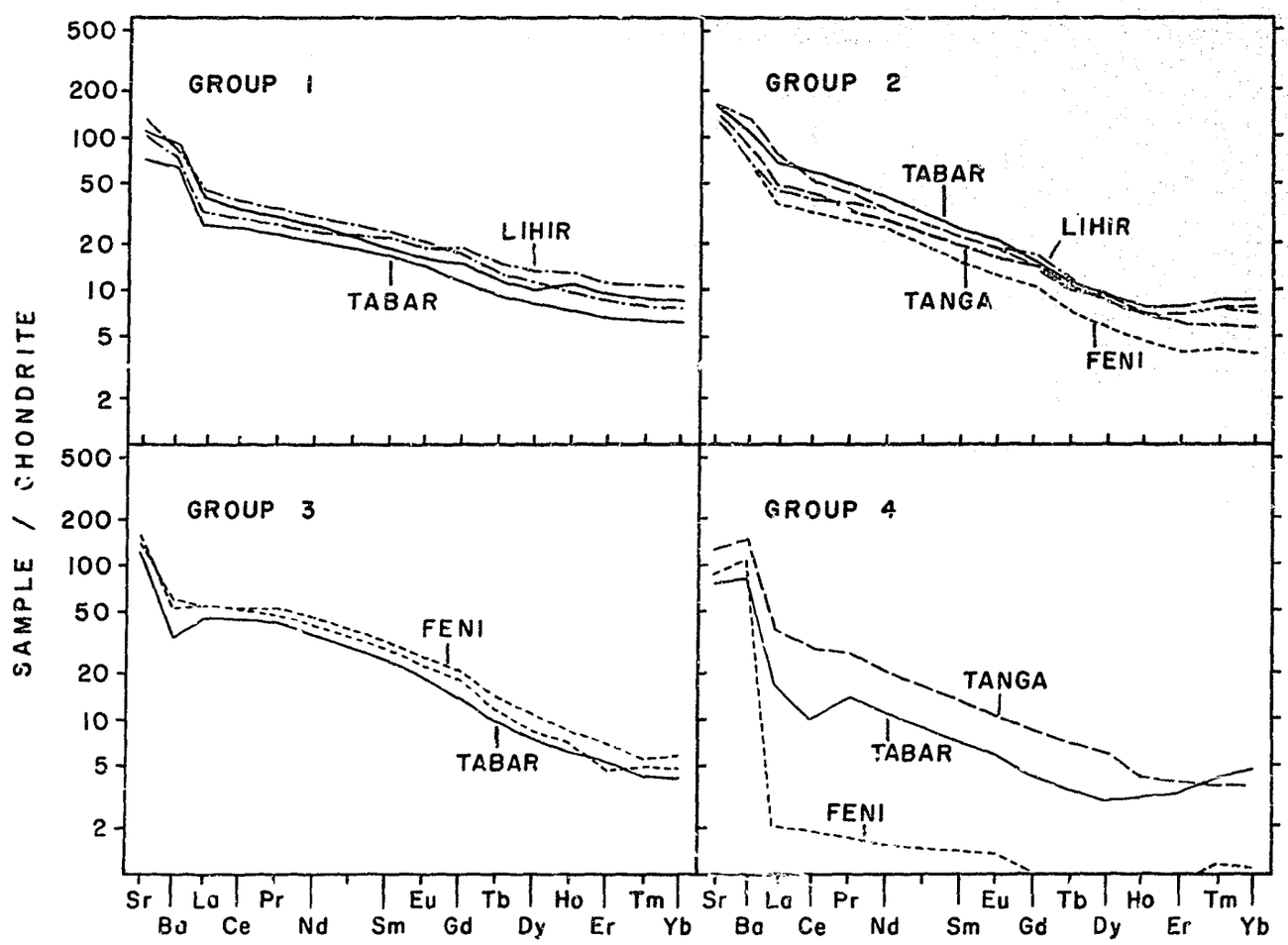

Figure 22. Chondrite-normalised trace-element patterns for the four petrological groups of the Tabar-to-Feni Islands. Unbroken lines represent Tabar rocks. Dot-dash lines represent Lihir rocks. Long-dash lines represent Tanga rocks. Short-dash lines represent Feni rocks.

similar to those of the undersaturated volcanic rocks of the Tabar Islands, suggesting a close genetic relationship. The volcanic rocks of the Tabar-to-Feni Islands were evidently derived from sources with long-term depletions of light-REE and Rb relative to heavy-REE and Sr, respectively. These sources are not isotopically distinct from those which generated volcanic rocks in the other arc provinces in Papua New Guinea and the Solomon Islands. Slight, but significant, differences between isotopic ratios, trace-element ratios, and REE patterns for each of the three alkalic groups on the Tabar-to-Feni Islands are evidence that different mantle sources, or a heterogeneous source, may have been involved in their petrogenesis. Substantial enrichments of some incompatible elements and light-REE in many of the samples may be evidence that the mantle beneath the Tabar-to-Feni Islands was enriched relatively recently and in different degrees in different areas. Intra-crustal melting leading to the production of quartz-trachytes, and geochemical modification of mafic lavas caused by crustal contamination, are also likely.

Summary of mineralogical results

The mineralogy of Tabar-to-Feni volcanic rocks is diverse and is dominated in mafic rocks by olivine, clinopyroxene, plagioclase, and magnetite. Amphibole and biotite are abundant in some types, and there are lesser amounts of apatite, haüyne-sodalite, analcite, leucite, nepheline, alkali feldspar, and pyrrhotite-chalcopyrite. The quartz trachytes contain alkali feldspar, orthopyroxene, and quartz that co-exist with amphibole and magnetite. Groundmass zeolites and calcite are present in a few samples. Clinopyroxene-rich and amphibole-rich (or both) plutonic cumulate blocks and inclusions are also present in the suite.

Olivine ranges widely in composition from phenocryst cores as mafic as Fo_{93}, to Fo_{50}, to rim and groundmass compositions of Fo_{42}. Clinopyroxene is salitic and contains inclusions of feldspar, magnetite, and apatite. Rims are typically enriched in Ti and Al relative to cores, and main compositional changes are in the components $CaTiAl_2O_6$-$NaFeSi_2O_6$-$CaAl_2SiO_6$. Feldspar compositions range widely throughout the suite, from An_{92} in the plutonic cumulates, through An_{89} in phenocryst cores, to co-existing groundmass oligoclase-anorthoclase/K-rich feldspar. Sanidine phenocrysts are present in the quartz trachytes. The most abundant spinel is a low-Ti magnetite (mostly much less than 10 weight

percent TiO_2) which is found both in the groundmass and as phenocrysts. However, there is an extensive overall compositional range - from chromite, through chromian magnetite, to magnetite. Rare, Cr-poor, Al-rich spinels are also present.

Amphibole compositions range mainly from magnesiohastingsite, through magnesiohastingsitic hornblende, to endenitic hornblende. Phenocryst tremolite co-exists with groundmass riebeckite in some quartz trachytes. Some amphiboles fall outside strict compositional limits (less than 5.75 Si cations per 23 oxygens). FeO contents in amphibole separates from cumulates and lavas (E. Kiss, personal communications, 1981) have been determined, and these correspond to relatively high oxidation states (FeO (analysed) = 0.427 FeO-total). Mica ranges from phlogopite to biotite. The felspathoids haüyne and sodalite have complex and unusual zoning patterns. For example, haüyne-rich cores in some phonolitic tephrites and trachyandesites are zoned through to rims that are intermediate in composition between haüyne and sodalite, to groundmass SO_3-free sodalite. Analcite is typically present in samples with high H_2O+ contents and high Na_2O/K_2O values. They appear to be secondary after leucite. Haüyne is present in rocks with high Na_2O contents (greater than 4.2 weight percent) and low H_2O+ values (less than 0.6 weight percent).

Noteworthy mineralogical features of these rocks are the persistently low TiO_2 contents of minerals such as clinopyroxene, amphibole, biotite, and magnetite which, in most other strongly silica-undersaturated rocks, are rich in TiO_2. The low TiO_2 contents are a reflection of the low TiO_2 content of the host magmas which, together with the overall low Nb contents in the suite, appears to be a feature of other island-arc volcanic rocks. The presence of haüyne phenocrysts, high Fe^{3+}/Fe^{2+} values for amphiboles (and whole rocks), and possibly some high Mg/Fe values in minerals such as olivine and pyroxene are consistent with high oxygen fugacities. However, more reduced groundmass equilibration conditions are indicated by the results of thermodynamic calculations for the assemblage olivine+plagioclase+leucite+magnetite (about $750^{o}C$, fO_2 10^{-22} bars).

ACKNOWLEDGEMENTS

D.A.W. and I.H.C. are indebted to Dr. R.A. Davies, formerly Senior Government Volcanologist at the Rabaul Volcanological Observatory, who gave the initial encouragement to survey the Tabar-to-Feni volcanoes in 1972-73. Those

of us involved in fieldwork also acknowledge the valuable assistance given at different times by Stuart Scriven, Principal Surveyor, Department of Lands, Rabaul, who permitted extensive use of the M.V. 'Lahara', and by the Captains and crews of the 'Lahara' whose seamanship and knowledge of local waters helped us greatly. The friendly assistance rendered by Graham Carson and Ray Lacey (Ambitle Island), Paul Jamison (Lihir Island), and Graham Dudley (Malendok Island), is also gratefully acknowledged. R. Freeman, W.B. Nance, and P. Oswald-Sealey provided valuable assistance in analytical work at ANU.

REFERENCES

ARCULUS, R.J., 1982 - Electron-microprobe chemical analyses of minerals and glasses in volcanic rocks from the Tabar, Lihir, Tanga and Feni Islands. Unpublished data catalogue, Bureau of Mineral Resources, Canberra.

ARCULUS, R.J., & JOHNSON, R.W., 1981 - Mineralogy of strongly silica-undersaturated volcanic rocks from the Tabar, Lihir, Tanga, and Feni Islands, Papua New Guinea. Abstracts Volume 1981 IAVCEI 'Arc Volcanism' Symposium, Tokyo and Hakone, 18-19.

ARCULUS, R.J., JOHNSON, R.W., & PERFIT, M.R., 1978 - Alkaline volcanic rocks from the Tabar-to-Feni Islands, Papua New Guinea: oceanic or island-arc magmas?. Abstracts of the International Geodynamics Conference, Tokyo, 1978, 200-201

BLAKE, D.H. & McDOUGALL, I., 1973 - Ages of the Cape Hoskins volcanoes, New Britain, Papua New Guinea. Journal of the Geological Society of Australia, 20, 199-204.

COLEMAN, P.J., & PACKHAM, G.H., 1976 - The Melanesian borderlands and India-Pacific plates boundary. Earth-Science Reviews, 12, 197-233

COOMBS, D.S. & WILKINSON, J.F.G., 1969 - Lineages and fractionation trends in undersaturated volcanic rocks from the east Otago volcanic province (New Zealand) and related rocks. Journal of Petrology, 10, 440-501.

DAMPIER MINING (1974). Prospecting Authority 353 (NG). Dampier Mining Company Ltd.

DAVIES, H.L., 1973 - Gazelle Peninsula, New Britain, 1:250 000 Geological Series. Bureau of Mineral Resources, Australia - Explanatory Notes SB/56-2.

DE BROIN, C.E., AUBERTIN, F., & RAVENNE, C., 1977 - Structure and history of the Solomon - New Ireland region. International Symposium on Geodynamics in South-West Pacific, Noumea. Editions Technip, Paris, 37-50

FINLAYSON, D.M., & CULL, J.P., 1973 - Structural profiles in the New Britain-New Ireland region. Journal of the Geological Society of Australia, 20, 37-48

FISHER, N.H., 1957 - CATALOGUE OF THE ACTIVE VOLCANOES OF THE WORLD INCLUDING SOLFATARA FIELDS. PART 5, MELANESIA. International Volcanological Association, Naples.

FOURNIER, R.O. & ROWE, J.J., 1966 - Estimation of underground temperatures from the silica content of water from hot springs and wet-steam wells. American Journal of Science, 264, 685-697

FURUMOTO, A.S., WEBB, J.P., OSEGARD, M.E., & HUSSONG, D.M., 1976 - Seismic studies on the Ontong-Java Plateau, 1970. Tectonophysics, 34, 71-90.

GALLASCH, H., 1974 - A solution cave in volcanolithic arenite - Lihir Island. Niugini Caver, 4, 31-33.

GLAESSNER, R., 1915 - Beitrage zur Kenntnis der Eruptivgesteine des Bismarck - Archipeligo und der Salomon Inseln. Beitrage Geologische Entforschung Deutschen Schutzgebiete, 10, 1-85

GULF RESEARCH AND DEVELOPMENT, 1973 - Regional marine geophysical reconnaissance of Papua/New Guinea. Gulf Research and Development Company and Australian Gulf Oil Company, Sydney.

HART, D., 1970 - Rainfall. In WARD, R.G. & LEA, D.A.M. (Editors), AN ATLAS OF PAPUA AND NEW GUINEA. Collins and Longman, Glasgow.

HEMING, R.F., 1979 - Undersaturated lavas from Ambittle [sic] Island, Papua New Guinea. Lithos, 12, 173-186

HOHNEN, P.D., 1978 - Geology of New Ireland, Papua New Guinea. Bureau of Mineral Resources, Australia, Bulletin 194.

IRVINE, T.N. & BARAGAR, W.R.A., 1971 - A guide to the chemical classification of the common volcanic rocks. Canadian Journal of Earth Sciences, 8, 523-548.

JOHNSON, R.W., 1979 - Geotectonics and volcanism in Papua New Guinea: a review of the late Cainozoic. BMR Journal of Australian Geology & Geophysics, 4, 181-207.

JOHNSON, R.W., MACKENZIE, D.E., & SMITH, I.E.M., 1978 - Volcanic rock associations at convergent plate boundaries: re-appraisal of the concept using case histories from Papua New Guinea. Geological Society of America-Bulletin, 89, 96-106.

JOHNSON, R.W., MUTTER, J.C., & ARCULUS R.J., 1979 - Origin of the Willaumez-Manus Rise, Papua New Guinea. Earth and Planetary Science Letters, 44, 247-260

JOHNSON, R.W., WALLACE, D.A., & ELLIS, D.J., 1976 - Feldspathoid-bearing potassic rocks and associated types from volcanic islands off the coast of New Ireland, Papua New Guinea: a preliminary account of geology and petrology. In JOHNSON, R.W. (Editor), VOLCANISM IN AUSTRALASIA, 297 - 316. Elsevier, Amsterdam.

KEAR, D., 1957 - Erosional stages of volcanic cones as indication of age. New Zealand Journal of Science and Technology, B, 38, 671-682.

MAMMERICKX, J., CHASE, T.E. SMITH, S.M., & TAYLOR, I.L., 1971 - BATHYMETRY OF THE SOUTH PACIFIC, CHART 11. Scripps Institute of Oceanography and Institute of Marine Science, La Jolla.

MURAUCHI, S., LUDWIG, W.J., DEN, N., HOTTA, H., ASANUMA, T., YOSHII, T., KUBOTERA, A., & HAGIWARA, K., 1973 - Seismic refraction measurements on the Ontong Java Plateau northeast of New Ireland. Journal of Geophysical Research, 78, 8653-8663.

NORRISH, K., & CHAPPELL, B.W., 1977 - X-ray fluorescence spectrometry. In ZUSSMAN, J. (Editor), PHYSICAL METHODS OF DETERMINATIVE MINERALOGY, 201-272. Academic Press, London.

PAGE, R.W., & JOHNSON, R.W., 1974 - Strontium isotope ratios of Quaternary volcanic rocks from Papua New Guinea. Lithos, 7, 91-100.

PEARSON, H.F., 1934 - Gold in Tabar Islands. Report by Asst. Warden Pearson. The Rabaul Times, no. 485, 3 August 1934, 3-4

PERFIT, M.R., ARCULUS, R.J., JOHNSON, R.W. & CHAPPELL, B.W., 1978 - Mineralogy, major, trace and isotope chemistry of volcanic rocks from the Tabar-to-Feni Islands, Papua New Guinea: an alkalic island arc? Geological Society of America - Annual Meeting, Abstracts, Toronto, 10, 470.

PERFIT, M.R., JOHNSON, R.W., & CHAPPELL, B.W., 1981 - Geochemistry and isotopic compositions of volcanic rocks from an alkalic island arc: Tabar-to-Feni Islands, Papua New Guinea. Abstracts Volume, 1981 IAVCEI 'Arc Volcanism' Symposium, Tokyo and Hakone, 290-291.

PERFIT, M.R., McCULLOGH, M.T., & JOHNSON, R.W., 1982 - Isotopic and trace-element differences in Late Cainozoic volcanic rocks from west Melanesia. Geological Society of America - Annual Meeting, Abstracts, New Orleans.

REED, S.J.B., & WARE, N.G., 1973 - Quantitative electron microprobe analysis using a lithium drifted silicon detector. X-ray Spectrometry, 2, 69-74.

REED, S.J.B., & WARE, N.G., 1975 - Quantitative electron microprobe analysis of silicates using energy-dispersive X-ray spectrometry. Journal of Petrology, 16, 499-519

REYNOLDS, M.A., 1956 - Notes on thermal activity at Lihir and Anir (Feni) Island groups. Bureau of Mineral Resources, Australia, Record 1956/25 (unpublished).

TAYLOR, S.R., & GORTON, M.P., 1977 - Geochemical application of spark-source mass spectrography - III: Element sensitivity, precision and accuracy. Geochimica et Cosmochimica Acta, 41, 1375-1380.

THORNTON, C.P., & TUTTLE, O.F., 1960 - Chemistry of igneous rocks I. Differentiation Index. American Journal of Science, 258, 664-684

WALLACE, D.A., 1976 - Preliminary investigation of the Ala River (Walo) thermal field, west New Britain. Geological Survey of Papua New Guinea, Report 76/19 (unpublished).

WARE, N.G., 1981 - Computer programs and calibration with the PIBS technique for quantitative electron probe analysis using a lithium-drifted silicon detector. Computers and Geosciences, 7, 167-184.

WHITE, D.E., 1957 - Magmatic, connate, and metamorphic waters. Geological Society of America, Bulletin, 68, 1659-1682.

WHITE, D.E., BARNES, I., & O'NEILL, J.R., 1973 - Thermal and mineral waters of nonmeteoric origin, California Coast Ranges. Geological Society of America - Bulletin, 84, 547-560

APPENDIX 1. MICROPALAEONTOLOGICAL REPORT

By D.J. Belford

Sample locations are shown on the relevant maps accompanying the main part of this report.

Simberi Island (Fig. 4)

The first three samples from Simberi Island all have the grid reference LC849099, and all four samples were collected by G.A.M. Taylor.

Sample 69400380. This sample is a fine-grained limestone containing abundant planktonic foraminifera - mainly Globigerinidae, including *Orbulina*, *Sphaeroidinellopsis*, and *Globoquadrina dehiscens*; rare Globorotaliidae, including *Globorotalia* of the *cultrata* type, are also present.

The sample is regarded as middle to late Miocene in age (Zones N.11 to N.18).

Sample 69400381. This detrital limestone contains foraminifera and algae. Larger foraminifera include *Lepidocyclina (Nephrolepidina)* sp., *Miogypsina (M)* sp., *Amphistegina* sp., and *Planorbulinella* sp. Planktonic foraminifera are similar to those in sample 0380, but are interpreted to be in channel infillings in an older limestone. The sample is thought to be early Miocene in age, and the infillings to be middle to late Miocene.

Sample 69400382. This sample is a detrital limestone similar to 0381, and contains larger and planktonic foraminifera. The larger foraminifera include *Lepidocyclina* (N) sp., *Miogypsina (M)* sp., *Amphistegina* sp.,*Carpenteria* sp., and *Heterostegina* sp. Planktonic foraminifera include *Orbulina*, *Sphaeroidinellopsis*, and *Globorotalia* of the *cultrata* group.

This sample is regarded as middle to late Miocene in age with reworked larger foraminifera.

Sample 69400453 (grid reference E385600, N9709900). This sample contains foraminifera, algae, mollusca, bryozoa, corals, and echinoid spines. Foraminifera are *Amphistegina* sp. (abundant), *Cycloclypeus* sp., *Planorbulinella* sp , *Gypsina* sp., *Carpenteria* sp., *Elphidium* sp., *Pulleniatina obliquiloculata*, *Globorotalia (G) tumida*, and ? *Sphaeroidinella*. The sample is regarded as

Pliocene or younger.

Lihir Island (Fig. 9)

Samples 73680049 and 73680050 (both collected at grid reference MB474579) and sample 73680066 from Mahur Island (MB609908) contain rare foraminifera (*Operculina, Acervulina,* fragments of *Carpenteria),* but these are insufficient for age determination.

Dr. B. Fordham has forwarded a cave sample from Lihir Island for examination; a report on this material has been made previously (Fordham, 1974). Free specimens identified from the sample are *Globorotalia (G.) tumida tumida* (Brady), *G. (G) cultrata* (d'Orbigny) group, *G. (Turborotalia) acostaensis pseudopima* Blow, *Globigerinoides quadrilobatus* (d'Orbigny) group, *Orbulina universa* d'Orbigny, *O.? suturalis* Bronnimann, *Sphaeroidinellopsis subdehiscens subdehiscens* (Blow) and *Amphistegina* sp. The thin section examined contains rare *Globorotalia (G.) cultrata* group, *Dentoglobigerina altispira altispira* (Cushman & Jarvis), possible *Sphaeroidinellopsis* sp., and indeterminable globigerinids.

This fauna is considered to be latest Miocene to Pliocene age (Zone N.18 to Zone N.20) using the zonation of Blow (1969). However, Berggren (1973) placed the base of the Pliocene for all practical purposes at the base of Zone N.18, and in this scheme the fauna is early Pliocene (PL1 to PL3).

Ambitle Island (Fig. 15)

Sample 73680056 (grid reference NA693538) contains abundant, well-preserved planktonic and benthonic smaller foraminifera. Planktonic foraminifera are: *Globigerina tripartita* Koch, *G. sellii* (Borsetti), *Gipraebulloides praebulloides* Blow, *G. ouachitaensis ciperoensis* Bolli, G. *angustiumbilicata* Bolli, *G.* sp *Globigerinita dissimilis* (Cushman & Bermudez), *G. unicava unicava* (Bolli, Loeblich & Tappan). This sample is middle to late Oligocene in age (planktonic zones No. 1 to No. 3).

Babase Island (Fig. 15)

Sample 73680057 (grid reference NA745549) contains *Calcarina, Acervulina,* and fragments of *Carpentaria* or *Sporadotrema,* and is not older than Pleistocene.

BERGGREN, W.A., 1973 - The Pliocene time scale: calibration of planktonic foraminiferal and calcareous nannoplankton zones. Nature, 243, 391-397.

BLOW, W.H., 1969 - Late middle Eocene to Recent planktonic foraminiferal biostratigraphy. Proceedings of the 1st International Conference on planktonic microfossils, Geneva, 1967, vol. 1, 199-422. Leidon, E.J. Brill.

FORDHAM, B.G., 1974 - In Gallasch, H., A solution cave in volcanolithic arenite - Lihir Island. Niugini Caver, 4, 31-33.

APPENDIX 2. ISOTOPIC AGE DETERMINATIONS OF FIVE VOLCANIC ROCKS

Five samples of volcanic rocks from the Tabar to Feni Islands were submitted to Amdel for K-Ar age determination. Sample locations are shown on the relevant maps accompanying this report. Results are as follows:

Sample No. and Locality	Rock	Method	% K	% Atmospheric Ar^{40}	Radiogenic Ar^{40}/K^{40}	Age m.y.
73680002, Babase Island, grid ref. NA742546	Mafic lava	Hornblende concentrate	0.916 0.918	77.2	0.00008942	1.53±0.15
FN1/28, Ambitle Island, grid ref. NA696489	Q-trachyte	Biotite extract	5.97 5.98	85.0 84.3	0.00003982 0.00002870	0.68 0.49±0.10
TG4/1, Bitbok Island, grid ref. NB232121	Q-trachyte	Biotite extract	6.68 6.69	67.0 69.9	0.00006679 0.00006307	1.14 1.08±0.08
73680018, Lif Island, grid ref. NB204126	Mafic lava	Total rock	3.23 3.22	78.2	0.00001094	0.187±0.02
TB3/11, Tabar Island, grid ref. LB845815	Q-trachyte	Plagioclase	3.57 3.58	70.1	0.00005762	0.986±0.08

APPENDIX 3. ANALYSES OF THERMAL WATERS

COLLECTED BY G.A.M. TAYLOR*. BY H.R. LORD

Sample	1		2		3		4				6	
Temp. °C	42		95		98		88		45		101	
pH	6.9		6.2		6.7		2.0		5.5		7.0	
S.C. at 23°C (micromho/cm)	4290		4740		12,150		3430		17,280		7090	
T.D.S. at 180°C (ppm)	3480		3450		9910		1285		12,460		5470	
	ppm	me/lt	ppm	me/lt	ppm	me/lt	ppm	me/lt	ppm	me/lt	ppm	me/lt
Ca	337	16.8	40	2.0	80	4.0	8	0.4	232	11.6	10	0.5
Mg	54	4.4	3	0.3	12	1.0	n.d.		300	24.6	n.d.	
Na	725	31.6	1150	50.4	3075	134	2	0.1	3750	163.0	1925	83.7
K	12	0.3	49	1.3	336	8.6	8	0.2	131	3.4	154	3.9
Fe	n.d.		1.1		n.d.		13.4	0.7	n.d.		n.d.	
Al	n.d.		n.d.		n.d.		4.8	0.5	n.d.		n.d.	
Mn	n.d.		n.d.		0.5		n.d.		0.6		n.d.	
Zn	n.d.		n.d.		0.02		0.01		0.05		n.d.	
Σ cations		53.1		54.0		148		2		203		88.1
Cl	1200	33.8	1300	36.7	2990	84.5	7	0.2	6560	185	2170	61.2
HCO_3	123	2.0	265	4.4	260	4.3	nil		460	7.6	54	0.9
SO_4	930	19.4	634	13.2	3080	64.1	930	19.4	800	16.7	1260	26.2
Σ anions		55.2		54.4		153		19.6		210		88.3
Σ ions	3200		3687		12,284		1275		11,839		5767	
SiO_2	119		164		161		282		168		80	
R_2O_3	<12		<12		<12		26		<12		<12	

continued on next frame

*The analyses listed here were originally presented in an unpublished BMR Laboratory Report (No. 98), dated 15 October 1969. No further details on the sample localities are known. S.C. refers to specific conductance, T.D.S. to total dissolved solids, and me/lt, to micro-equivalents per litre. n.d. presumably means 'not detected', although no detection limits are given in the original report.

Appendix 3 continued

Sample localities

1. Sambuari Bay, Tatau Island, Tabar Islands.
2. Nis Nis, Ambitle Island, Feni Islands.
3. Luise Harbour (Sample A), Lihir Island.
4. Luise Harbour (Sample B), Lihir Island.
5. Malendok Island, Tanga Islands.
6. Waramung, Ambitle Island, Feni Islands.